

AD-A127 503

PERFORMANCE LIFE AND OPERABILITY TRADE-OFFS IN VCE

1/2

(VARIABLE CYCLE ENGINE.. (U) GENERAL MOTORS CORP

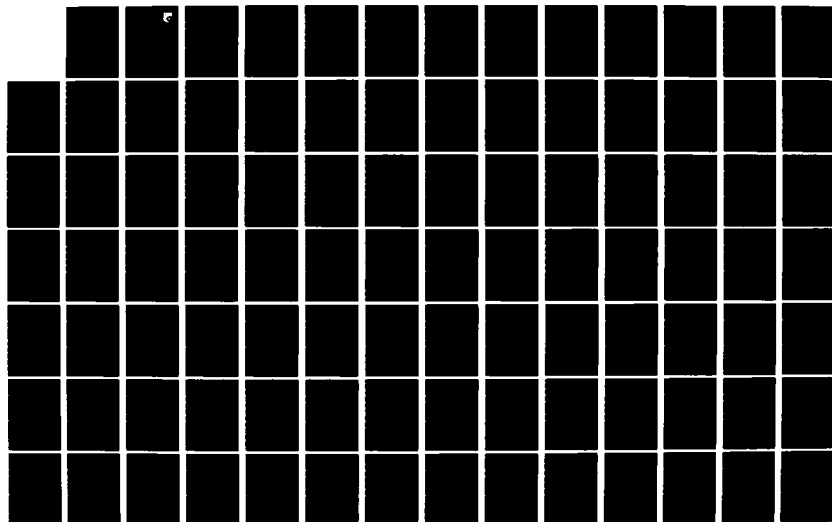
INDIANAPOLIS IN DETROIT DIESEL ALLISON DI.. JUL 81

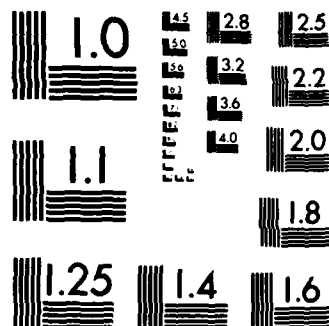
UNCLASSIFIED

DDA-EDR-10456 AFWAL-TR-81-2060

F/G 21/5.

NL





MICROCOPY RESOLUTION TEST CHART  
NATIONAL BUREAU OF STANDARDS-1963-A

AFWAL-TR-81-2060

AD 1127 3



# **Performance, Life, and Operability Trade-offs in VCE Control Logic Design**

**Detroit Diesel Allison  
P. O. Box 894  
Indianapolis, Indiana 46206**

**July 1981**

**Final Report for Period August 1978 to November 1980**

**APPROVED FOR PUBLIC RELEASE; DISTRIBUTION UNLIMITED**

**Aero Propulsion Laboratory  
Air Force Wright Aeronautical Laboratories  
Air Force Systems Command  
Wright-Patterson Air Force Base, Ohio 45433**

88 05 62 032


UNCLASSIFIED COPY


# NOTICE

When Government drawings, specifications, or other data are used for any purpose other than in connection with a definitely related Government procurement operation, the United States Government thereby incurs no responsibility nor any obligation whatsoever; and the fact that the government may have formulated, furnished, or in any way supplied the said drawings, specifications, or other data, is not to be regarded by implication or otherwise as in any manner licensing the holder or any other person or corporation, or conveying any rights or permission to manufacture use, or sell any patented invention that may in any way be related thereto.

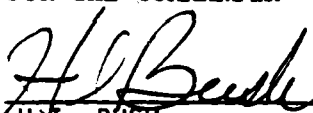
This report has been reviewed by the Office of Public Affairs (ASD/PA) and is releasable to the National Technical Information Service (NTIS). At NTIS, it will be available to the general public, including foreign nations.

This technical report has been reviewed and is approved for publication.

  
\_\_\_\_\_  
PAUL T. ADAMS, JR.  
Project Engineer  
Components Branch

  
\_\_\_\_\_  
LESTER L. SMALL  
Technical Area Manager  
Controls and Diagnostics  
Components Branch

FOR THE COMMANDER

  
\_\_\_\_\_  
H. I. BUSH  
Director  
Turbine Engine Division  
Aero Propulsion Laboratory

"If your address has changed, if you wish to be removed from our mailing list, or if the addressee is no longer employed by your organization, please notify AFWAL/POTC W-PAFB, OH 45433 to help us maintain a current mailing list".

Copies of this report should not be returned unless return is required by security considerations, contractual obligations, or notice on a specific document.

UNCLASSIFIED

SECURITY CLASSIFICATION OF THIS PAGE (When Data Entered)

REPORT DOCUMENTATION PAGE		READ INSTRUCTIONS BEFORE COMPLETING FORM
1. REPORT NUMBER AFWAL-TR-81-2060	2. GOVT ACCESSION NO.	3. RECIPIENT'S CATALOG NUMBER
4. TITLE (and Subtitle) PERFORMANCE, LIFE, AND OPERABILITY TRADE-OFFS IN VCE CONTROL LOGIC DESIGN	5. TYPE OF REPORT & PERIOD COVERED Final Report for Period Aug 78 to Nov 80	
	6. PERFORMING ORG. REPORT NUMBER EDR 10456	
7. AUTHOR(s)	8. CONTRACT OR GRANT NUMBER(s) F33615-78-C-2021	
9. PERFORMING ORGANIZATION NAME AND ADDRESS Detroit Diesel Allison P. O. Box 894 Indianapolis, IN 46206	10. PROGRAM ELEMENT, PROJECT, TASK AREA & WORK UNIT NUMBERS 30660377 62203F	
11. CONTROLLING OFFICE NAME AND ADDRESS Aero Propulsion Laboratory (AFWAL/POTC) Air Force Wright Aeronautical Laboratories (AFSC) Wright-Patterson Air Force Base, OH 45433	12. REPORT DATE July 1981	
	13. NUMBER OF PAGES 142	
14. MONITORING AGENCY NAME & ADDRESS (if different from Controlling Office)	15. SECURITY CLASS. (of this report) UNCLASSIFIED	
	15a. DECLASSIFICATION DOWNGRADING SCHEDULE	
16. DISTRIBUTION STATEMENT (of this Report)  Approved for public release; distribution unlimited.		
17. DISTRIBUTION STATEMENT (of the abstract entered in Block 20, if different from Report)		
18. SUPPLEMENTARY NOTES		
19. KEY WORDS (Continue on reverse side if necessary and identify by block number) Variable Cycle Engine                      Operability Controls Trade-Off Analysis              Engine Life Consumption Aircraft Performance		
20. ABSTRACT (Continue on reverse side if necessary and identify by block number) The baseline engine control requirements were generated from previous control design experience. The control requirements for the 680-B1 (next generation engine) were then generated from a "top down" analysis of mission (weapon system), aircraft, and engine requirements. The performance, operability, and engine component life parameters were then varied to determine the trade-offs with each other. It was clearly demonstrated that the control logic can perform trade-offs in these parameters through the choices made throughout the logic design procedure,		

# TABLE OF CONTENTS

	<u>Page</u>
I. INTRODUCTION.....	1
II. CONTROL REQUIREMENTS.....	3
Introduction.....	3
Derivation of Requirements.....	4
Performance Requirements.....	6
Life Requirements.....	11
III. MISSIONS.....	17
Stick Missions.....	17
Air-to-Air Combat.....	19
Realistic Throttle Histories.....	21
IV. ENGINE AND CONTROL SYSTEM DESCRIPTION.....	29
Engine Description.....	29
Control Description.....	29
V. ENGINE SIMULATION.....	38
General Steady-State Performance Deck.....	38
Special Features of Engine Simulation.....	43
VI. CONTROL SIMULATION.....	50
Baseline Control Mode.....	50
Actuator Models.....	59
Control Simulation.....	62
VII. ENGINE/CONTROL SIMULATION RESULTS.....	68



A

# TABLE OF CONTENTS (continued)

	<u>Page</u>
VIII. ANALYTICAL METHODOLOGY.....	75
Steady State Evaluation.....	75
Dynamic Analysis.....	78
IX. ANALYSIS TOOLS.....	85
Introduction.....	85
Steady-State Performance Deck.....	86
Mission Evaluation.....	88
Life Utilization.....	89
X. STEADY STATE RESULTS.....	95
Control Mode Development.....	95
Performance Optimization.....	106
Control Schedules.....	111
Steady State Evaluation.....	116
XI. DYNAMIC ANALYSIS.....	131
Evaluation of Life Consumption with Dynamics.....	131
XII. CONCLUSIONS & RECOMMENDATIONS.....	141

# LIST OF FIGURES

	<u>Page</u>
Figure 1 Maximum Customer Bleeds & Horsepower Extraction.....	9
Figure 2 Inlet Airflow Corridor.....	14
Figure 3 Typical Wartime Mission.....	20
Figure 4 Typical Training Mission.....	22
Figure 5 Sample Combat History.....	24
Figure 6 Combat Simulation Profile.....	26-28
Figure 7 System Configuration.....	30
Figure 8 HPT Actuation System.....	34
Figure 9 Generalize Engine Simulation Structure.....	39
Figure 10 Typical Layered Map.....	41
Figure 11 Nozzle Simulation.....	42
Figure 12 Engine Cycle Match Flowchart.....	45
Figure 13 Engine/Control Simulation Flowchart.....	48
Figure 14 Fuel Control Logic.....	51
Figure 15 Fuel Limiting Logic.....	53
Figure 16 Geometry Control Logic.....	55
Figure 17 $R_C$ & $N_H$ Select Logic.....	57
Figure 18 Fuel System Block Diagram.....	60
Figure 19 Control Output Sample.....	64
Figure 20 S.L.S. Transient Response -- Idle to Int.....	69
Figure 21 S.L.S. Transient Response -- Idle to Max.....	70
Figure 22 $0.8 M_N/36,000$ Ft Transient Response -- Int. to Max.....	71
Figure 23 $0.8 M_N/36,000$ Ft Transient Response -- Idle to Max.....	72
Figure 24 $0.8 M_N/50,000$ Ft Transient Response -- Idle to Max.....	73
Figure 25 Basic Technical Approach.....	76
Figure 26 Steady State Evaluation.....	77
Figure 27 Deep Strike Mission.....	79



# LIST OF FIGURES (continued)

	<u>Page</u>
Figure 28 Supercruiser Mission.....	80
Figure 29 Training Mission.....	81
Figure 30 Life Utilization Analysis.....	82
Figure 31 Dynamic Analysis.....	84
Figure 32 Variable Engine Mission Analysis Program.....	90
Figure 33 Fixed Engine Mission Analysis Program.....	90
Figure 34 Mechanical LCF.....	91
Figure 35 Thermal LCF.....	93
Figure 36 Effect of Engine Limits.....	109
Figure 37 Installed Operating Line.....	110
Figure 38 Speed Schedule #1.....	112
Figure 39 Speed Schedule #2.....	112
Figure 40 Operating Line.....	113
Figure 41 EPR Schedule #1.....	113
Figure 42 EPR Schedule #2.....	114
Figure 43 Corrected Flow Schedule.....	115
Figure 44 Nozzle Temperature Schedule.....	116
Figure 45 EPR at Max Thrust.....	119
Figure 46 Gas Stream & Metal Temperature During Critical Period.....	126
Figure 47 Gas Stream & Metal Temperature During Combat Turns.....	136
Figure 48 Mission Life Control Transients.....	140

# LIST OF TABLES

	<u>Page</u>
Table I High Altitude Attack Mission.....	18
Table II Boeing Supercruiser Mission.....	18
Table III GMA400 Sensor Requirements.....	37
Table IV GMA400 Control Mode Summary.....	58
Table V Sensor Table.....	66
Table VI Scheduled Control Mode Errors Due to Engine Variations.....	103
Table VII Baseline Control Mode Errors Due to Engine Variations.....	104
Table VIII Non-Trim Control Mode Errors Due to Engine Variations.....	105
Table IX Minimum SFC Evaluation.....	120
Table X Minimum RIT Evaluation.....	122
Table XI Minimum Speed Evaluation.....	123
Table XII Derated Control Evaluation.....	127
Table XIII Trim Mode Evaluation.....	129
Table XIV Baseline Min SFC Comparison.....	132
Table XV Baseline Min $N_H$ Comparison.....	133

# LIST OF SYMBOLS

A	Area
A <sub>e</sub>	Nozzle Area
A <sub>Teff</sub>	Effective Nozzle Area
ACCEL*	Output of Acceleration Schedule
A8	Nozzle Geometric Area
ATEGG	Advanced Turbine Engine Gas Generator
BLD1	Turbine Blade Cooling
BLD2	Aft Section Cooling
CD	Convergent-Divergent
CDP	Compressor Discharge Pressure
C <sub>T</sub>	Thrust Coefficient
C <sub>T-D</sub>	Thrust to Drag Coefficient
C <sub>Tint</sub>	Internal Thrust Coefficient
DCEL*	Output of Deceleration Schedule
EHSV	Electro-Hydraulic Servo Valve
EPR	Engine Pressure Ratio
EPREQ*	Engine Pressure Ratio Required
FASP	Frequency Analysis of Systems Program
FEBA	Forward Edge of Battle Area
FN	Net Thrust
GOVERL*	Governor Error after the Lag
HPC	High Pressure Compressor
HPT	High Pressure Turbine

\*Noted variables are associated with the control logic.

IECMS	Inflight Engine Condition Monitoring System
IGV	Inlet Guide Vane
ISA	Inlet Standard Air
JTDE	Joint Technology Demonstrator Engine
LVDT	Linear Variable Differential Transformer
$K_I$	Integral Gain
$K_p$	Proportional Gain
LPT	Low Pressure Turbine
$M_N$	Mach Number
N	Speed Derivative
NHCFBK*	Corrected Speed Feedback
NHCOMAP*	Corrected Speed for Map Look-up
NHCOMAX*	Maximum Corrected Speed
NHCOMNR*	Minimum Corrected Speed (based on inlet corridor)
NHCOMX*	Maximum Corrected Speed (computed)
NHCOMXR*	Maximum Corrected Speed (based on inlet corridor)
NHCREQ*	Requested Corrected Speed
NHMAX*	Maximum Mechanical Speed
NPR	Nozzle Pressure Ratio
PA	Ambient Pressure
psi	Pounds per Square Inch
psia	Pounds per Square Inch (absolute)
PLA	Power Lever Angle
PPH	Pounds per Hour
P1	Compressor Inlet Pressure

\*Noted variables are associated with the control logic.

P3	Compressor Exit Pressure
P3MAX*	Maximum $P_3$
P3MIN*	Minimum $P_3$
R	Rankine
$R_c$	Compressor Pressure Ratio
RCMAX*	Maximum Compressor Pressure Ratio (based on inlet corridor)
RCMIN*	Minimum Compressor Pressure Ratio (based on inlet corridor)
RCMNM*	Minimum Compressor Pressure Ratio
RCMXM*	Maximum Compressor Pressure Ratio
RCREQ*	Requested Pressure Ratio
RIT	Rotor Inlet Temperature
rpm	Revolutions per Minute
TBT	Turbine Blade Temperature
T/C	Thermocouple
TIMEF*	Final Time
TNOZ	Nozzle Metal Temperature
T1	Inlet Temperature
T3	Compressor Discharge Temperature
T4	Turbine Inlet Temperature
T5	Turbine Outlet Temperature
VCD	Vortex Controlled Diffuser
VCE	Variable Cycle Engine
$W_f$	Fuel Flow
WFACCEL*	Accel Fuel Flow Limit
WFCOM*	Fuel Flow Command
WFDCEL*	Decel Fuel Flow Limit
WFNOM*	Nominal Fuel Flow

\*Noted variables are associated with the control logic.

$\gamma$	Ratio of Specific Heats
$\theta$	Fuel Valve Position
$\Delta N *$	Speed Derivative Limit Exceedance
$\Delta NHC *$	Corrected Speed Limit Exceedance
$\Delta TBT *$	Turbine Blade Temperature Limit Exceedance
$\Delta TNOZ *$	Nozzle Metal Temperature Limit Exceedance
$\Delta T3 *$	Compressor Discharge Temperature Limit Exceedance
$\Delta T4 *$	Turbine Inlet Temperature Limit Exceedance
$\Delta T5 *$	Turbine Outlet Temperature Limit Exceedance
$\Delta W_f *$	Fuel Flow Adjustment for Limit Exceedance

\*Noted variables are associated with the control logic.

## I. INTRODUCTION

Turbine engine control systems historically have undergone a gradual evolutionary development. However, three major factors in combination recently have had a revolutionary impact on this process, and have caused significant changes in control design techniques. These factors are: (1) the development of engines with several controlled variables, (2) the development of ruggedized electronics for use in engine-mounted controls, and (3) the development of powerful, mathematically sophisticated transient control techniques.

One result is that control mode design techniques are becoming highly dependent on engine simulations. Consequently, the control designer must become more involved in establishing the nature of and defining limitations of this control design tool. Key characteristics of the control-oriented engine simulation are: (1) control-type inputs rather than performance inputs with implied control modes, (2) bandwidth consistent with control requirements and hardware constraints, (3) inclusion of actuator and sensor dynamics, (4) an all-digital simulation that will run efficiently. In some aspects these characteristics tend to be mutually exclusive. However, a workable blend must be established in order to permit efficient and effective control design.

A second result is the potential of using the control of an engine to perform performance, stability, and life management. For example, initial life usage studies of variable turbine area have stressed the performance improvement potential of the technology when applied to aircraft and missions studies. Recent work has also demonstrated that it is possible to enhance weapons systems performance and stability by providing the control with sufficient logic to perform trades in flight to respond to changing aircraft needs. Now it is time to consider engine life usage as an additional trade factor in the control design.

A turbine engine has inherent life potential or capability that in principle can be roughly described by various measurable factors; e.g., hot section life (times at temperature), low-cycle fatigue cycles, etc. The control system cannot modify these basic characteristics nor can it modify the installation or utilization characteristics of the weapons system. However, within these constraints, there is opportunity for controls to modify the rate at which these life resources are consumed. However, in order for these results to be useful to the Air Force, it is necessary that any performance penalty associated with these control modes be identified in a quantitative manner, just as potential improvements in life consumption rates are to be quantified.

Consequently, this program was directed toward the derivation of the methodology and tools required by the controls designer to produce propulsion system controls that meet weapons system and mission needs and take maximum advantage of the life capabilities inherent in an engine design. The first step in this process is the direct derivation of control requirements from weapons system needs without any assumptions concerning presumed set point schedules. The second step is the structuring of an engine model in such a manner that a controls designer can easily investigate the trade-offs involved in simultaneously providing required performance and stability levels and making the best use of engine life potential. The third step is the use of the model to generate control set points recognizing their influence on engine life and a quantification of the resultant performance cost/life benefit payoffs. It is recognized that these payoffs are highly weapons system and mission dependent and it is, therefore, necessary that the aircraft and missions selected for analysis be realistic. Finally, a formalization of the above process of controls development is required.



## II. CONTROL REQUIREMENTS

### Introduction

Advanced propulsion systems operating at or near design limits require precision control of speed, pressure, temperature, and airflow to attain maximum performance while maintaining engine durability. An accurate and reliable control system is required to ensure optimal engine performance and operational stability throughout the flight envelope. The control system must respond to pilot commands within the constraints imposed by airframe requirements and critical engine parameters and provide total engine control over the full range of operation. Mission, airframe, and engine requirements are combined to generate control criteria which, although they may differ in details for various missions, aircraft, and propulsion systems, will comprise the same general characteristics. The control requirements can be broken into three major categories: (1) performance, (2) engine life, and (3) operability.

The high concern for aircraft performance has placed the major emphasis in engine and control design on performance and operability in most existing engines. The extreme operating conditions obtained on today's engines to achieve the required high levels of performance have extracted a high penalty in engine life and some degradation in operability. Therefore this program was initiated to develop a methodology and criteria for evaluating various control systems by performing trades between engine life, performance and operability. The control requirements are presented here under these three categories to facilitate the trade studies in later tasks. Also, to permit meaningful trade studies, a distinction between hard requirements and goals is made. In this context, all systems considered in a trade study must meet the requirements and the trade-offs will be made on how well each system approaches the goals.

## Derivation of Requirements

The control requirements are often taken from MIL-SPEC 5007D. This has led to control systems that were overdesigned in some areas and underdesigned in others when applied to a specific engine/aircraft/mission environment. In this program the MIL SPEC was used as a guide in determining the 680-B1 control requirements. Each item was evaluated with respect to engine/aircraft/mission requirements and appropriate values established. In those cases where no realistic requirement could be established, the MIL SPEC was treated as a goal.

The control requirements must be generated through a "top down" analysis of mission (weapon systems), aircraft, and engine requirements. Mission requirements were examined first to determine

- 1) engine operating envelope
- 2) critical power points
- 3) critical SFC points (cruise and loiter)
- 4) turning rates
- 5) climb rates

Some of the above data is used in the engine design and sizing. The control can not compromise these points if the engine is sized properly (not overdesigned). Other mission requirements affect excess power and possibly acceleration times which can be reflected into the control requirements. Finally, mission related items like envelope (Reynolds number), turning rates (distortion), and power requirements (after burning light-off) have a major affect on control operability requirements.

Next, the aircraft requirements and capabilities were investigated, the latter often being emphasized unless the airframer is willing to allow the control to limit the aircraft performance. Generally, the engine is sized at a few critical points like static sea level (S.S.L.) for take-off, a cruise condition

and a combat point, and the engine/aircraft combination dictates the capabilities for the remainder of the mission envelope. The aircraft capabilities generally exceed the mission requirements. Thus, it is important to justify aircraft requirements (often really desired capabilities) with specific mission requirements to prevent undue requirements from being placed on the engine and control system.

Discussions were held with airframers on control requirements. A majority of the discussions were held with McAir, a subcontractor on this project, who acknowledged that it was difficult to determine actual engine and control requirements and most discussions were centered on present performance rather than hard requirements. Thus, aircraft requirements will generally be treated as goals rather than hard requirements.

Finally, the control requirements must reflect the engine related requirements in the areas of start up, engine stability, engine protection, and engine life.

One main theme continued to surface during the review of the control requirements with the engine project manager. Increased engine life is a prime consideration of the 680-B1 engine and the baseline control requirements were oriented toward performance. The control should put considerable emphasis on accurate control of engine life critical parameters while achieving important thrust and SFC performance goals. Thus, the overall scope of this program has become an integral part of the engine/control system design.

As a starting point, the baseline requirements were generated from TF41, GMA200 ATEGG, and GMA 200 JTDE control development experience. In addition, the control requirements for the F100 multivariable control design (Technical Report AFAPL-TR-76-74) were reviewed as representative of today's supersonic engine control requirements. A preliminary review held within DDA was concerned mainly with establishing all the design constraints of the engine and questioning performance criteria. Then, a review of the controls requirements was held with McAir to define the critical criteria with respect to the air-

craft and establish realistic performance requirements. This was followed by review by AFAPL personnel to interject a wider background in supersonic engine control criteria based upon actual experience. The following requirements are the result of several iterations between the above parties and reflect the requirements and goals for the 680-B1 engine in the areas of

- o Performance
- o Stability
- o Life

at the beginning of Task III of this program.

#### Performance Requirements

The engine/control performance requirements spelled out in MIL-Spec 5007D include

- Control linearity
- Control repeatability
- Acceleration response time
- Deceleration response time

Since none of these requirements could be quantified based upon mission or engine requirements, they were discussed extensively with McAir and Air Force personnel.

#### Control Linearity

The linearity and repeatability requirements are subjective to the pilots "feel of the aircraft" and represent a "goodness" rather than a hard requirement. However, these factors cannot be ignored for many unsubstantiated control removals are due to a pilots "poor handling" complaints that affect reliability and cost. The only real requirement is that the control cannot have

any thrust discontinuities as a function of pilot input (PLA) and thrust must increase monotonically with PLA. The following goals have been established.

Thrust Modulation -- The relationship between thrust and power lever should be linear within +2% without discontinuities.

Repeatability -- Stabilized thrust at any power lever position should be repeatable.

### Transient Response

McAair admitted that it was difficult to determine actual transient response requirements and thus the discussions addressed present performance rather than hard requirements. The following goals were derived from the meeting.

- o Idle to MIL (Military or Maximum Thrust): 4 seconds
- o 15% IRP (Intermediate Rated Power) to MIL: 3.3 seconds
- o 35% IRP to MIL: 2.2 seconds
- o At 15% IRP a 5% thrust change should be achieved in 0.3 sec.  
a 10% thrust change should be achieved in 0.6 sec.
- o At 35% IRP a 5% change should be achieved in 0.25 sec.  
a 10% change should be achieved in 0.30 sec.  
a 15% change should be achieved in 0.50 sec.

(No engine today meets all of these although the J79 (F4), F100 (F15) and F404 (F18) propulsion systems meet various parts of the requirements).

The above goals are for standard static sea level conditions and specify the time required to achieve 95% of the thrust change. Stable steady-state values should be achieved in an additional 10 sec. Additional assumptions are no customer bleed, no anti-ice, and no customer horsepower extraction. The MIL SPEC will be used to extrapolate the above goals to other flight conditions. Included are an additional 7 seconds for the idle to intermediate response for

conditions above 10,000 feet and a twenty-five percent increase in response time for non-standard day, bleeds, horsepower, extraction, and inlet distortion. Maximum customer bleeds and horsepower extraction are given in Figure 1. Additional goals include:

Thrust Response -- For increases or decreases in power lever angle, engine thrust must be a monotonically increasing or decreasing function of time, respectively.

Control Overshoots -- The maximum overshoot on speed and temperature shall be

$N_H$  overshoot less than 2%

$T_3$  overshoot less than 5%

$T_{4.1}$  overshoot less than 5%

As a goal, there will be no undershoot on thrust, speed, or temperature on a decel to idle. (It will be shown later that undershoots have a minimal effect on life consumption. From an aircraft handling point of view, overshoots are not undesirable.)

#### Additional Aircraft Related Requirements

The discussion with McAir revealed two other performance goals which are

- o Idle thrust should not exceed 2 percent of minimum aircraft weight. The F15 without stores and landing fuel load taxies at 80 to 100 MPH. The pilots find it "sporty" and it wears out brakes and tires.
- o Current engines do not operate well at non standard day conditions. McAir believes that propulsion companies design them for standard day, test cell operation and not for use in airplanes. The 680-B1 control

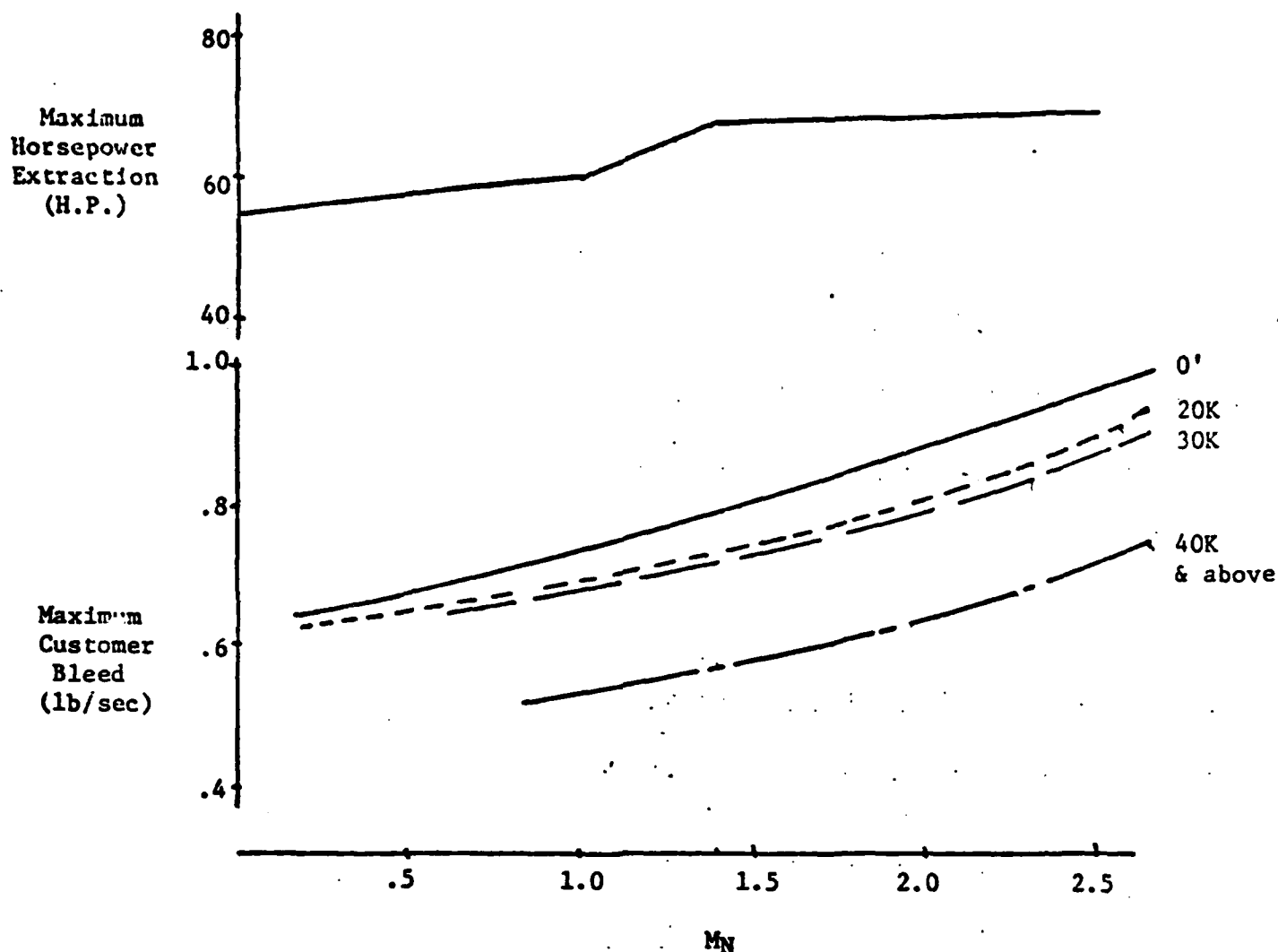


Figure 1. Maximum customer bleeds and horsepower extraction.

designs must address non standard day conditions and distortion. The real world tends to be hotter than Inlet Standard Air (ISA) below 40K' and colder than ISA above 40K'.

- o Selectable control modes such as cruise and combat are desirable.
- o Additional engine handling qualities required of today's aircraft include

No surge  
Air start capability  
Distortion tolerance  
No loss of handling quality with engine deterioration

The last point deals with the broad area of control system trim. The typical variations due to build tolerances and deterioration of performance are summarized below.

<u>Parameter</u>	<u>Variation</u>	
Compressor efficiency	+2%	-2%
Compressor flow	+1%	-3%
Compressor pressure ratio	+4%	-4%
Turbine efficiency	+2%	-2%
Turbine flow	+2%	-1%
Burner pressure drop	+1%	-1%

#### Engine Fluctuations

Under steady-state operating conditions between idle and maximum continuous thrust, engine thrust fluctuations must not exceed +1 percent of intermediate thrust or +5% of the thrust available at the power lever position and flight condition, whichever is less. During engine transients, the variation of engine airflow from the corresponding steady-state values of the power setting selected must not cause propulsion system instability (The Inlet Airflow Corridor is needed to quantify this requirement).

#### Combustion Stability

The following control requirements are tied directly to the efficient operation of the burner

- o The minimum fuel-air-ratio (F/A) to support steady state combustion shall be (.002) and the minimum burner pressure is 10 psia.



- o Flow control shall direct fuel to pilot burners until  $F/A = .025$  is reached. It then directs fuel also to the main fuel burners while maintaining .025 in the pilot stage. After main burner stage  $F/A$  reaches .025, main and pilot fuel flow is maintained equal.

### Life Requirements

There are four basic areas of the control requirements that have a great effect on engine life. These are

- o Engine limits
- o Life utilization
- o Reliability
- o Engine stability

#### Engine Limits

There are two different levels of limiting for most engine parameters that must be observed to protect the engine. The lowest level is usually the steady-state maximum (or minimum) value used to evaluate overall engine life. Exceeding these steady-state values will reduce engine life. The second limit is the maximum (or minimum) value the parameter may obtain during a transient. This relaxing of engine protection during the transient occurs for such a brief period that it generally has minimal effect on engine life. Most of these limits occur at maximum power. The variable geometry allows the engine to satisfy many of these limits simultaneously at maximum power, making the control at maximum power the single most challenging control problem.

Maximum engine parameter values that must not be exceeded to ensure adequate protection of the engine are described in the following paragraphs. These limits are hard requirements.

## Temperature Limits

The actual temperatures that must be maintained within limits to protect the engine are TBT (turbine blade metal temperature),  $T_{noz}$  (nozzle skin temperature),  $T_3$  (compressor discharge temperature), and  $T_4$  (turbine rotor inlet gas temperature). The  $T_3$  limit is based on titanium temperature limits. The RIT (rotor inlet temperature) limit is based on a maximum allowable turbine vane metal temperature and turbine life considerations. The steady state limits based upon engine life considerations are

TBT max	=	1660°F
$T_{noz}$ max	=	1800°F
$T_3$ max	=	(classified)
$T_4$ max	=	(classified)

Simulations and analyses are used to correlate measurable gas stream temperatures with unmeasurable limiting temperatures. Normally, the gas temperature is allowed to exceed the maximum value for a very short period of time because of the thermal lag between gas stream temperature and metal temperature. The maximum transient values for  $T_3$  and  $T_4$  (amount and time) are

$T_3$  may exceed the steady state maximum by 50°F for less than 0.5 seconds.

$T_4$  may exceed the steady state maximum by 60°F for less than 0.3 seconds.

In addition, there are absolute maximums for the metal temperatures that, if exceeded, will destroy the engine. These are

TBT limit = 2000°F (Lamilloy unbonding)

$T_{noz}$  limit = 2000°F (Lamilloy unbonding)

### Inlet Airflow Corridor

The area of aircraft inlet and engine compatibility is dependent on the selection of a specified aircraft/inlet configuration. Although a supercruiser aircraft has been selected as the prime candidate for the 680-B1, the present DDA models assume a "perfect" inlet with no spillage drag -- only ram recovery.

Specific inlet information for this type of future aircraft was unobtainable for this project. DDA has a McAir FX type inlet simulation which produces an air flow corridor, ram recovery, and drag as a function inlet capture area and pre-programmed inlet geometry. The correct approach to defining the proper inlet for the aircraft and engine would be an iteration between parametric engine and inlet simulations with both inlet parameters and engine cycle or operating line as variables to maximize thrust in the critical regions of the flight envelope.

The output of the design would be a schedule of inlet capture area and inlet geometry to optimize installed thrust. The operating line of the engine would also most likely be redefined in this study. With the aircraft and inlet design in hand, the engine inlet distortion profiles can be generated for various aircraft maneuvers and flight conditions.

However, such an inlet design is outside the scope of this program or the GMA400 ATEGG program and an alternate approach was taken. A communications link between the inlet and engine controls was assumed. This allows the inlet to know the engine airflow requirements and "optimize" the inlet capture area rather than scheduling the area. The existing internal ramp schedules were used in computing ram recovery and drag losses since "optimizing" these schedules was outside the scope of this project. This produced the inlet airflow corridor shown in Figure 2 in which an arbitrary buzz limit was imposed for this study since no real inlet data exists.

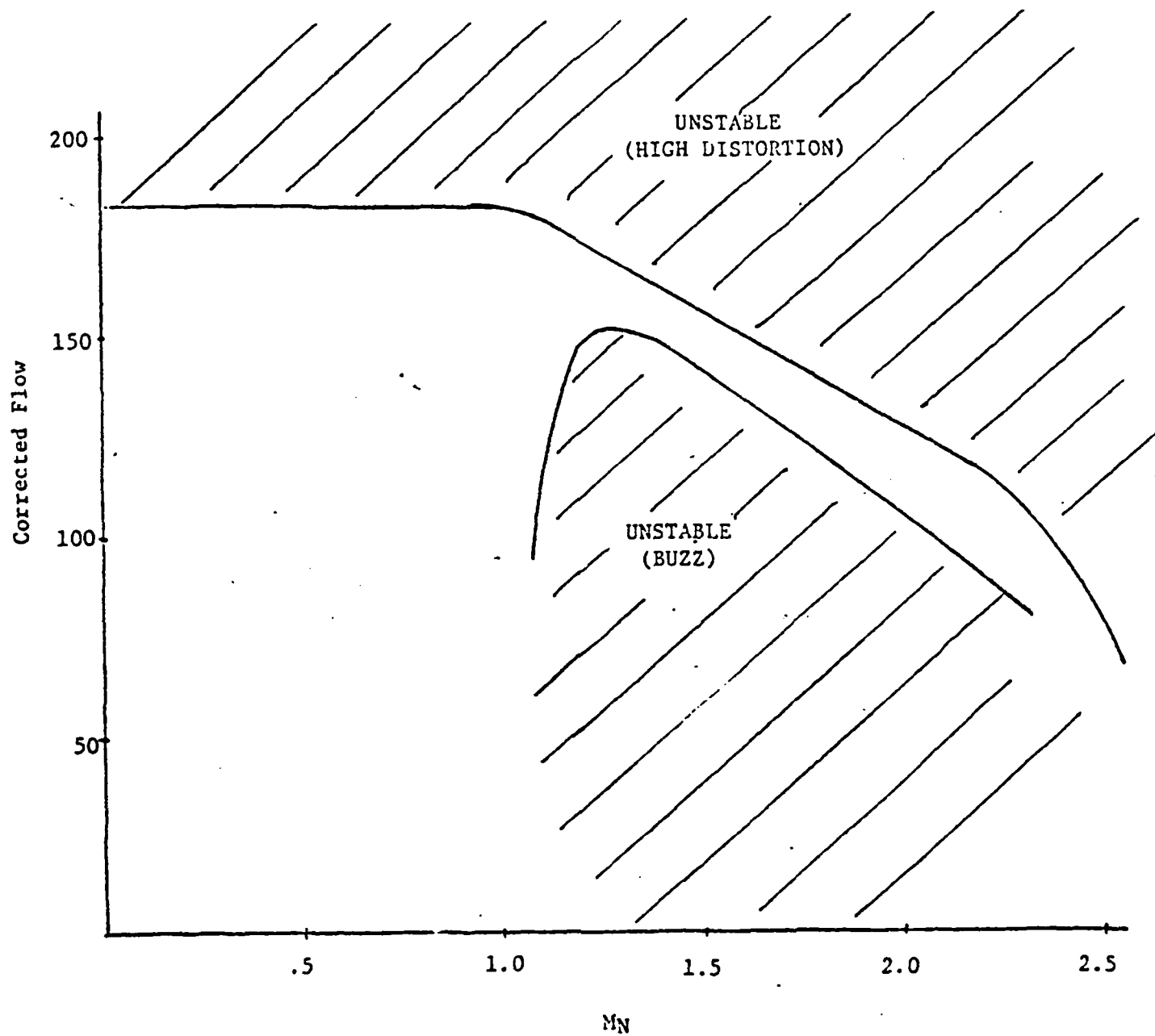


Figure 2. Inlet airflow corridor.

### Distortion Tolerance

The variable cycle engine affords the control designer many tools to shift the operating line of the engine and provide additional surge margin for the compressor during accelerations and in the face of inlet distortion. From the controls standpoint, the distortion problem can be divided into two categories based upon bandwidth of the control system required to accommodate distortion. In general, a very high bandwidth (fast response) control system is required to compensate for distortion. A four year funded program to study distortion in the 680-B1 high flow through compressor is now underway and will help define the response requirements. However, work on a fixed compressor indicates a bandwidth greater than 10 cycles is required to compensate for distortion detected at the inlet.

In some cases, when it is possible to predict slowly varying distortion, such as with aircraft maneuvers, a much slower control system will work adequately because of the lead introduced by the prediction. The control for the 620-B1 will compensate for predictable distortion. The distortion data from the 5 stage high flow through compressor rig tests in late 1979 will be used in the control design along with available test data from an existing supersonic inlet for the Mach 2.0 to 2.5 range. This data consists of a 90 degree and a 180 degree distortion pattern (Realistic patterns will not be available until approximately 2 years into the 4 year program).

### Engine Stability

The minimum steady-state compressor surge margin should be 20 percent for a nominal engine and control, and surge margins should not be less than 10 percent during transients. The actual requirements may be adjusted to reflect the confidence in the engine model (i.e., the limits may be lowered as the model is adjusted to reflect rig test data or actual engine performance). At this point, hard requirements are a minimum steady state surge margin of 10 percent and a minimum transient surge margin of 5 percent.

In addition compressor variable geometry must be scheduled to avoid any flutter region of the compressor. No flutter regions for the 680-B1 compressor have been identified after two rig tests of "similar" high flow compressors.

#### Failure Accommodation

The electronic engine control must automatically provide safe operation of the engine in the event of any single control element failure. Actuators must fail to a safe-operating position to the maximum possible extent (obviously impossible for all failure modes). In the case of a sensor failure, the control will provide an alternate control mode (including scheduled geometry positions or fixed geometry) or utilize a synthesized signal. In the case of a computer failure (except single I/O channels), or multiple failures, the control will either shut the engine down (test stand or multi-engine aircraft) or revert control to a back-up (electronic or hydromechanical) control. I/O channel failures will be considered the same as sensor or actuator failures.

Range and Rate checks will be performed on all I/O data for reasonableness to determine failures. Error counters for each signal will be maintained and a failure indicated to the control logic when a preset error count is exceeded. Test routines for the CPU, memory sum check, and I/O wrap-around will be run at a slower rate than the basic logic cycle and appropriate failures indicated to the control logic. The control logic will continuously monitor the failure indicators on each control logic cycle and make the necessary control adjustments specified above.

### III. MISSIONS

The primary mission for the 680-B1 engine is the supercruiser mission as presented in the proposal and updated by Boeing (Mach Number on the supercruiser leg changes slightly). The secondary mission for this study is the "deep strike" mission as described in the proposal. A supercruiser training mission was developed by DDA based upon current training missions for supersonic aircraft. The combination of the supercruiser mission, deep strike mission, and a realistic training mission will provide a good cross-section of the life-usage expected for the 680-B1 engine. These stick missions are described below.

#### Stick Missions

##### High Altitude Attack Mission

The high-altitude attack mission selected has a total nominal mission radius of 550 nautical miles, which is compatible with a 51,000 lb aircraft and the 22,900 lb thrust engine. The actual range depends on the control mode. The ratio of the subsonic cruise leg to the supersonic cruise leg will be approximately 2:1. The supersonic maximum thrust combat turn is considered in combination with the outbound dash and is altitude optimized for minimum fuel. The air-to-ground stores are expended during the turn. A supersonic dash Mach Number of 2.0 is considered typical for the time period and mission. A description of the mission is given in Table I.

##### Boeing Supercruiser Mission

The supercruiser mission is similar to the high-altitude attack mission. The total mission radius will be nominally 555 nautical miles, consistent with 47,000 lb aircraft with 21,200 lb thrust engine. The precise baseline mission range will be determined by the simulation program for the given control mode.

Table I. High Altitude Attack Mission

<u>CONDITION</u>	<u>TIME</u> (Min)	<u>ALT.</u> (K FT.)	<u>MN.</u>	<u>POWER</u> <u>SETTING</u> (PCT)
Idle	15.0	0	0	6
T.O.	.2	0	0-.25	100
Accel	5.2	0	.25-.85	100
Climb	1.1	0-33	.85	100
Cruise	38.4	34	.85	24
Accel & Climb	1.7	30-36	.85-2.0	100
Dash Out	10.5	50	2.0	62
Combat-Turn	4.5	50	2.0	100
Dash In	10.5	60	2.0	66
Cruise	43.1	42	.85	22
Loiter	<u>20.</u>	0	.85	7
150.2 Min				

Both the dash-out and dash-return Mach numbers are 2.2, representative of the mission and the time period. The dash-out and combat turn are altitude optimized for minimum fuel. Combat is at 64,000 ft and all air-to-ground stores are expended during the turn maneuver. Both missions have a 20-minute loiter capability at the end and a 5 percent fuel allowance. A description of the mission is given in Table II.

Table II. Boeing Supercruiser Mission

<u>CONDITION</u>	<u>TIME</u> (Min)	<u>ALT.</u> (K FT.)	<u>MN.</u>	<u>POWER</u> <u>SETTING</u> (PCT)
Idle	15	0	0	6
T.O.	.18	0	0- .22	100
Accel.-Climb	3.9	0-62	.25-2.2	100
Cruise Out	24.3	62-64	2.2	75
Combat	3.2	64	2.2	100
Cruise In	26.3	64-70	2.2	38
Loiter	<u>20.0</u>	0	.4	8
92.88 Min.				



### Training Mission

One of the noncombat training missions being developed for the turbine life usage program is a composite profile of TF41-A-1 flight operations and has proportional segments related to the different missions flown by the A-7D aircraft. The total cycle is 1 hour and 40 minutes long, which is representative of the average A-7D mission length. The length of each segment of the mission represents the percentage of time the average TF41 is exposed to that segment. The cycle contains only training segments-combat and maintenance-related activities are not included. The cycle has the following percentage breakdown:

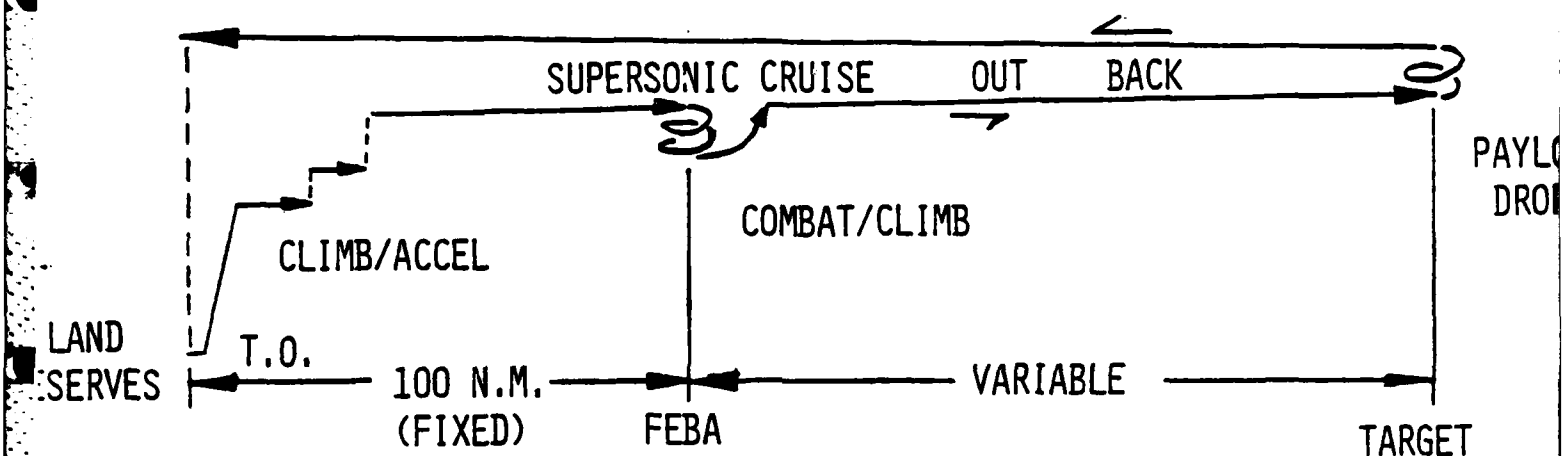
Takeoff	2
Climb	8
Medium cruise	18
Low-level cruise	22
Ground attack	25
Air-to-air	8
Descent	10
Traffic pattern	<u>7</u>
	100%

### Air-to-Air Combat

A combat phase was added to the high altitude attack and supercruiser missions to add realism to these missions. The supersonic dash in the Boeing mission was reduced to Mach 2.0 to be compatible with the other mission. The new supercruiser mission is shown in Figure 3. In addition to adding realism, the max g turns yield maximum data for distortion studies. They also increase the range of engine operation during the missions to make them more sensitive to control variations in evaluating future life conserving modes.

A large number of peacetime missions for current supersonic aircraft were studied to derive the above training mission. This information was integrated into the TF41 training mission to produce a realistic training mission for a

MISSION SHOWN: SUPERSONIC PENETRATOR (DESIGN MISSION)



- MISSION FEATURES:
- o START WITH FULL INTERNAL FUEL
  - o 15 MINUTE TAXI/WARMUP
  - o CRUISE AT CONSTANT SUPERSONIC MACH NUMBER AT BEST ALTITUDE FOR MAX RANGE
  - o 5000 LB PAYLOAD
  - o 20 MINUTE LOITER BEFORE LANDING
  - o 5% MISSION FUEL RESERVE

Figure 3. Typical wartime mission.

supersonic aircraft. However, no supersonic flight is included since present restrictions on supersonic training have reduced such flights to less than 1% of training hours. The peacetime training mission developed for this study is shown in Figure 4.

### Realistic Throttle Histories

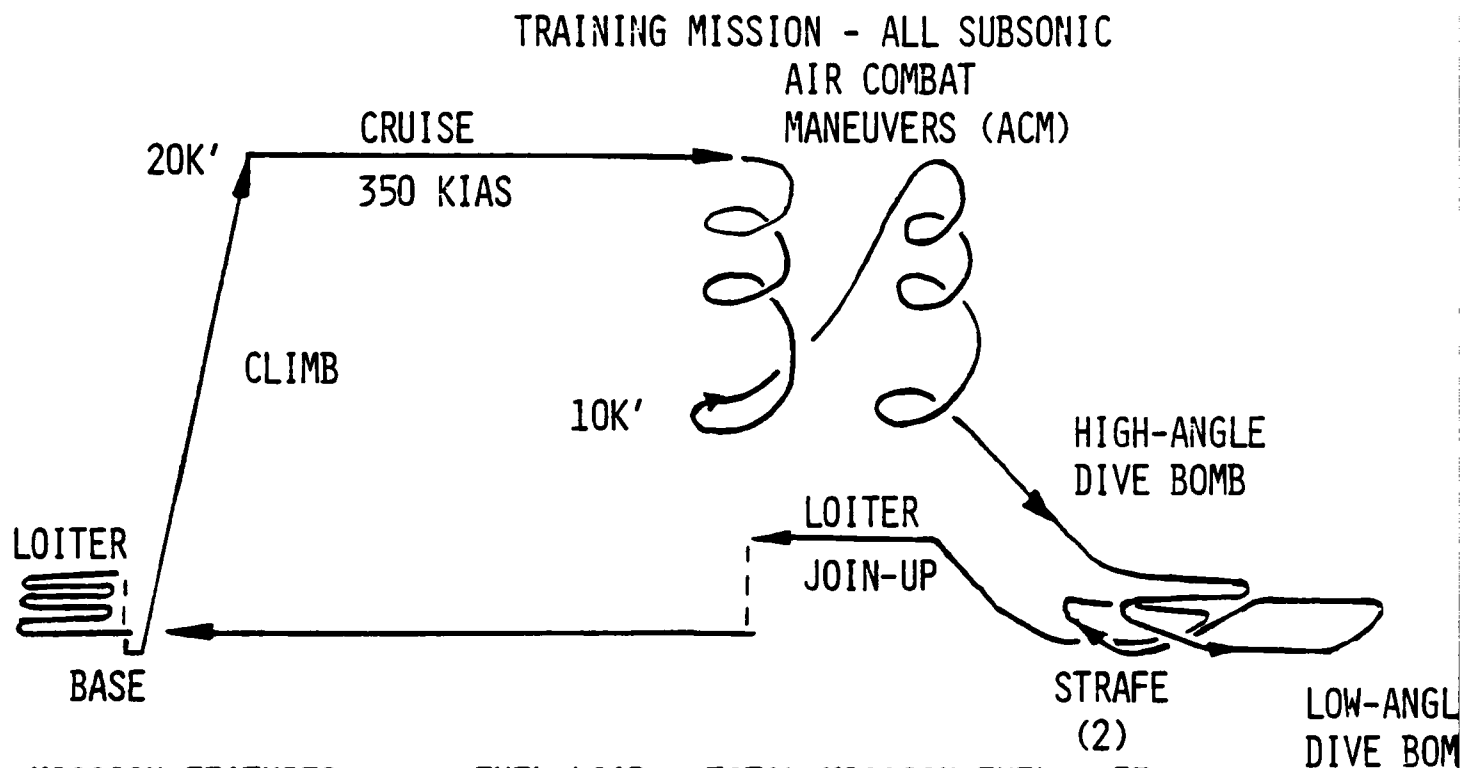
A final degree of realism was added to the mission by superimposing pilot "throttling jockeying" on top of the stick missions. Two data sources were used to derive realistic throttle movements.

### TF41 Data

DDA presently has data from 25 real TF41 missions including leaders and wingmen. After examining the available continuously recorded A-7E/TF41-A-2 Inflight Engine Condition Monitoring System (IECMS) data, eleven of the available 25 flights were selected for use in the life usage program. Selection was based on applicability and continuous recording quality. The eleven missions were a mix of A-7E mission types shown in the table below.

<u>Mission Type</u>	<u>No. of Mission Records</u>
Air Combat	2
Formation Leader	1
Strike-Bomb	4
Check Flight	2
Carrier Qual.	2

Each mission record has been segmented into types of operation to provide a "Dynamic segment library" of data which can be drawn on to enhance any conceptual stick mission on a segment by segment basis. Dynamic enhancement exists for the following mission segments.



MISSION FEATURES:

- o FUEL LOAD = TOTAL MISSION FUEL + 5%
- o 15 MINUTE TAXI/WARMUP
- o MANUAL CRUISES, CONSTANT KIAS, ALTITUDE
- o DISTANCE TO WEAPONS RANGE 100 N.M.
- o 2000 LB PAYLOAD (2 - 1000 LB DROPS)
- o 20 - 30 MINUTES OVER WEAPONS RANGE
- o 20 MINUTE LOITER BEFORE LANDING

Figure 4. Typical training mission.

Combat  
Descent  
Landing  
Manual Cruise  
Taxi

Four mission segments are presumed locked throttle at some constant power, they are: ACCEL, CLIMB, CLIMB/ACCEL, TAKEOFF. An additional flight segment which is presumed to have no throttle dynamics is a cruise segment at speeds above Mach 1. Nearly without exception supersonic flight is subject to automation with the engine and airframe controlled jointly by autopilot to maintain a cruise speed and heading (this generally produces a different type of throttle motion for which no data was available at DDA).

An additional modification is the superposition of throttle chops during maneuver or combat situations. Examination of A-7E gunnery range and air combat thrust transients and vehicle most movements showed that chops to low part-power operation were common and likely used to quickly decelerate or change aircraft heading -- either for range convenience or combat survival. Because the thrust/weight ratio of the A-7E/TF41-A-2 is quite low, the IECMS dynamics could not be relied on to provide throttle chop simulation of a more vigorous airplane. However, some limited data were available from the F-14 and F-15 aircraft which provided guidance (see Figure 5 - flight simulation data supplied by McAir). The chops which were inserted into the mission consist of reduction to 20 percent max power for a 10 second duration and a throttle slam to the next power requirement. They have been added at 90 - 180 or 360 degree increments of combat turns and at the beginning of a gunnery range pass. Usually the number and interval between throttle chops is qualitatively determined by examination of flight data for similar maneuvers and/or judgment concerning the pilots environment and stress.

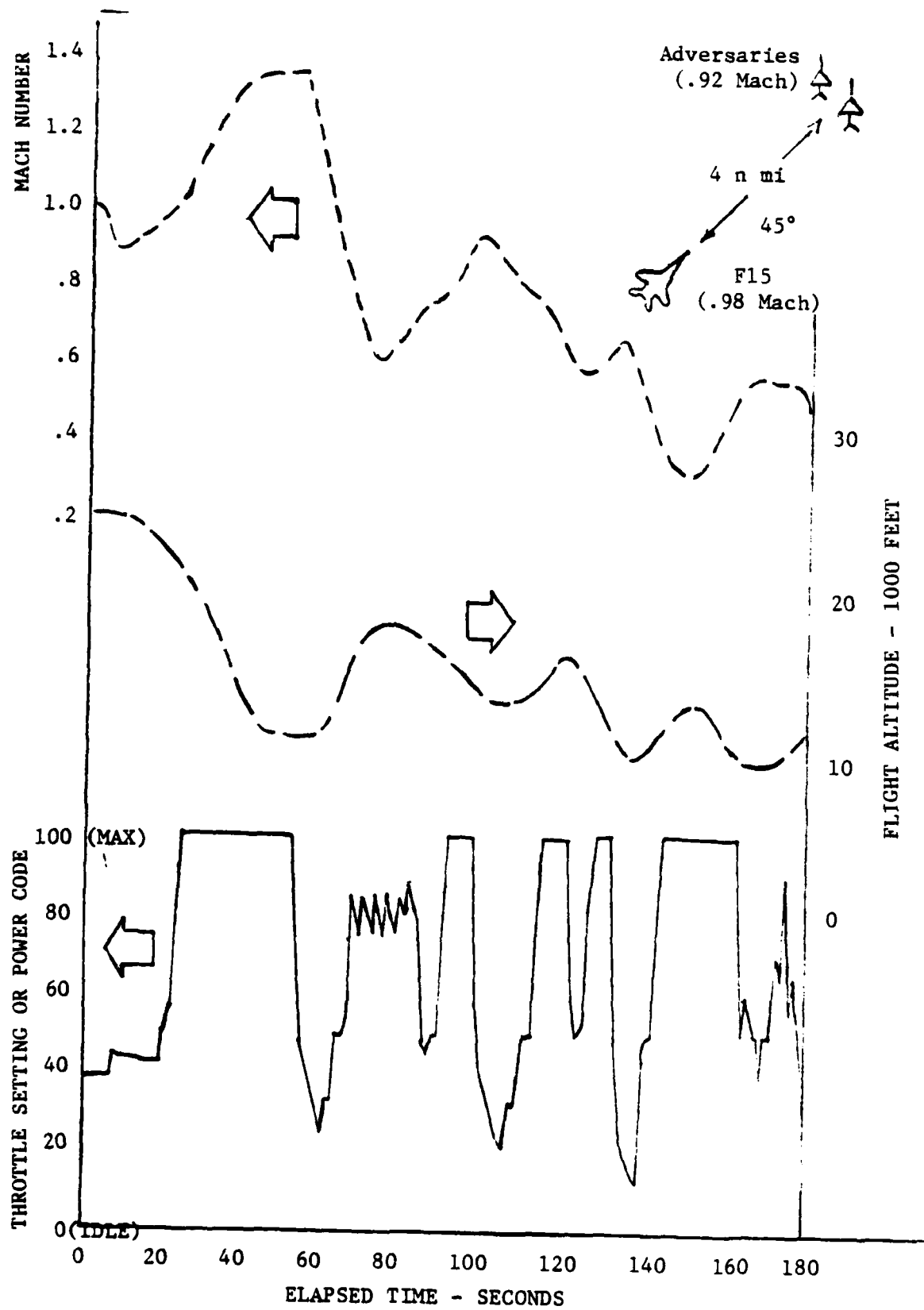
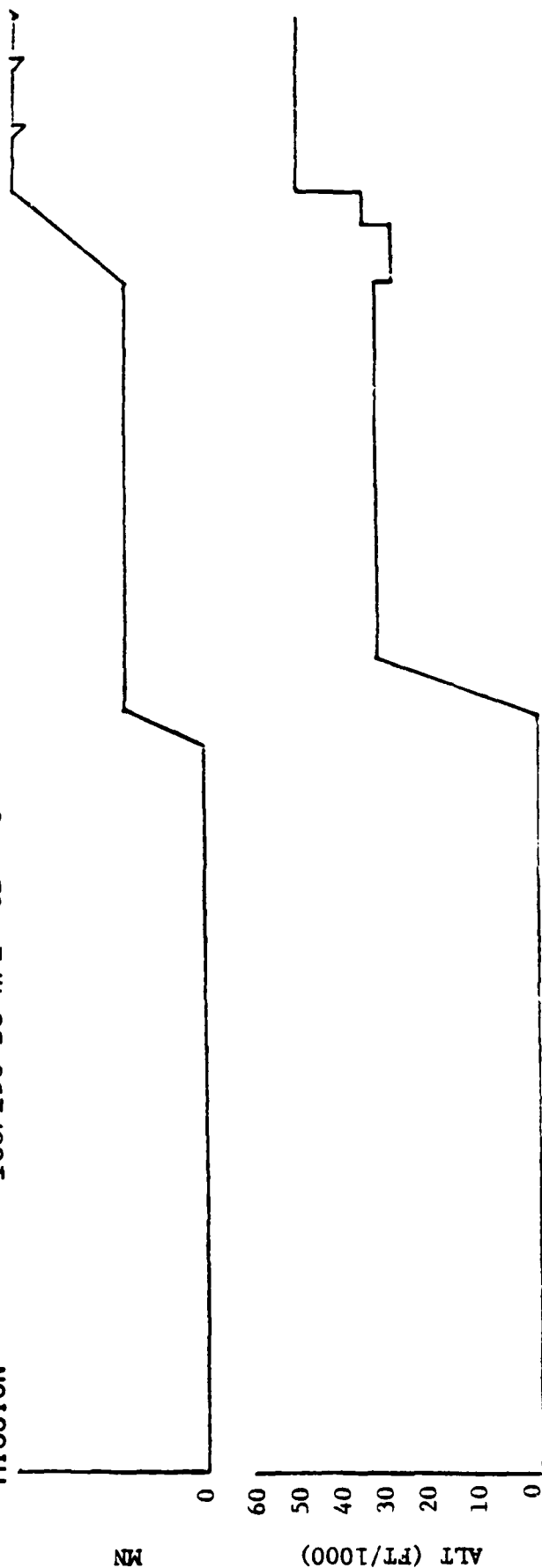


Figure 5. Sample combat history.

### Enhanced Missions

A computer plot of a mission histogram which has been dynamically enhanced using the rationale just described is shown in Figure 6. All of the enhancement features discussed can be observed in the FN (PCT) (percent maximum thrust) trace of the figure. The combat and turn segments have employed both IECMS throttle dynamics and input throttle chops to enhance their dynamic contribution to utilization of LCF life.

MISSION = 100/150 DS W/2 CB + C



26

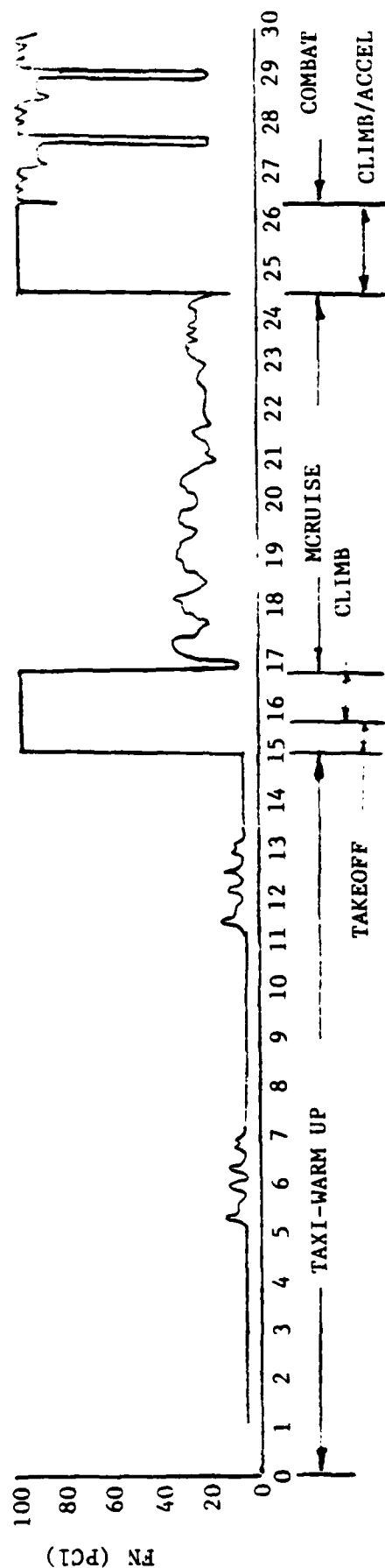


Figure 6. Combat simulation profile.



MISSION = 100/150 DS W/2 CB + C

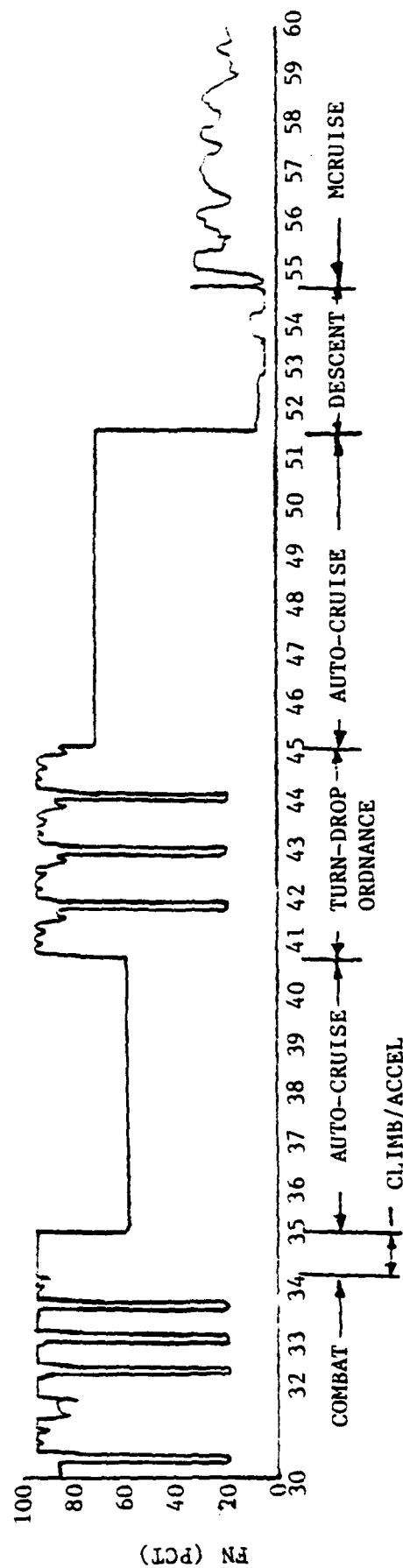
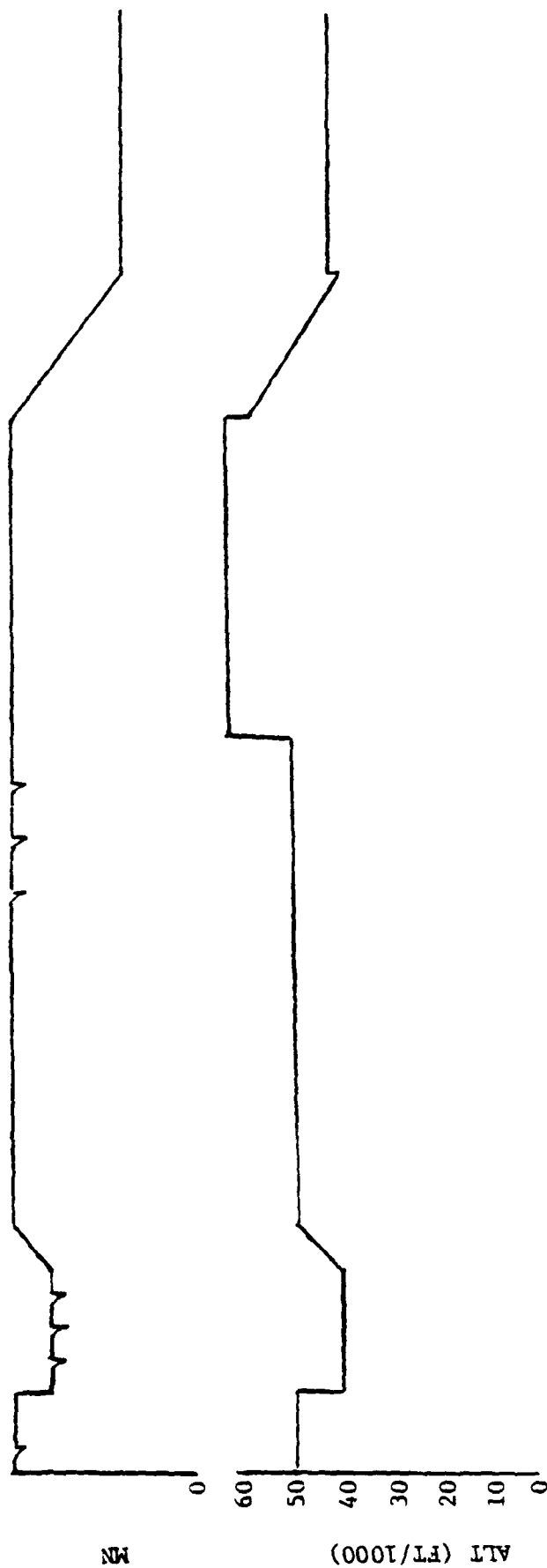


Figure 6. Combat simulation profile (continued)

MISSION = 100/150 DS W/2 CB + C

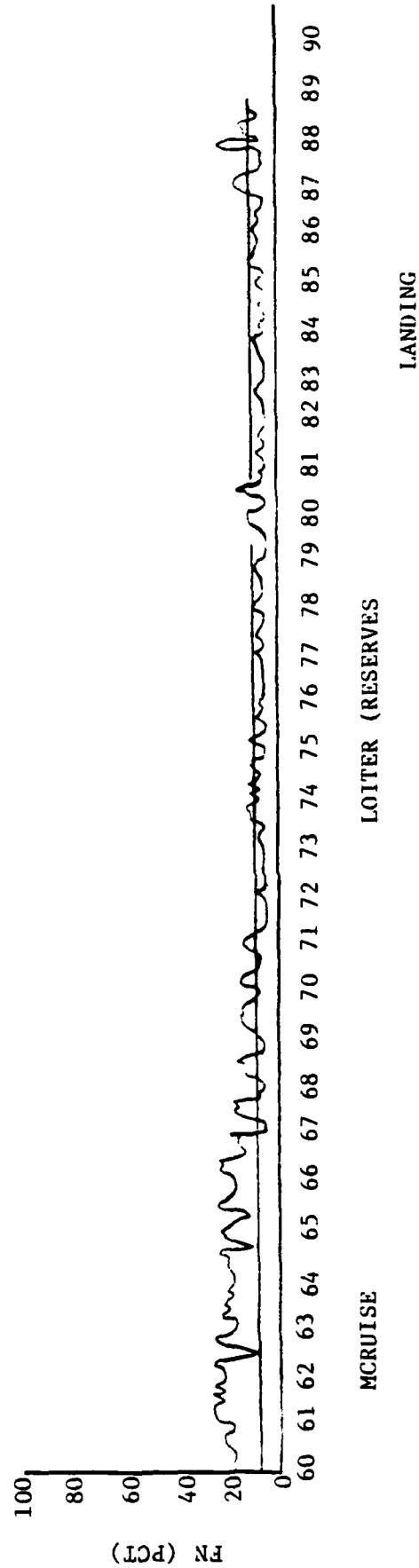
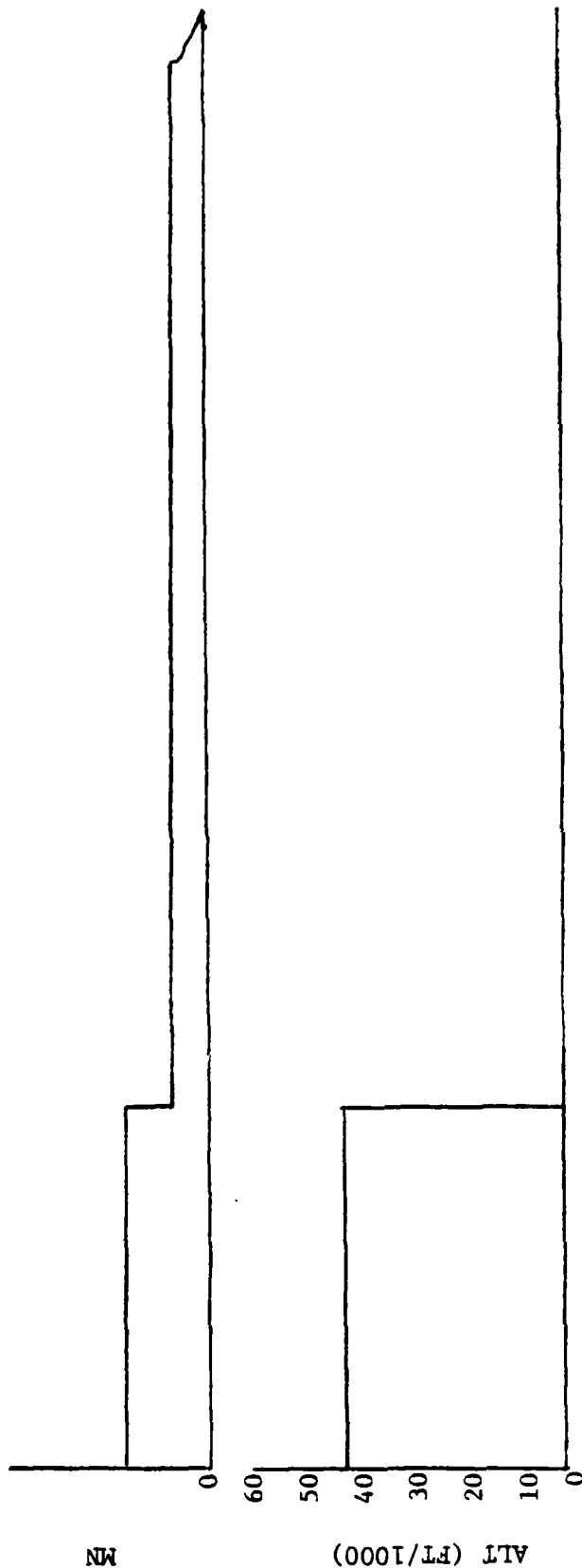


Figure 6. Combat simulation profile (continued).

#### IV. ENGINE AND CONTROL SYSTEM DESCRIPTION

##### Engine Description

The 680-B1 engine used in this program is an advanced high temperature turbojet VCE envisioned for the late 1980's as a derivative of the DDA GMA 400 ATEGG gas generator. The 680-B1 is a single spool, variable geometry, high through-flow dry turbojet with high "temperature augmentation" providing the performance of an after-burning turbojet.

The compressor is a six-stage, high-flow compressor with all vanes variable (including IGV's). The combustor consists of a vortex controlled diffuser (VCD), a Lamilloy\* combustor liner, and two "zones" of fuel nozzles. The single-stage turbine has variable vanes and modulated cooling air to the Lamilloy turbine blades. Modulated cooling air is also supplied to the other Lamilloy structures in the aft section. Exhaust gas exits through a variable area convergent-divergent (CD) nozzle.

##### Control Description

A digitally implemented control system was selected for the 680-B1 engine based upon complexity of the control problem and the versatility of the digital controller. The general system configuration is shown in Figure 7. The hardware can be broken down into the following categories and items:

- (1) Digital Controller
- (2) Fuel System
  - Pump
  - Metering Valve
  - Flow Splitter
  - Main Fuel Shut-off Valve

---

\*Lamilloy is a registered G.M. trademark.



(3) Actuators

- Compressor Geometry
- Turbine Geometry
- Turbine Blade cooling modulation
- Aft cooling modulation
- Nozzle

(4) Control Feedback

- Fuel flow and fuel split
- Cooling bleed positions
- Compressor geometry position
- Turbine geometry position
- Nozzle geometry position

(5) Engine Sensors

- Inlet temperature
- Inlet total pressure
- Inlet static pressure
- Compressor discharge temperature
- Compressor discharge static pressure
- Turbine discharge total pressure
- Turbine exit temperature
- Nozzle metal temperature
- Nozzle total pressure
- Turbine blade metal temperature
- Speed Sensors

(6) Electrical System

- PMG
- Exciters
- Igniters
- Wiring harnesses

These items will now be discussed in detail as currently defined for the 680-B1.

## Digital Controller

The GMA400 will have a new state-of-the-art digital controller based upon microprocessor technology. The digital controller receives information from the aircraft data systems, engine sensors, control sensors, and the inlet, computes the specified control logic, and issues commands to the control actuators and other special systems as shown in Figure 7. In addition, the controller monitors its own condition and automatically switches to a parallel hydromechanical back-up control when a failure is detected. The controller also monitors the condition of the engine and other control components and takes the appropriate action specified in the control logic when an abnormality is detected. The details of the computer are not important to this project since no attempt will be made to simulate computer characteristics such as I/O quantization, computational accuracy, or data skew in the dynamic control digital simulation.

## Fuel System

The 680-B1 will have a new TRW pump and Woodward metering system. The fuel pump and control assembly will have the fuel flow capacity of 42,000 PPH max. The fuel pump/control assembly consists of 1) an inducer element which keeps the main centrifugal element filled with fuel at all inlet pressure conditions, 2) a retracting vane starting pump, 3) a high pressure centrifugal impeller surrounded by a free wheeling rotating diffuser to reduce drag friction, and 4) a pressure drop type metering control which consists of a metering valve, torque motor operated fuel servo, throttling valve, and pressurizing valve.

The metering valve control assembly will be built by Woodward Governor, Rockford, Illinois and supplied to TRW where the combined fuel pump/control assembly will be assembled and tested prior to being shipped to DDA. The metering control contains a torque motor which uses a signal from the digital electronic control to operate a fuel servo valve which in turn positions a rotary fuel metering valve. The fuel metering valve controls the amount of

fuel going to the engine. Downstream of the metering valve is a throttling valve whose function is to control the pressure drop across the metering valve to a fixed value. Since fuel flow is a function of metering valve area and its pressure drop, fuel flow to the engine is controlled directly by the electrical signal to the torque motor servo. Throttle valve position is determined by a spring and a regulated fuel pressure which is generated by a differential pressure sensor which measures pressure drop across the metering valve. A pressurizing valve is located downstream of the throttle at the control exit. Its function is to maintain a more nearly uniform gain over the flow range.

The 680-B1 will also have an integral flow divider and shut-off valve. The present conceptual design requires the digital controller to calculate fuel-air ratio and to generate an electrical signal which is used in the flow divider to operate a fuel servo valve. The servo valve meters fuel to the main fuel nozzle system in order to maintain scheduled fuel-to-air ratios for the primary and main fuel nozzles over the flow range.

The flow divider also incorporates a main shut-off valve which prevents fuel from leaking from the pump/control assembly into the combustion chamber, collecting there and causing a hot start when the control metering valve is at the minimum flow stop setting. Its location near the fuel nozzles also minimizes fuel system fill time during starts. When the shut-off valve is closed, the main and primary fuel nozzles are purged of fuel and vented overboard via the nozzle and flow divider by means of combustion chamber gas pressure. The start valve is controlled by a solenoid operated fuel servo valve which is activated open (manifold drains closed) during a start and activated closed (mainfold drains open) during shutdown by a discrete signal.

#### Compressor Geometry Actuation System

The compressor vane actuation system will probably be a fuel powered hydraulic actuation system controlled on corrected speed by the digital controller

through an Electro-Hydraulic Servo Valve (EHSV) and a position transducer. A pair of hydraulic cylinders will actuate a bell crank system to each vane actuation ring, one per stage of variable vanes. LVDT's sense actuator travel and provide position feedback to the controller.

### Turbine Geometry Actuation System

The turbine actuation system was developed on a Navy contract to survive the high temperature environment of the GMA 200 JTDE. The turbine actuation system, shown in Figure 8, has a pneumatic motor which drives multiple planocentric actuators located around the periphery of the engine by means of a high speed flexible drive cable system. The actuators in turn position a synch ring. An electrical signal from the digital controller modulates the air supply to the motor to control the synch ring rotational rate and direction. Resolvers provide position feedback to the controller.

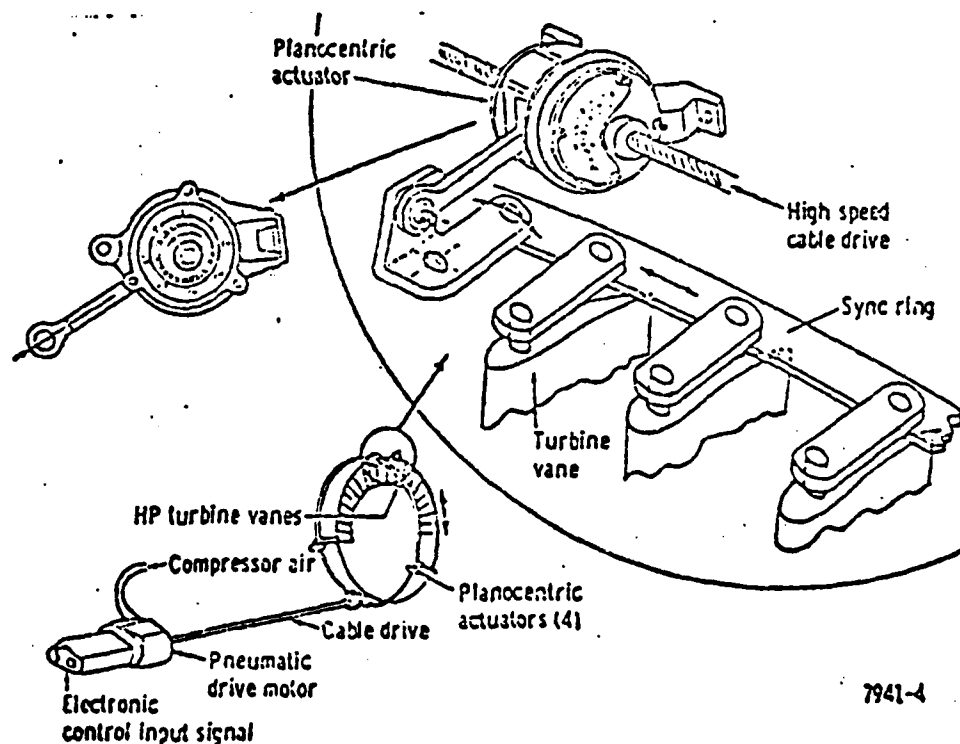


Figure 8. HPT actuation syste.



### Aft Section Cooling Modulation

This system will probably consist of a ring-valve similar to the LPT turbine "jet flap" control on the JTDE. An air motor and planocentric could be used here because the ring valve and planocentric drives would be in the rear support area (hot section) and the air motor in the compressor section similar to the HPT arrangement.

### Nozzle Area Actuation System

The nozzle actuation system will be an airmotor drive through ball-screw jacks to move the mechanically linked convergent and divergent sections of the nozzle. This arrangement is similar to the current F100 system in which the ball screw jacks survive well in the hot section while the airmotor is located in the cooler compressor section.

### Actuator Feedback

The following feedback devices for the actuators will be assumed as presented in the individual actuator system description:

- |    |               |    |          |
|----|---------------|----|----------|
| 1) | Fuel flow     | -- | resolver |
| 2) | Flow divider  | -- | LVDT     |
| 3) | HPC           | -- | LVDT     |
| 4) | HPT           | -- | resolver |
| 5) | Blade cooling | -- | none     |
| 6) | Aft cooling   | -- | resolver |
| 7) | Nozzle        | -- | resolver |

### Engine Sensors

The pressure sensors are included in the digital controller. The compressor inlet and discharge temperature are measured with Chromel/Alumel Thermocouples

with multiple parallel elements. The turbine exit temperature is measured with multiple single element thoriated Platinum/Platinum-40% Rhodium thermocouples. An optical pyrometer is used to measure the turbine blade temperature. A series of "painted-on" Chromel/Alumel thermocouples is used to measure the nozzle section metal temperature. Magnetic speed pick-ups are used for redundant speed sensors. The GMA 400 instrumentation is summarized in Table III.

#### Other Electrical

The permanent magnetic alternator will be of standard design utilizing samarium cobalt technology with multiple windings for exciters and d.c. rectified power. Dual exciters and igniters will also be used.

Table III. GMA400 Sensor Requirements

<u>Variable</u>	<u>Type of Probe</u>	<u>Range</u>	<u>Conversion Circuitry</u>
Compressor Inlet Total Pressure	Multiple Rakes- Manifolded	2 to 50 psia	Bendix Digital Quartz
Compressor Inlet Static Pressure	Multiple Rakes- Manifolded	2 to 50 psia	Transducer in EH-K2
Compressor Dis-charge Total Pressure	Multiple Rakes- Manifolded	5 to 400 psia	Bendix Digital Quartz Transducer in EH-K2
Nozzle Total Pressure	Multiple Rakes- Manifolded	10 to 150 psi	Bendix Digital Quartz Transducer in EH-K2
Rotor Speed No. 1	Magnetic		Digital Pulse Counters in EH-K2
Rotor Speed No. 2	Magnetic		Digital Pulse Counters in EH-K2
Compressor Inlet Temperature	Chromel/Alumel T/C Multiple Parallel Elements	350 to 800°R	Amplifier in EH-K2
Compressor Dis-charge Temperature	Chromel/Alumel T/C Multiple Parallel Elements	300 to 1650°R	Amplifier in EH-K2
Turbine Exit Temperature	Thoriated Platinum/Platinum -40% Rhodium- Single Element	400 to 3250°R	Amplifier in EH-K2
Turbine Blade Metal Temperature	Optical Pyrometer	1700 to 2200°R	Amplifier Circuitry External to EH-K2
Nozzle Metal Temperature	Chromel/Alumel or Platinel T/C - Multiple "painted- on" parallel elements	600 to 1800°R	Amplifier in EH-K2

## V. ENGINE SIMULATION

### General Steady-State Performance Deck

#### General Structure

DDA computerized steady-state performance programs are designed on the building block concept and consist of a controlling logic routine which links a system of generalized component subroutines into any desired type of engine configuration defined by inputs (see Figure 9). Additional specialized calculations can be easily and efficiently incorporated with only minor modification which allows maximum flexibility in studying a variety of cycle arrangements. The system also features rapid cycle matching procedures and direct transfer from design point to off-design calculation modes.

Transient analysis of a system is rapidly accomplished by interfacing additional dynamic routines with the steady-state simulation. These additional routines perform the control of time functions, rotor dynamics, and heat storage effects to produce engine response time history characteristics. Thus, the dynamic simulation is achieved with little change to the steady-state model and makes maximum use of component characteristics prepared for the steady-state analysis.

#### Inlet

The inlet characteristics utilized in the installation of the turbojet engine performance data were obtained from McDonnell Douglas Aircraft Corporation. The subject inlet is an external compression, two-dimensional overhead ramp type incorporating variable capture area with a movable upper lip or cowl to reduce spillage drag. The above mentioned documents provided to DDA the procedures and curves necessary to calculate inlet recoveries and the associated throttle dependent/independent drag components as listed below for both supersonic and subsonic operations.

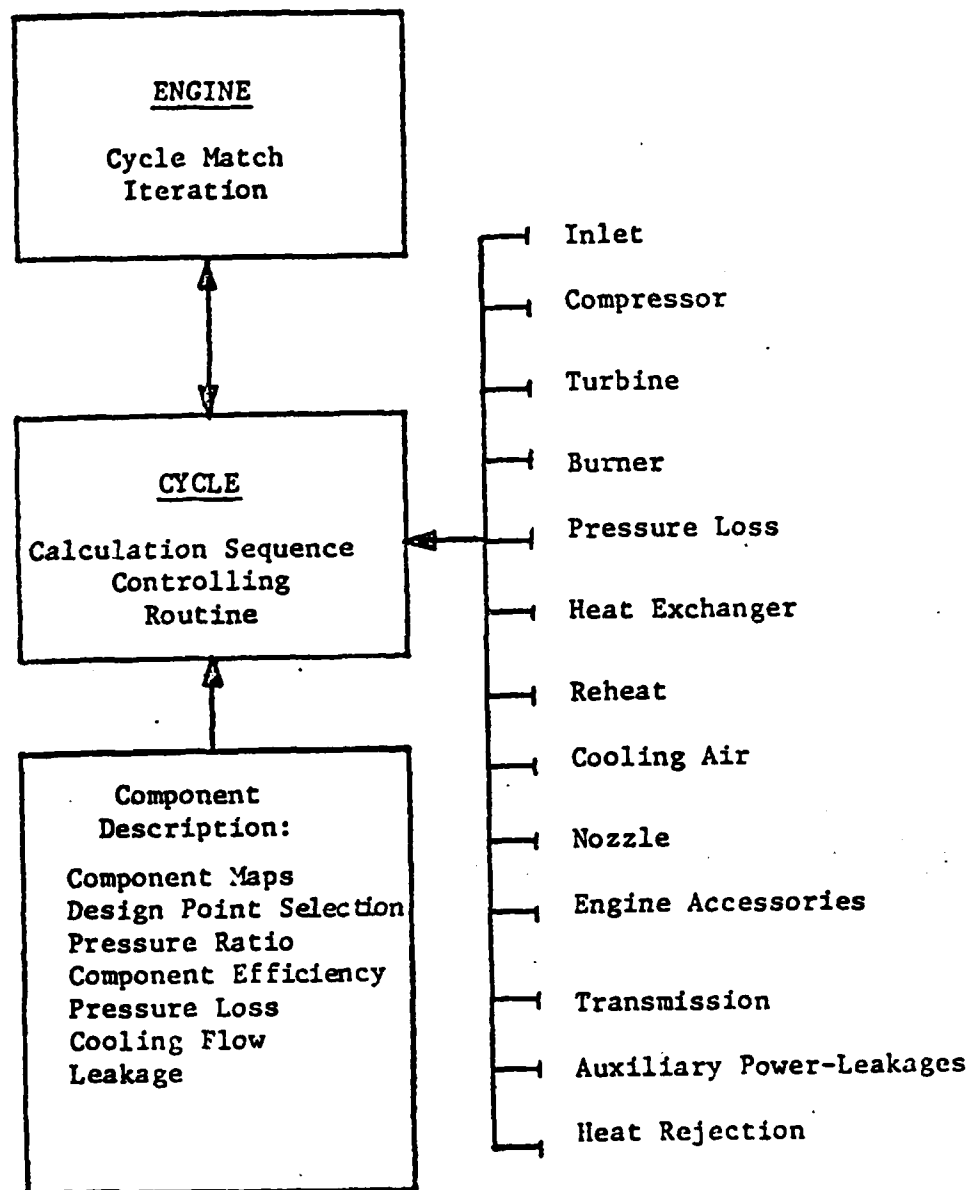


Figure 9. Generalized engine simulation structure.

Supersonic Inlet  
Drag Components

subcritical spill drag  
sidespill drag  
bypass drag  
bleed drag  
leakage drag  
Environmental Control System drag  
cooling drag  
engine allowance (airflow drag)  
upper cowl drag  
lower cowl drag  
critical drag

Subsonic Inlet  
Drag Components

subcritical spill drag  
no sidespillage  
assumed not possible  
assumed not possible  
does not occur  
full ram drag penalty  
full ram drag penalty  
assumed to be zero  
upper cowl drag  
assumed to be zero  
critical drag

Compressor and Turbine

Calculation procedures have been developed and incorporated into the basic system for simulating variable geometry rotating components by a generalized approach of layered characteristics representing a range of geometry settings or schedules as illustrated in Figure 10. This layered map approach is applicable to a variety of variable geometry definitions without program changes. Thus, engine component performance is easily and rapidly modified to reflect changes in component design or test results. This approach is used for the variable area turbine, and high pressure compressor with variable scheduling of all stators. All component maps, cycle constants, control schedules and other necessary model data are compiled into the program with provision for overriding by input data.

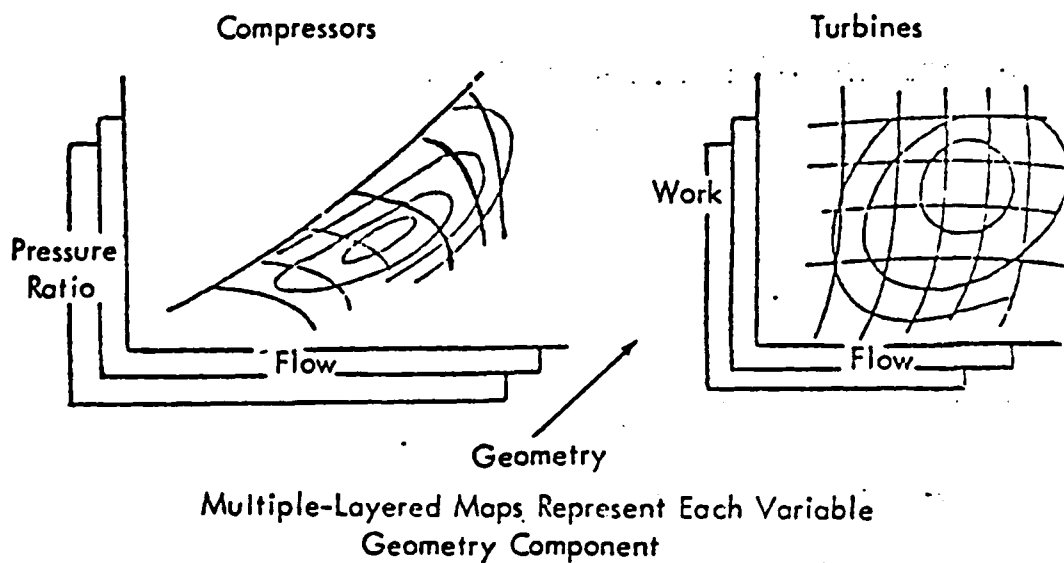
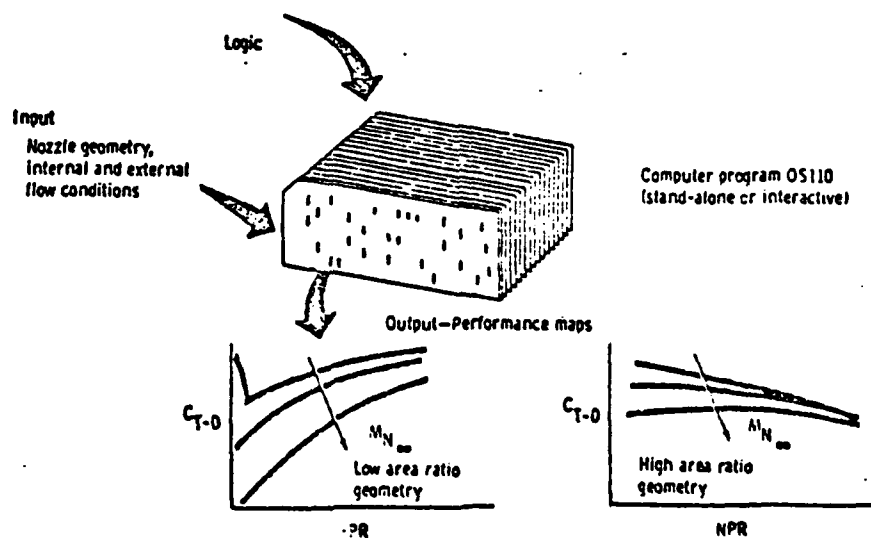
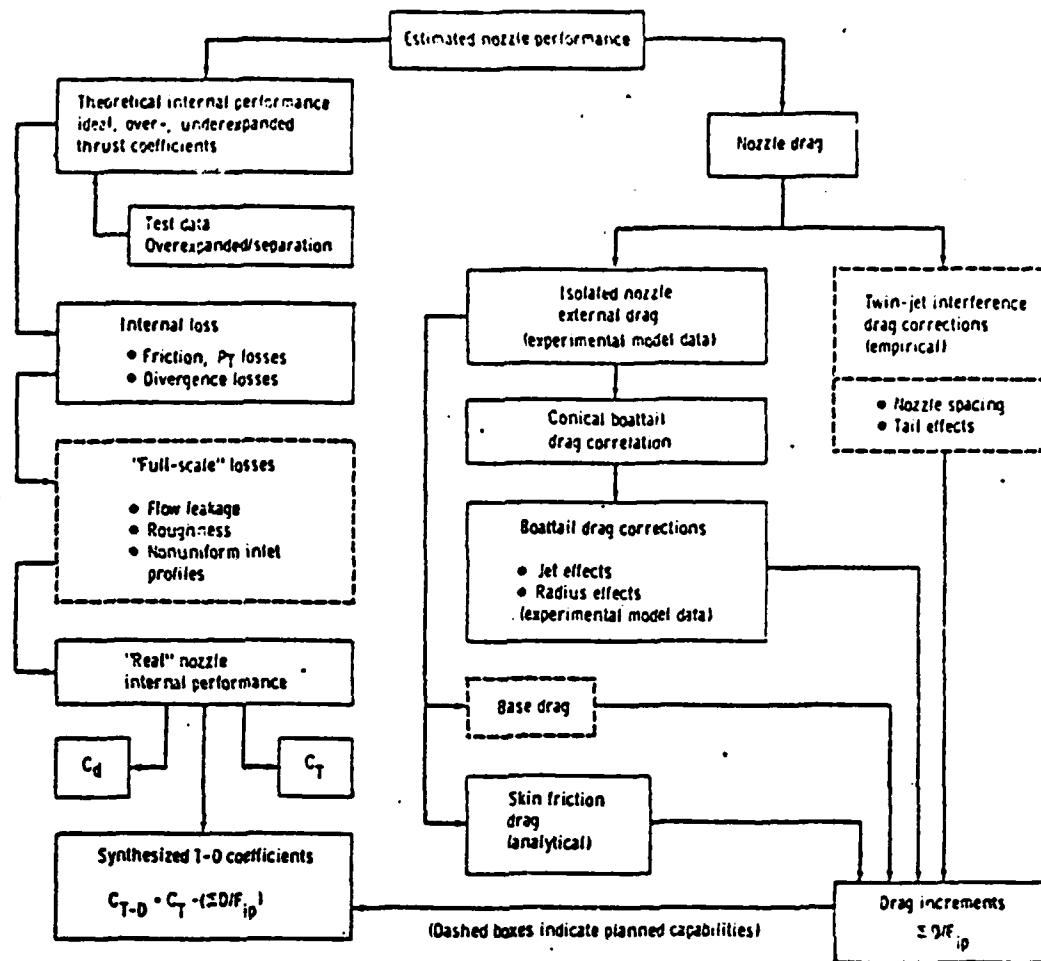


Figure 10. Typical layered map.

### Nozzle

The nozzle simulation is based upon the DDA isolated axisymmetric nozzle thrust minus drag coefficient ( $C_{T-D}$ ) synthesizer computer program. Figure 11 illustrates the basic approach used in this program. This program uses ideal one-dimensional nozzle flow equations to generate the ideal internal thrust coefficient ( $C_{Tint}$ ) maps as a function of nozzle area ratio ( $A_e/A_{Teff}$ ), nozzle pressure ratio (NPR), and specific heat ratio ( $\xi$ ). The ideal  $C_T$  is converted to  $C_{Tint}$  by subtracting analytical thrust decrements for real nozzle internal losses which include the exit divergence loss, internal friction, total pressure losses, full-scale leakage, and roughness losses. (At unchoked and highly overexpanded conditions, experimental data from available nozzle model testing are more reliable than available prediction methods and are generally used to establish the internal  $C_T$  levels.)



TE-9201

Figure 11. Nozzle simulation.



An experimental data base from DDA and available industry nozzle afterbody model tests was used to obtain nozzle isolated conical boattail drag coefficient "maps" as a function of free-stream Mach Number, boattail angle, and  $A_{base}/A_{nacelle}$  ratio. Experimental data from DDA and industry sources have been correlated to provide estimated corrections to the conical boattail drag coefficients as a function of initial boattail corner radius ratio, ranging from conical to full circular arc and for jet effects (boattail pressure coefficient downstream recompression effects) as a function of NPR. Using the boattail drag coefficient "maps", external nozzle drag values are calculated for the nozzle boattail at each condition analyzed and normalized by ideal thrust to form drag decrements. External skin friction drag is analytically calculated using the Prandtl-Schlichting skin friction drag coefficient equation as a function of Reynolds Number and Mach Number. The skin friction drag is also normalized into a drag decrement. The summation of the external drag decrements are subtracted from the internal thrust coefficient to obtain the synthesized thrust minus  $C_{T-D}$ . The simulation program results have been compared with model test data with good agreement and are extensively used by DDA for preliminary design estimates of convergent-divergent nozzle  $C_{T-D}$  performance. The program can be interactively operated as a subroutine to the engine performance card deck to supply  $C_{Tint}$  and  $C_{T-D}$  estimates over the engine operating range.

### Special Features of Engine Simulation

#### Structure of the Cycle Match

The cycle match within the ENGINE subroutine essentially does an iteration on a set of variables to satisfy a set of error equations and constraint equations. For a steady-state "match point", the error equations consist of the continuity equation and the horsepower balance equation. For transient conditions, the horsepower equations and speed variables are dropped and rotor dynamics are used to provide the balance. The multiple constraint system is employed to provide greater flexibility in the steady-state mode. In general,

the required selection of cycle match variables and equations, as well as the constraints, is made by program inputs without reprogramming. The ENGINE subroutine calls the CYCLE routine for its description of the engine as seen in Figure 12. This subroutine structure allows easy changes to the engine definition by the performance analysis section during the preliminary design. In this program, the control designer could change his simulation down through the ENGINE subroutine, but the CYCLE definition and component subroutines always contain the latest engine data. In this manner, through close cooperation between the two groups, the control designer is always working with a current engine model.

#### Offset Derivative

The above ENGINE subroutine is used in special control design programs which were not directly utilized in this study. The first is an offset derivative program that computes all the partials for sensitivity analysis. The second is an error analysis program. The third expands the offset derivative to develop "state-space" linear models of the engine. These linear models can include the rotor dynamics and pressure dynamics. The latter feature is especially useful in judging the requirement for pressure dynamics in the transient simulation. Each of these digital programs are written in reasonably general terms so that any "ENGINE" can be used with minor modifications.

#### Steady-State Engine Deck

A special steady-state simulation was generated with many extra features like design point calculation, off-design calculations, limited parametric studies, engine parameter optimization, control geometry optimization, and steady-state performance evaluation for control geometry position schedules and control engine parameter schedules.

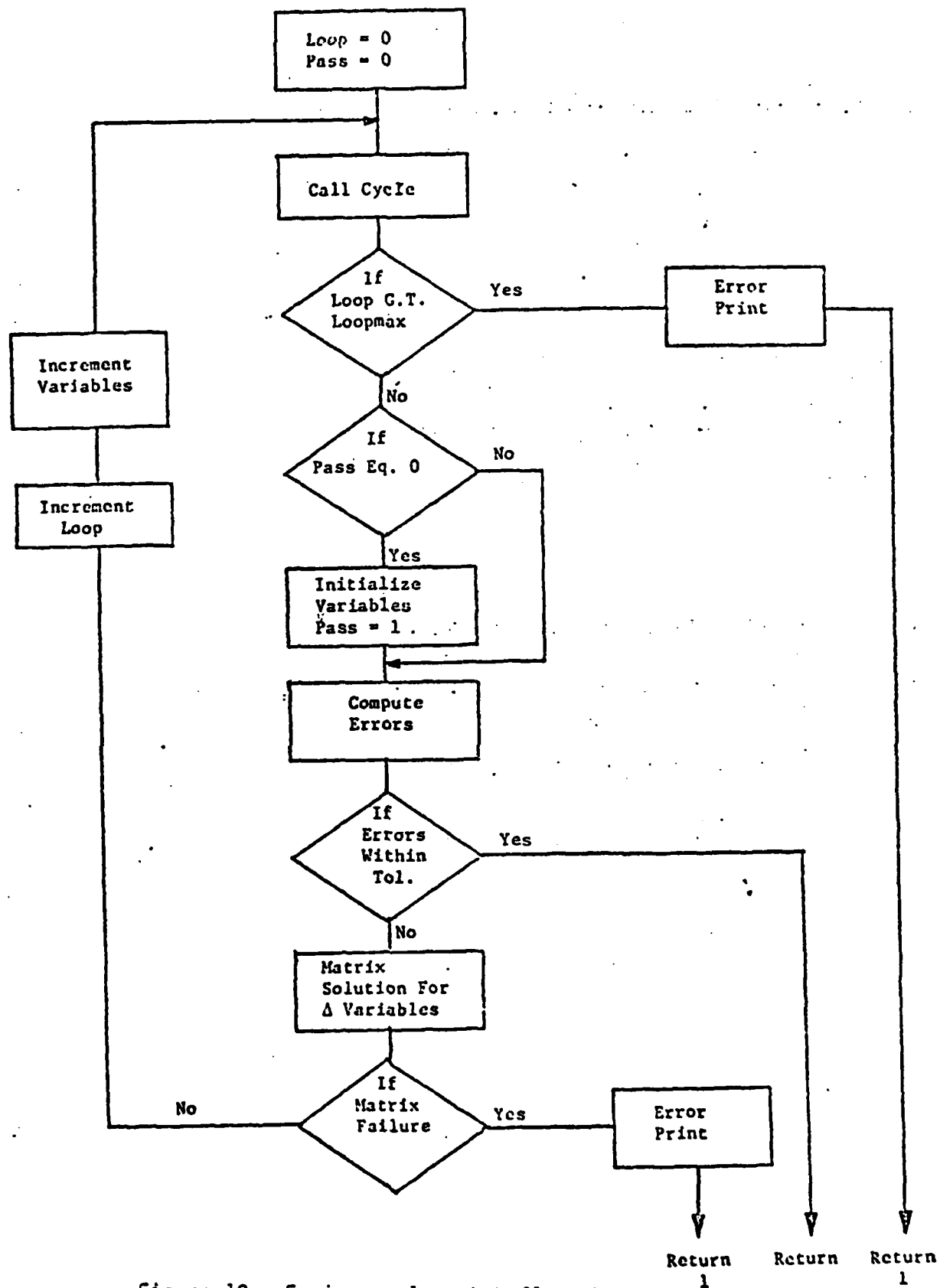


Figure 12. Engine cycle match flow chart.

This simulation utilizes the same CYCLE routine called by the above ENGINE routine to assure the same engine definition between this steady-state deck and the transient Engine/Control simulation described below. However, this steady-state deck does not utilize the above ENGINE subroutine because it is necessary to integrate the cycle-match, multiple constraint system, and optimization program for efficient computation. Also, design point computations require a different variable set-up for the cycle-match.

It should also be noted that a transient "optimization" was also achieved with this "steady-state" deck by optimizing speed for incremental time segments (within the engine limits and surge margin constraints) until 90% speed is achieved, and then changing the optimization function to reflect maximizing thrust. The "steady-state" configuration is used by setting the horsepower unbalance error function to reflect the required rotor speed rather than a zero horsepower unbalance for true steady-state.

The normal steady-state option can be utilized when the control schedules specify geometry positions. However, the constraint system is utilized when the control schedules are in terms of engine parameters (i.e., speed governor for fuel flow). For a VCE, multiple constraint systems are required so that a particular constraint (engine parameter) can be associated with a particular geometry variable. This approach will yield the same answer as a full engine/control system simulation running transiently until steady-state is reached if the control loops have integrators to achieve zero steady-state control errors. This is true even if engine limiters are reached since the constraint system holds the engine limit while the geometry moves to a physical limit in an attempt to satisfy the control schedule. The cost of a computer run using this approach is only 5% of the cost of running a full dynamic control/engine simulation transiently to achieve steady-state solutions with the control schedules. Also, this approach is somewhat independent of the control mechanization which is often unknown during the preliminary design phase of the engine.

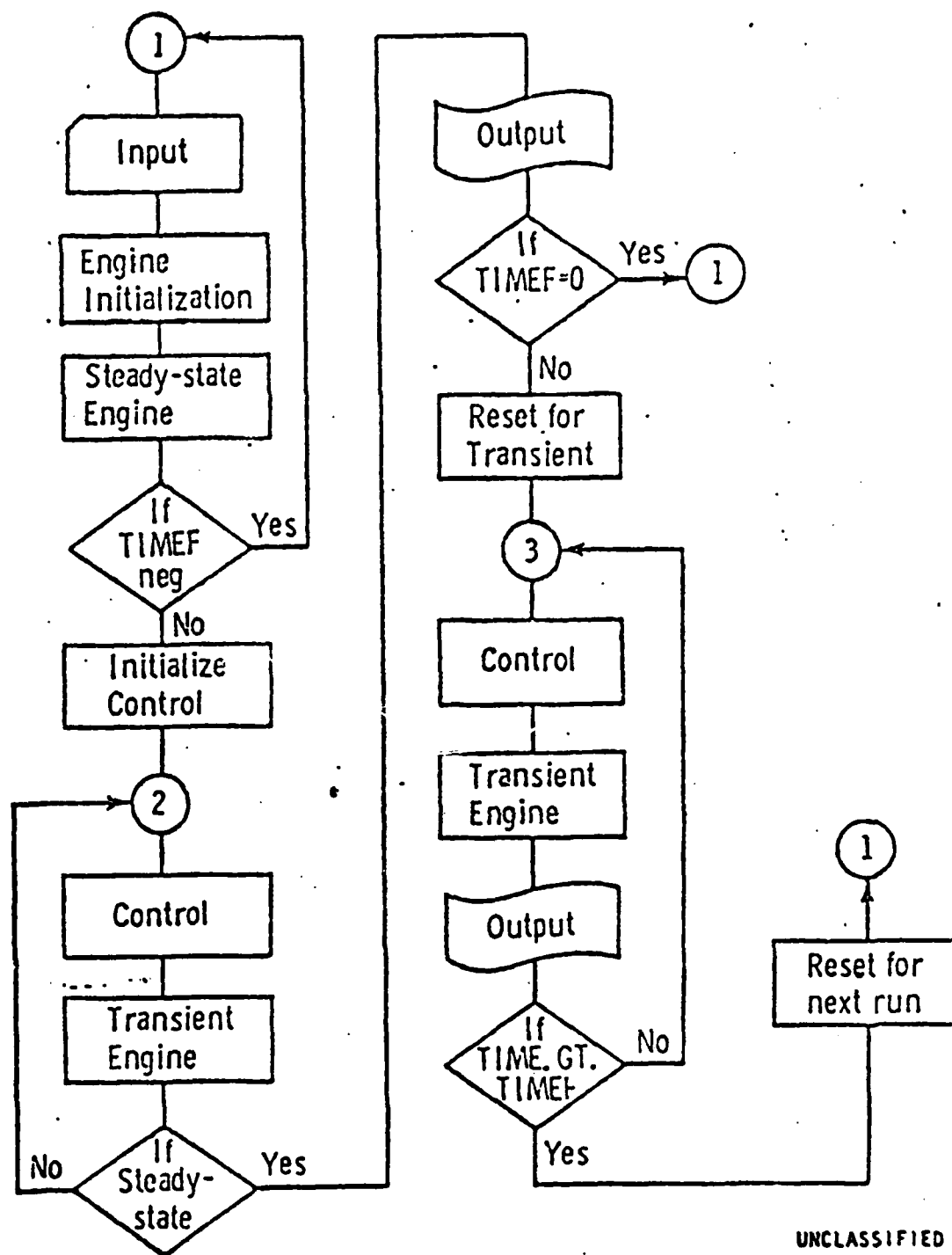
## Engine/Control Simulation Structure

The GMA 400 engine/control simulation, depicted by the flow diagram of Figure 13, can be operated in three modes determined by an input denoting final time (TIMEF). For TIMEF negative, the engine is exercised steady-state with control inputs supplied as input data. With TIMEF = 0, a steady-state point is determined for the engine and control system with flight conditions and throttle position (PLA) as input. The steady-state point is determined by running the simulation transiently with fixed inputs until engine and control derivatives (horsepower unbalances and control errors) are simultaneously within specified tolerances. A counter is provided to terminate this mode after a maximum number passes (i.e., 5-second transient) to avoid "hanging up" on an oscillatory or divergent steady-state solution.

Finally, a transient capability with the control is provided when TIMEF is positive. Note that although the program structure is general, with the control and engine as modules, the engine/control program has been written from scratch to provide efficient coding. Experience has shown that any generalized structure generally results in inefficient computation times.

The engine model retains the component performance characteristics (maps) to facilitate model updating during the engine evolution. The compressor, combustor, and turbine are integrated thermodynamically to generate engine performance. Rotor dynamics provide the transient capability of the model, and an advanced "cycle match" procedure matches the gas flows. The engine model presently includes the following features.

1. Fixed inlet with ram recovery.
2. Compressor maps of flow and efficiency with degradation capability.
3. Turbine maps of flow and efficiency with degradation capability.
4. Bleed and horsepower extraction.
5. Reynolds Number effects on compressor and turbine flow and compressor surge margin.



UNCLASSIFIED

Figure 13. Engine/control simulation flowchart.

The engine model has been stripped of many of the features necessary for cycle selection and sizing (design point, selectable inlets and nozzles, etc.) to increase computational speed. A faster cycle match procedure and a faster gas properties routine developed for the parametric decks have been incorporated into the GMA 400 deck. These changes have reduced the computing time an estimated 35%.

## VI. CONTROL SIMULATION

### Baseline Control Mode

#### General

A variable cycle engine such as the GMA 400 can be operated in a variety of ways. Each of the variable components, i.e. - turbine area, nozzle area, compressor area and fuel flow can influence the steady state (or transient) engine operating condition. It is the job of the control designer to construct a control law that will simultaneously modulate these control variables to achieve consistent, responsive and stable engine operation over the full flight envelope.

The major objective in the baseline control mode design was to achieve reliable thrust control along a minimum SFC operating line. Thrust control cannot be achieved directly since thrust is not easily or accurately measured, so an alternate method was needed. Control of compressor operating line (and therefore compressor flow) in conjunction with engine pressure ratio (EPR) will provide accurate though indirect thrust control. The compressor operating line is held by controlling corrected speed with the fuel flow and compressor pressure ratio with the turbine area. Engine pressure ratio is held by modulating the nozzle area. A detailed description of the baseline control mode follows.

#### Fuel Control

The GMA 400 fuel control (See Figure 14) is a rotor speed governor with standard accel and decel schedules, start logic and fuel limiters. The speed governor seeks to hold a requested rotor speed by adjusting the fuel flow. The error between requested speed and actual speed is amplified by the proportional plus integral gains (pph/rpm) and added to a nominal fuel flow to form



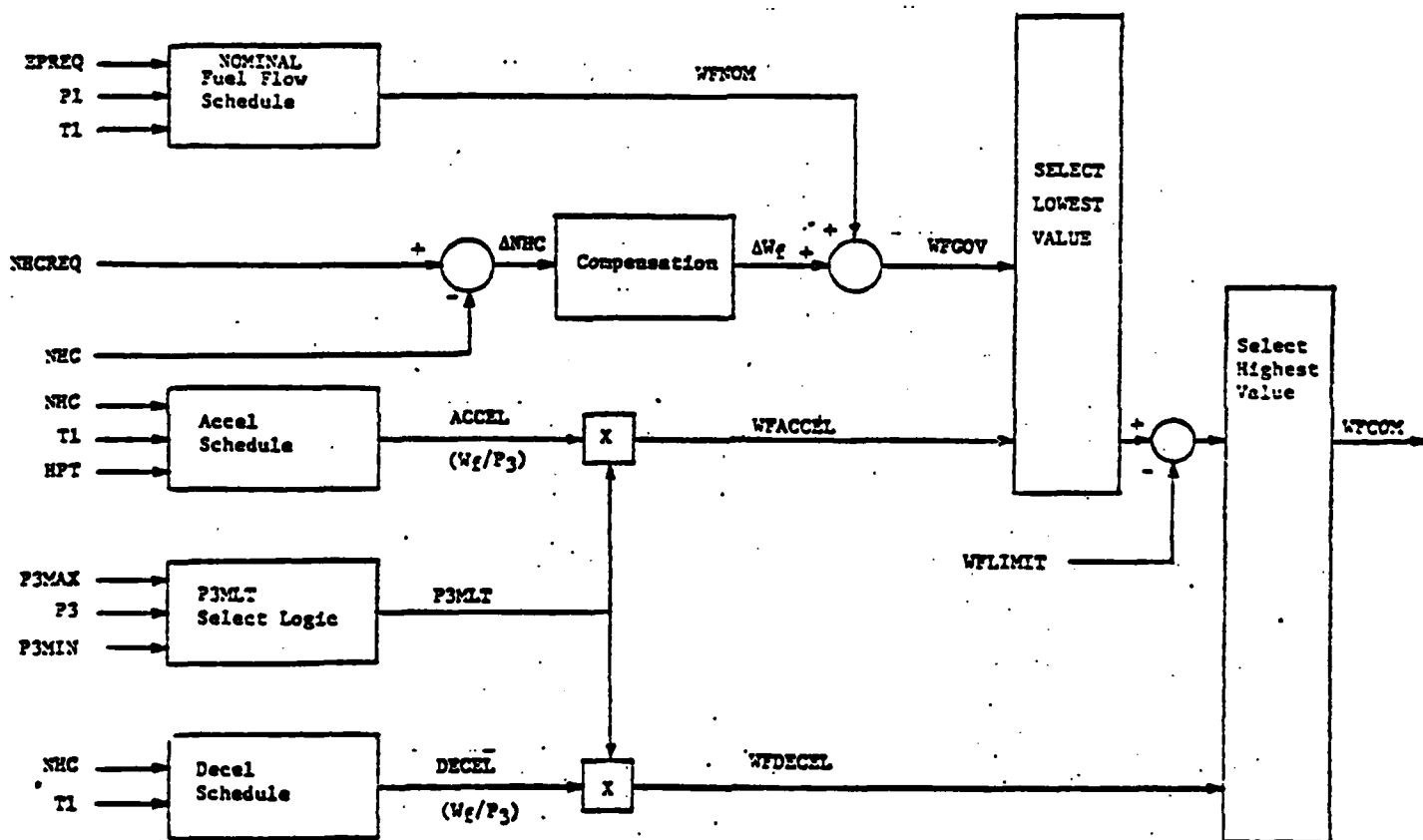


Figure 14. Fuel control logic.

a governor fuel request. The fuel is modulated in such a fashion as to zero out the speed error. The speed governor fuel request (WFGOV) is bounded by calculated maximum and minimum allowable fuel flows (WFACCEL and WFDECEL, respectively) and by the fuel limiter pulldown (WFLIMIT), which is added to the governor or accel fuel flow. It should be noted that WFLIMIT is constrained to always be negative. During the majority of steady-state engine operation condition, commanded fuel flows should equal WFGOV and the speed error should be close to zero. This will happen whenever WFLIMIT is zero, i.e. - no limits violated, and when WFGOV is between WFACCEL and WFDECEL. During a transient, WFGOV will generally trespass outside the area bounded by the accel and decel fuel flows because of the high speed errors, and commanded fuel flow will be constrained by the accel or decel schedule. If a limit is violated WFLIMIT will further subtract from the fuel flow request.

A unique feature of this particular fuel control is the considerable select logic employed to determine the speed request command. The command issued from the governor table is checked for compatibility against known engine speed limits and further constrained to be consistent with calculated compressor ratio maximum and minimum limits. This alleviates the necessity for including compressor discharge pressure (CDP) maximum and minimum limits in the fuel limiter circuitry. The decel, accel, and governor fuel flows, along with any fuel pulldown contributed by the limiters, control fuel in the PLA range 60-95. A PLA below 60 is within the start range, and the corrected speed request (NHCREQ) is designed to drive the fuel control onto the ACCEL schedule during this process. Thus the starting fuel flow is determined by the accel schedule which can be modified by WFLIMIT if any engine limits are exceeded during starting.

### Limiters

The fuel limiter circuitry, Figure 15, determines fuel limiter pulldown (WFLIMIT).

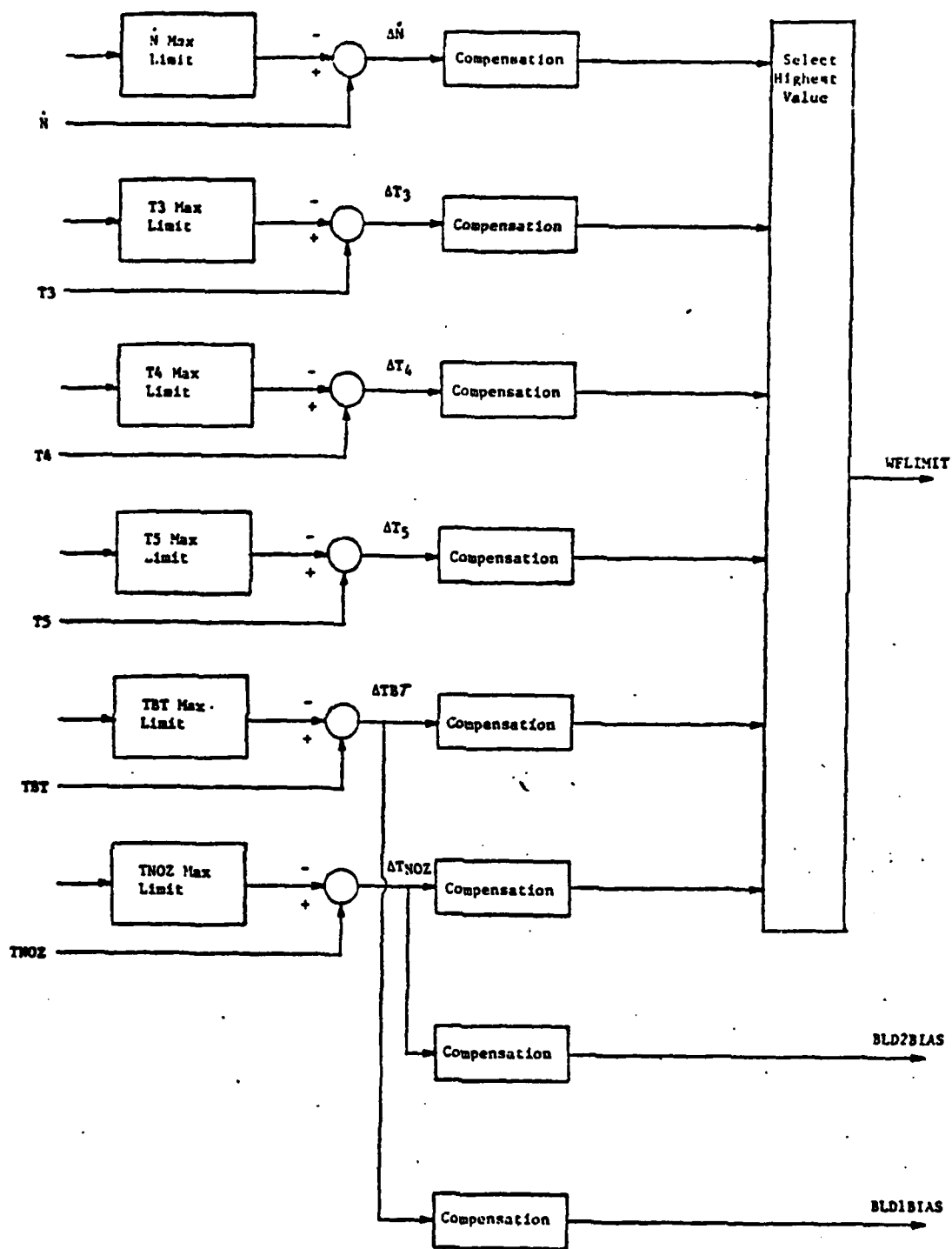


Figure 15. Fuel limiting logic.

The fuel limiter circuitry provides reliable parameter limiting via fuel flow pulldown. The limited parameters are speed derivative ( $N$ ), compressor discharge temperature ( $T_3$ ), synthesized turbine inlet temperature ( $T_4$ ), turbine exit temperature ( $T_5$ ), turbine blade metal temperature (TBT), and nozzle metal temperature (TNOZ). A limit fuel flow is calculated for each parameter. The reference or maximum allowable values for each parameter are predetermined from simulation data. In most cases these are constants, but may be graphical or analytical functions of geometry positions, speeds, ambient conditions, etc. An error is formed by comparison to sensed or synthesized signals. This error is multiplied by a gain and lead/lag compensation to form the particular limiter fuel pulldown.

Each output limit fuel flow is constrained to be negative, since a positive limit fuel flow results from engine operation within the defined "safe" region. A maximum fuel pulldown assigned for each parameter further constrains the outputs. The most negative, i.e. - the most limiting, fuel flow is selected to be equal to WFLIMIT which is then added to commanded fuel flow.

### Geometry

The geometry control schematic is shown in Figure 16. The geometry variables include turbine area (HPT), nozzle area (A8), compressor vane position (HPC), turbine blade cooling flow (BLEED 1) and aft section cooling flow (BLEED 2). HPC, BLEED 1 and BLEED 2 are scheduled variables and do not pose major problems to the control design. HPT and A8 are closed loop on engine parameters. BLEED 1 and BLEED 2 position commands are biased by metal overtemperature readings at the turbine blade and nozzle wall respectively (computed in the limiter logic). The A8 and/or the HPT position commands may be biased open by corrected speed error during transients to increase the surge margin during the transients. In the cases investigated in this study, only the nozzle bias was required because the turbine is held open by special logic in the compressor pressure ratio ( $R_c$ ) schedule selection discussed below. A brief description of the individual geometry controls follows.

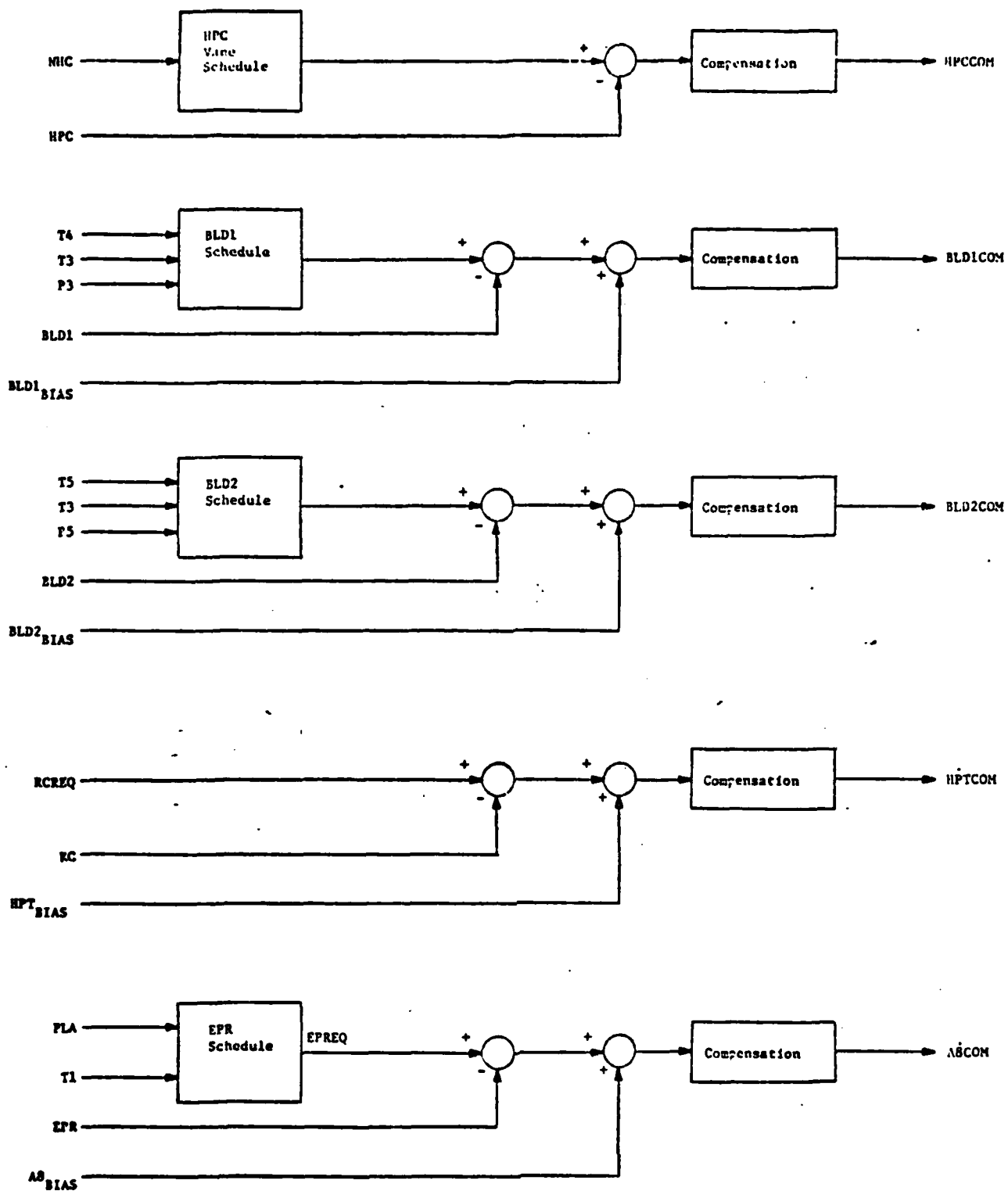


Figure 16. Geometry control logic.

HPT A desired compressor pressure ratio is chosen via the select logic shown in Figure 17. The turbine area is controlled to maintain this ratio. An  $R_c$  is selected as a function of NHCMP. This nominal  $R_c$  is compared to calculated maximum and minimum  $R_c$  and the limited  $R_c$  forms the output request. NHCMP is equal to NHCREQ except during a transient when it is equal to NHCGBK. The special logic during a transient minimizes the  $R_c$  error term and keeps the HPT from closing down during a transient and reducing compressor surge margin. Setting NHCMP equal to NHCREQ during steady-state alleviates much of the cross-coupling due to loop interactions because NHCREQ is a function of PLA only. The specific select logic statements are diagrammed in flowchart form in Figure 17. Provision is made for a position bias based on corrected speed error to hold the turbine open during transients but this is not used presently.

A8 A desired engine pressure ratio is selected as a function of PLA and T1. The nozzle area is controlled to maintain this pressure ratio. The nozzle position command is biased during transients to minimize the corrected speed error. The bias holds the nozzle open to allow for a quicker rotor acceleration.

HPC A desired HPC position is selected as a function of corrected speed. The compressor vane position is controlled to maintain this position.

BLEED 1 A desired turbine blade cooling flow is selected as a function of T3, synthesized T4, and P3. The bleed actuator is modulated to maintain this flow. The flow is biased open in case of a turbine blade temperature overlimit.

BLEED 2 A desired aft cooling flow is selected as a function of T3, T5, and P3. The bleed actuator is modulated to maintain this flow. The flow is biased open in case of a nozzle metal temperature overlimit.

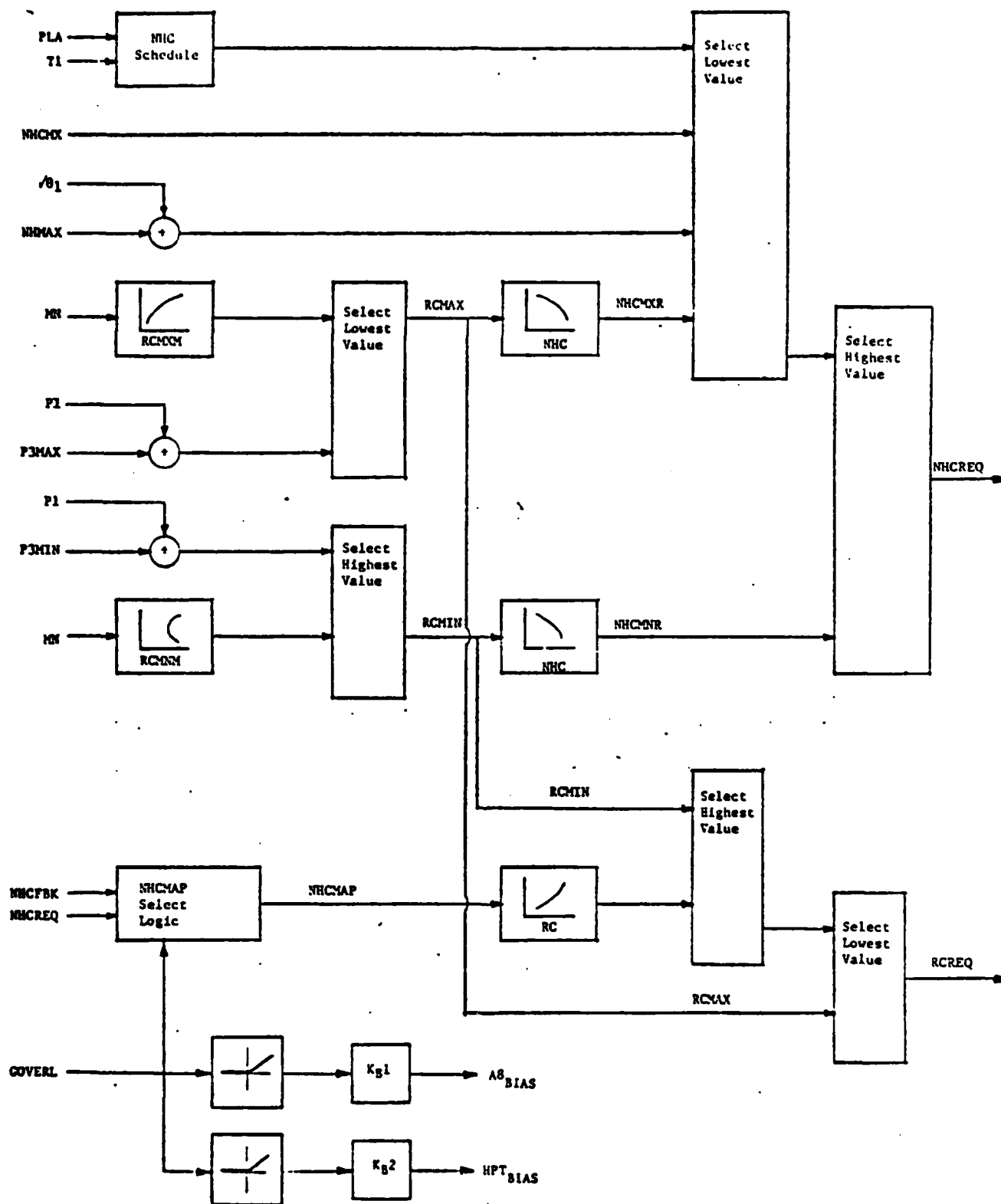


Figure 17.  $R_C$  &  $N_H$  select logic.

#### 4a.5 Summary

The control mode for the 680-B1 is summarized in Table IV. The system basically features a fuel governor and closed loop control of the compressor pressure ratio by the turbine to maintain a compressor operating line. The nozzle provides closed loop control of engine pressure ratio to maintain the desired thrust. The compressor geometry is scheduled on corrected speed to provide "optimal" surge margin. The cooling bleeds are scheduled on engine gas temperatures and pressures to assure sufficient cooling air to maintain safe metal temperatures. A large number of limiters and biases are included to protect the engine and improve dynamic performance.

Table IV  
GMA 400 Control Mode Summary

<u>Controlled Variable</u>	<u>Primary Control Mode</u>	<u>Bias/Limiter Parameters</u>
Wf	Closed loop on $NHC = f(PLA, T_1)$	NHC T3 T4 T5 TNOZ TBT $ACCEL = f(NHC, T_1, P_3, HPT)$ $DECEL = f(NHC, T_1, P_3)$
HPT	Closed loop on $R_c = f(NHC)$	-
A8	Closed loop on $EPR = f(PLA, T_1)$	Biased by NHC error during transients
HPC	Scheduled vs NHC	-
Bleed 1	Scheduled vs T3, Synthesized T4 and P3	Limiter on TBT
Bleed 2	Scheduled vs T3, T5 and P3	Limiter on TNOZ



## Actuator Models

Dynamic models for each of the actuation systems were derived in frequency response form based upon theoretical models and/or hardware test data. In general, complex nonlinear models have been reduced to simple linear transfer functions with the same dynamic characteristics. The effects of many of the typical actuation nonlinearities such as deadband and hysteresis are reduced by the high gain position feedback loop that was introduced to minimize these nonlinearities and provide the required fail-safe position feature. Therefore, the linearized transfer functions given below provide an adequate dynamic representation of the actuators for this study. The details of the model development are discussed in the following sections.

### ACTUATOR MODELS

$$WF_{COM} = \frac{(43.5)^2}{s^2 + 40.89s + (43.5)^2} \cdot \frac{1}{.065s + 1} WF_{OUT}$$

$$A8_{COM} = \frac{1.099 (-.012s + .91)}{.0013s^2 + .03s + 1} A8_{OUT}$$

$$HPT_{COM} = \frac{1}{.00158s^2 + .0374s + 1} HPT_{OUT}$$

### Fuel System

The fuel system block diagram is shown in Figure 18. The EH-K2 control computer and fuel actuation system hardware are depicted. The digital/analog interface is shown by a dashed line. The TRW fuel valve, pump and RVDT are modeled to the right of the dashed line. The models are based on TRW/Woodward design data, test data, or theoretical analysis. The EH-K2 sample and hold circuitry, input conditioning, and the proportional plus integral controller are shown to the left of the dashed line. The EH-K2 is modeled via the Z-transform in order to properly account for the digital operation.

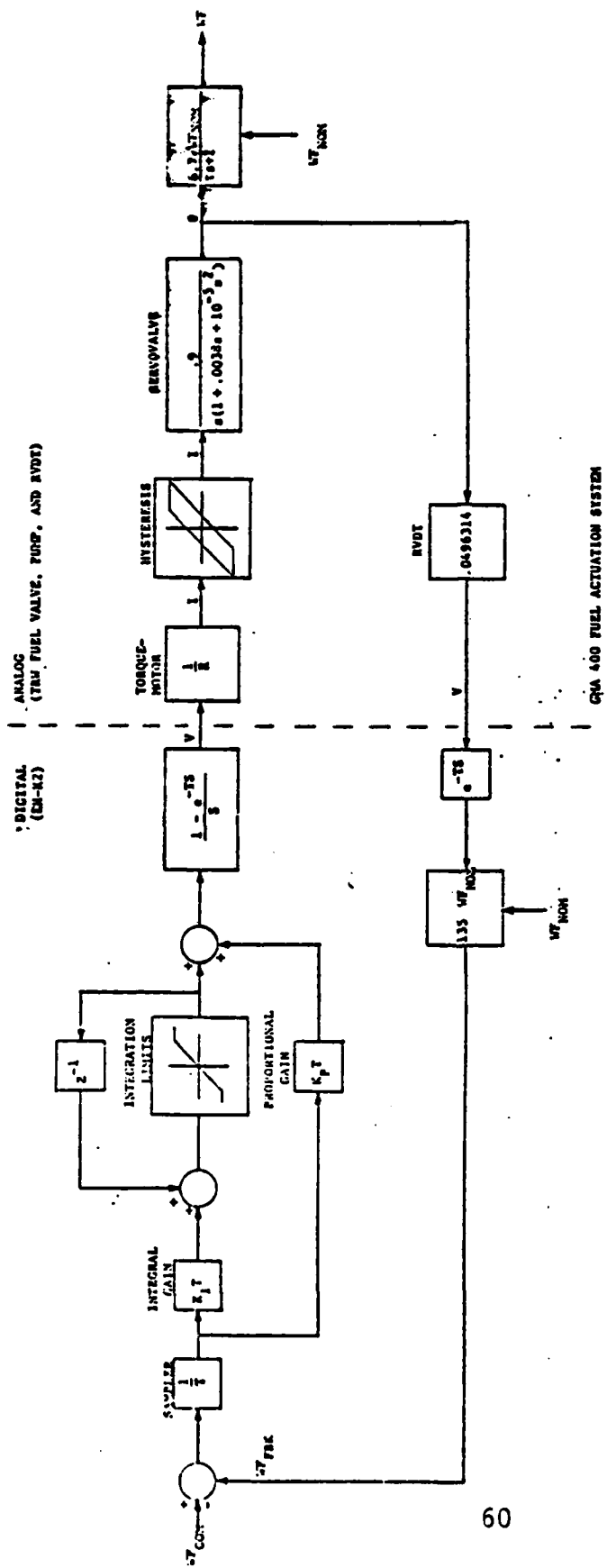


Figure 18. Fuel system block diagram.

The position loop shown from  $WF_{COM}$  to is closed within the computer such that the control gains  $K_p$  and  $K_I$  are digitally implemented. The addition of the closed position loop around the torque motor servovalve provides better control over commanded fuel flow and diminishes the observable effects of hysteresis, wear, stiction or other small nonlinearities.

The position loop from  $WF_{COM}$  to was programmed for computer analysis into FASP (Frequency Analysis of Systems Program). The gains,  $K_p$  and  $K_I$ , were adjusted to achieve good closed loop response. A quadratic transfer function representation was fitted to the resulting frequency response plots. The transfer function generated along with the pump transfer function is

$$WF_{COM} = \frac{(43.5)^2}{s^2 + 40.89s + (43.5)^2} \cdot \frac{1}{.065s + 1} WF_{OUT}$$

#### Turbine Actuation

The GMA400 turbine vane actuation system is identical to the GMA200 JTDE turbine vane actuation system. The GMA200 JTDE turbine vane actuation system was tested and the results were reported in Bendix Report ENCD-866-19410R. The results of this test were used to verify a Bendix detailed non-linear model of the turbine actuation system. The verified model was then used to generate closed loop response from HPT position to HPT command. Data was supplied for several supply pressures and an intermediate pressure was selected as being representative of average operating conditions. A quadratic transfer function was fitted for this intermediate pressure. The transfer function representation used in the simulation is

$$HPT_{COM} = \frac{1.099 (-.012s + .91)}{.0013s^2 + .03s + 1} HPT_{OUT}$$

## Nozzle Actuation

The nozzle actuation system for the GMA 400 is undefined. In all probability the final design will use a test stand nozzle very similar to the JTDE secondary nozzle or the ATEGG primary nozzle. Data was obtained from an ATEGG nozzle simulation at Bendix and a quadratic transfer function was fitted to this data to produce the following transfer function

$$A8_{COM} = \frac{1}{.00158S^2 + .0374S + 1} A8_{OUT}$$

**4b.4 HPC and Modulated Bleeds Actuation** The actuation system for the compressor vanes has been designed and modeled, but is not included in the simulation. The effects of actuation system inaccuracies are not included in the present simulation because of a lack of available data on off-design compressor performance. Therefore the simulation assumes that the compressor vanes are perfectly scheduled. This removes the requirement for a compressor actuator model in the simulation. It should be noted that this is not a serious omission since the compressor vanes are scheduled, and therefore transient interactions are not affected appreciably by the compressor vane control loop.

The bleeds for nozzle cooling and turbine blade cooling are modulated flow bleeds. The actuation systems for these bleeds are still being designed. Currently there is no provision for controlled bleed modulation in the simulation. These facts, coupled with the insignificant effects on control stability or transient interaction caused by modulated bleeds, dictated the decision to not include any bleed actuation system dynamics in the simulation.

## Control Simulation

A digital simulation of the control system, including actuators, sensors and control laws, was written and married to the engine simulation. A new main-

line program was required to provide the program sequencing and interface between the engine and the control. Descriptions of the mainline and major control subroutines follows.

### Mainline

This program sets up the input/output, computes the initial conditions, selects the proper steady state or transient running mode and issues diagnostic messages in case of an error. The mode selection is determined by the sign of the input final time (negative, zero, or positive). The modes are steady-state without the control, steady-state with the control, and transient time response with the control. The steady-state with control is derived by letting the engine and control run transiently with fixed inputs and automatically stopping the transient when engine derivatives and control errors are simultaneously within specified tolerances.

The three print options are available at independently selectable time intervals. The options are the full engine printout supplied with the engine routine, the full control printout showing parameter requests, feedbacks, errors and position commands for all the control and limiter loops, and a one line edited engine/control printout. An example of the full control output is shown in Figure 19.

### Subroutine CNTROL

Subroutine CNTROL is the control executive routine called by mainline. The subroutine is used to issue the call statements to the control subroutines in a predetermined sequence. The return is to the mainline at the end of the execution.

Time = 12.000	PLA = 100.00 Reference	Limit Code = 0 Feedback	Error	WFC = 23730. Proportional	Integral	Total
0 - Governor	99.947	99.909		31.613	614.401	23729.527
1 - Accel Limit						30310.730
2 - Decel Limit						4879.031
3 - DP/P Surge	0.0	0.0	0.0	0.0	0.0	0.0
4 - BOT			0.0	0.0	0.0	0.0
5 - Corrected NH	105.000	99.909	5.091	0.0	0.0	0.0
6 - T3			281.434	0.0	0.0	0.0
7 - TNOZ			1240.899	0.0	0.0	0.0
8 - TBT			136.724	0.0	0.0	0.0
9 - P3 Pressure	370.000	191.609	0.0	0.0	0.0	0.0
0 - NH Dot	10000.000	0.024	0.0	0.0	0.0	0.0
HP Compressor (HPC)	0.0	0.0	0.0	0.0	0.0	0.0
HP Turbine (HPT)			0.003	0.004		
Primary Nozzle (ABC)			0.003	0.006		

Figure 19. Control output sample.

### Sensors

The sensors are modeled as first order lags in Subroutine SENSOR. A table of the sensed parameters and their respective time constants is shown in Table V. The thermocouple time constants are non-constant functions of the airflow. The first order lags are mechanized as closed form recursive formulas derived from the Z-transform representation (Ref. TDR AX.1200-059, see discussion under Actuators) Subroutine SENSOR returns to the CNTROL subroutine at the end of execution.

### Fuel Law

The fuel control logic is programmed in WFLAW which calculates the accel, decel and governor fuel flows as well as all of the limiter fuel flows. A code, LIMITR, is generated that tells the user which limit has been violated and if the fuel command is on the accel or decel schedule. The return is to Subroutine CNTROL at the end of execution.

### Geometry Laws

Subroutines HPTLAW and A8CLAW are called from subroutine CNTROL. In HPTLAW the first portion of the logic determines the intermediate value used in the calculation of the  $R_c$  schedule request, HPTSCH. An error is then calculated and appropriate compensation applied before subroutine RATE is called. RATE integrates the actuator flow request to form a position command. RATE also checks that the rate requested is within permissible maximum and minimum flow limits for the particular actuator. HPTLAW returns to subroutine CNTROL at the end of execution.

In A8CLAW an EPR request is calculated and an error formed. A bias error, A8BIAS, is also formed based on the fuel control speed error. A8BIAS is set

Table V  
SENSOR TABLE

<u>Sensed Parameter</u>	<u>Sensor Lag Value</u>
Inlet pressure (P1)	.02 seconds
Compressor discharge total pressure (P3)	.02 seconds
Compressor discharge static pressure (P3S)	.02 seconds
Exhaust nozzle pressure (P7)	.02 seconds
Rotor speed (N1)	.01 seconds
Inlet corrected flow (WRTZD1)	.0015 seconds
Fuel flow ( $W_f$ )	.0015 seconds
HPT feedback position (HPTFBK)	.0015 seconds
Nozzle feedback position (A8FBK)	.0015 seconds

Temperature Sensors (Thermocouples)

$$TAU_{TEMP} = TAU_{NOM} * \frac{W_{AIRNOM}}{W_{AIR}}$$

<u>Temperature</u>	<u>Lag Value (Nominal)</u>	<u>Airflow (Nominal)</u>
Inlet (T1)	.5 seconds	109.5 lbs/sec
Compressor discharge (T3)	.5 seconds	166.5 lbs/sec
Nozzle inlet (T7)	.5 seconds	175.6 lbs/sec
Turbine blade (TBT)	.8 seconds (Models heat storage)	
Nozzle metal (TNOZ)	.3 seconds (Models heat storage)	



to zero when the speed request is no longer changing and the speed request is satisfied or "exceeded". The flow request is calculated as the sum of proportional gain K1, times the EPR error (A8CER) and proportional gain K2, times the A8BIAS. Subroutine RATE is then called and an actuator position command is returned. A8CLAW returns to Subroutine CNTROL at the end of execution.

The schedules for the compressor geometry and modulated cooling are built into the engine simulation. The compressor schedules are incorporated into the compressor maps while the cooling flows are computed as a function of compressor discharge pressure and temperature and the pressure and gas temperature at the cooling point.

### Actuators

The actuator subroutines called from CNTROL are WFVALV, for the fuel valve, HPTACT, for the turbine geometry, and NOZZLE, for the nozzle geometry. The actuator subroutines are very simple and are not flowcharted. A digital actuator model for each of the geometry components is mechanized in the respective routines based on frequency response modeling discussed earlier. The transfer functions are implemented in the simulation via general closed form solutions. Subroutines have been written to provide time responses to generalized inputs for a first order filter, second order filter, and second order transfer function with complex roots. Recursive formulas have been derived for each subroutine using Z-transform techniques. (Zero order hold assumed at the input). These recursive formulas yield the desired closed form solutions thereby insuring high accuracy and computational stability. Third order (or higher) transfer functions, such as the fuel system, are modeled by concentrating first and second representations.

## VII. ENGINE/CONTROL SIMULATION RESULTS

The control mode began as an uncoupled closed loop control where each geometry is controlled closed loop on a single engine parameter. The fuel loop is primarily a speed ( $N_H$ ) governor, the turbine geometry is used to hold the compressor pressure ratio ( $R_C$ ), and the nozzle controls the engine pressure ratio (EPR). The compressor geometry is scheduled on corrected speed to "optimize" compressor surge margin and the cooling bleeds are scheduled to provide nominal cooling requirements.

However, as the design evolved, it was necessary to "bias" various geometry control loops with error terms from other loops to provide the necessary interaction to counteract the coupling provided through the engine. For example, it is necessary to bias the turbine towards an open position during an accel to provide the required surge margin. However, if the turbine opens too much, the acceleration capability of the turbine is diminished considerably. Also, it is necessary to avoid closing the nozzle too fast during an accel. Therefore, the control evolved to a multi-variable control structure through classical design procedures in order to achieve the desired performance.

Linear analysis was used to determine the approximate system gains. However, with the additional cross-coupling, final adjustments to the control gains in the simulation were completed by trial and error to permit the control to meet the acceleration goals at other than static sea level conditions. In general, the system will accel from "idle" to intermediate in 3.5 seconds with no overshoot and from "idle" to max. in 4.5 seconds with no appreciable overshoot.

Typical transient responses at several different flight conditions are shown in Figures 20 - 24. In each case the PLA movement begins at 0.5 seconds. In general, the rise time to intermediate is less than 3.5 seconds and the rise time to maximum thrust is less than 4.5 seconds. The rise time for accels from intermediate to maximum power are approximately one second because the rotor speed remains constant and the fuel and variable geometry are adjusted for the additional power.

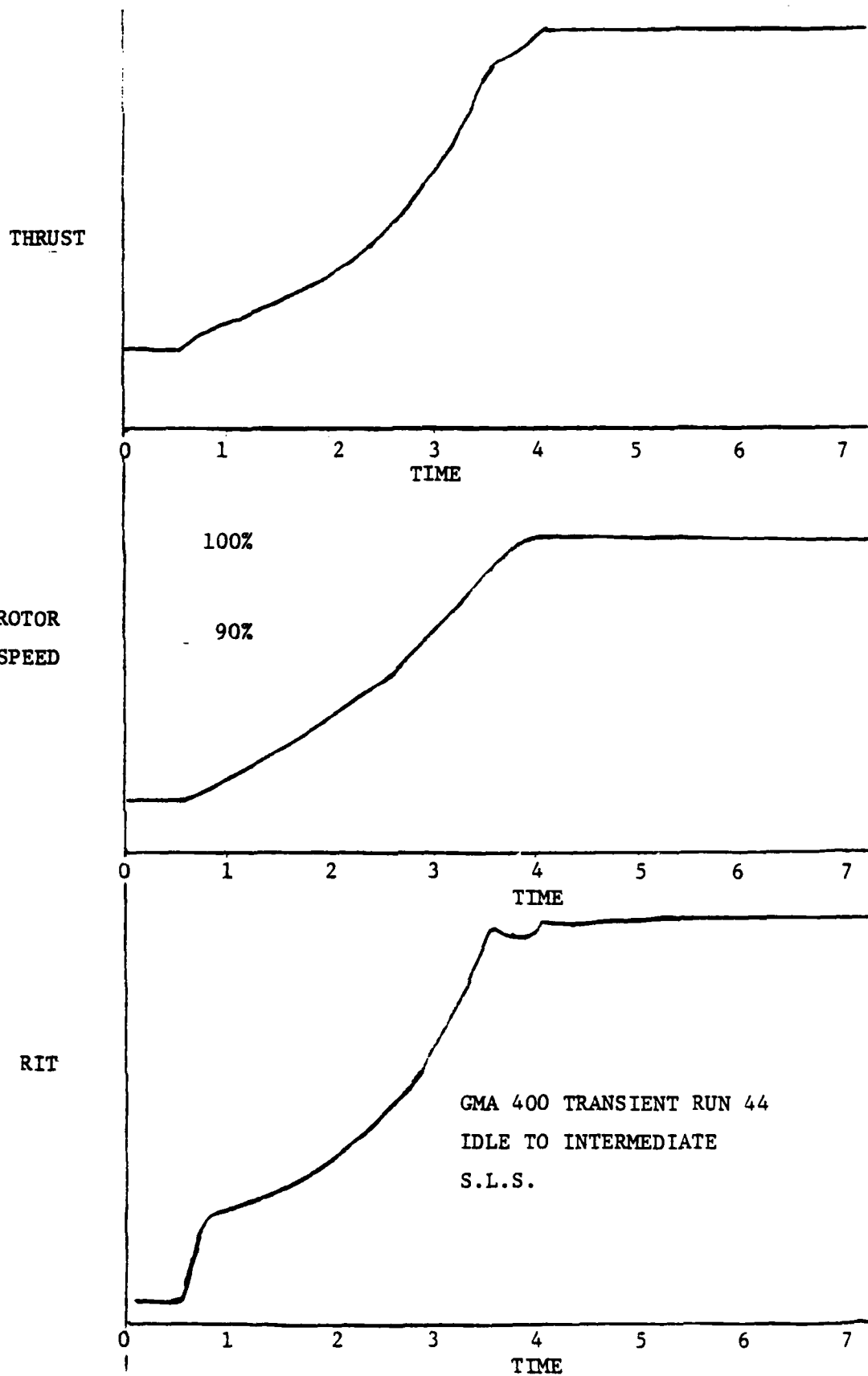


Figure 20. S.L.S. transient response - idle to intermediate.

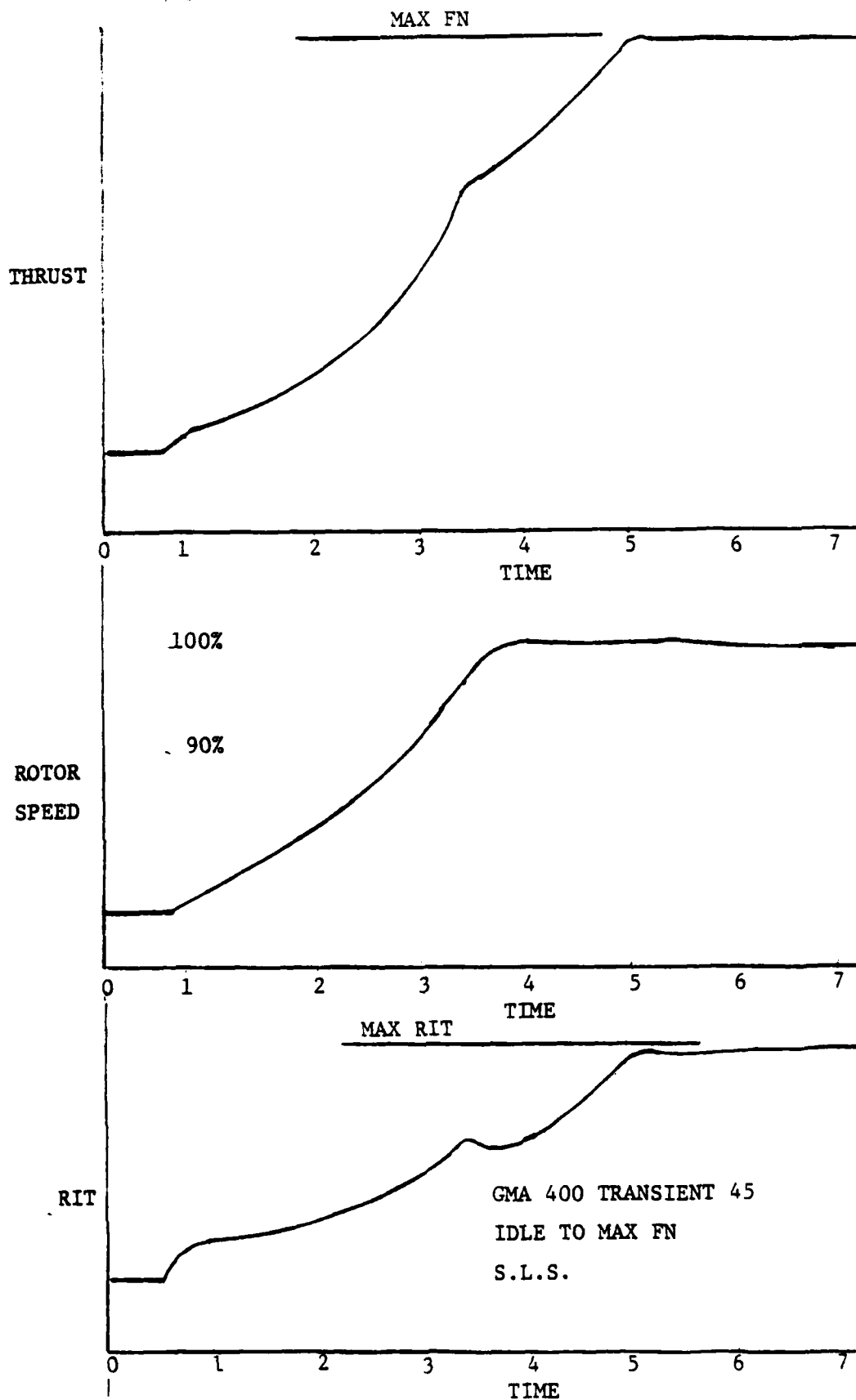


Figure 21. S.L.S. transient response - idle to maximum.

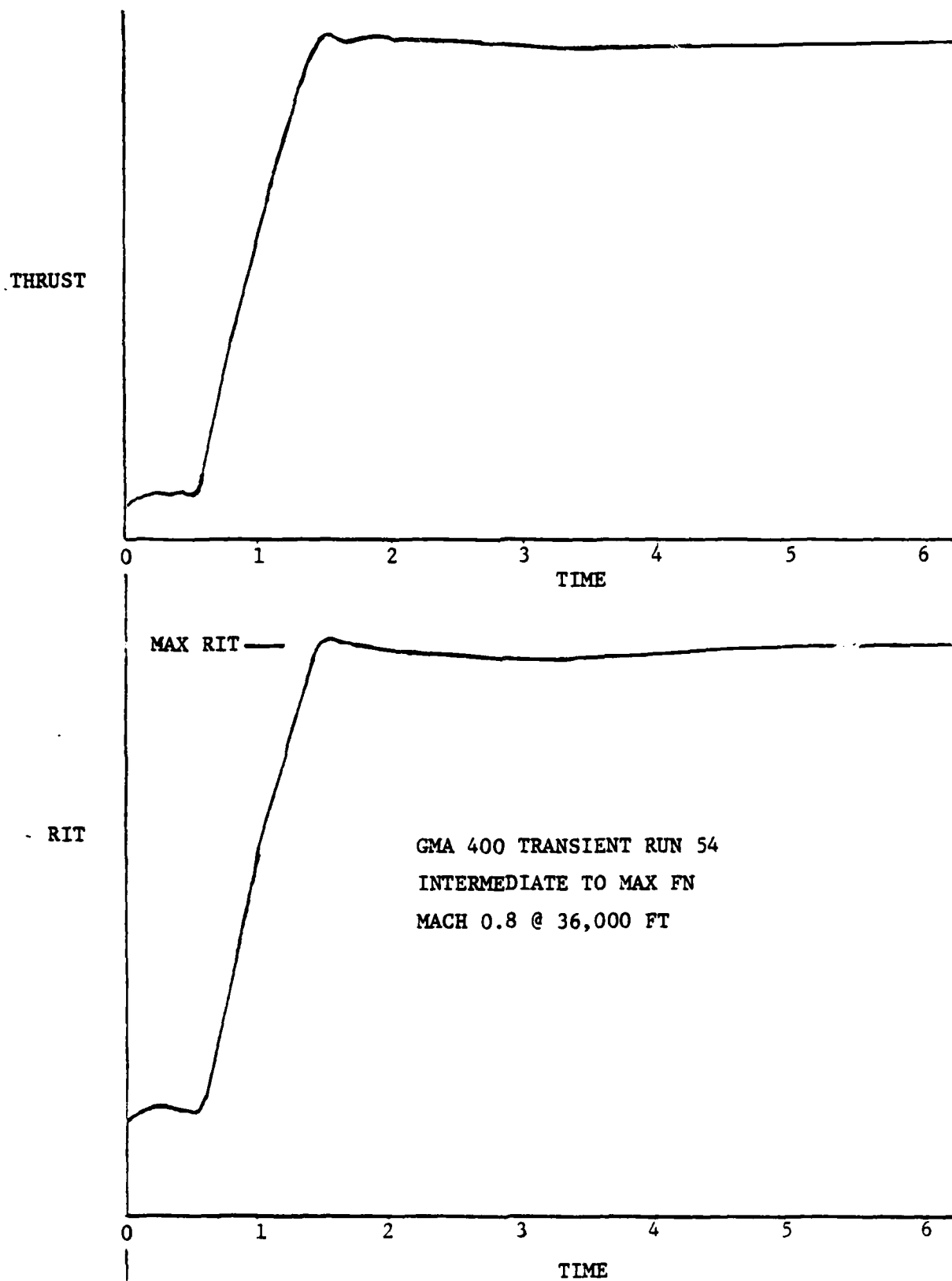


Figure 22. 0.8  $M_N$ /36000 ft. transient response - intermediate to maximum.

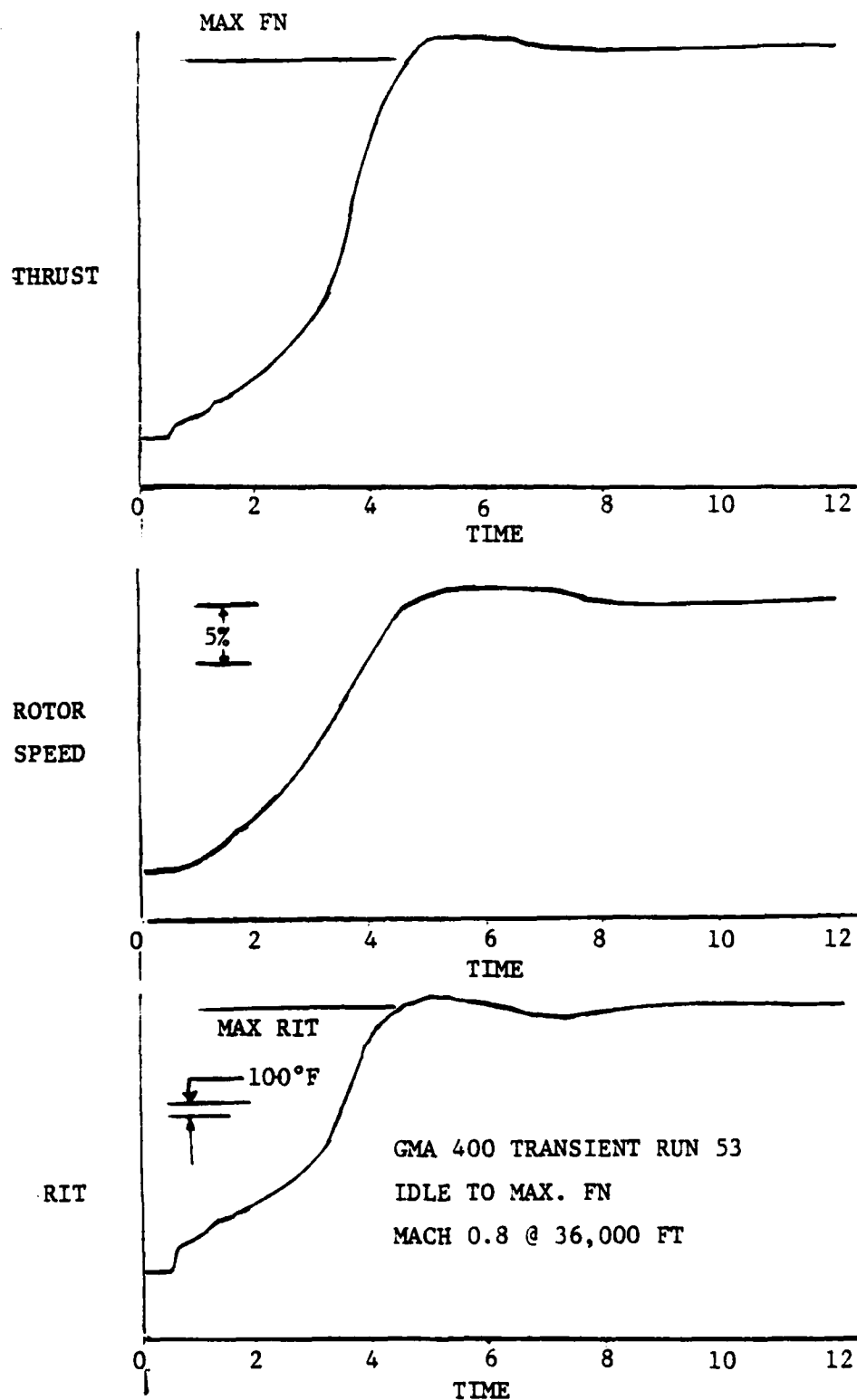


Figure 23. 0.8  $M_N$ /36000 ft. transient response - idle to maximum.

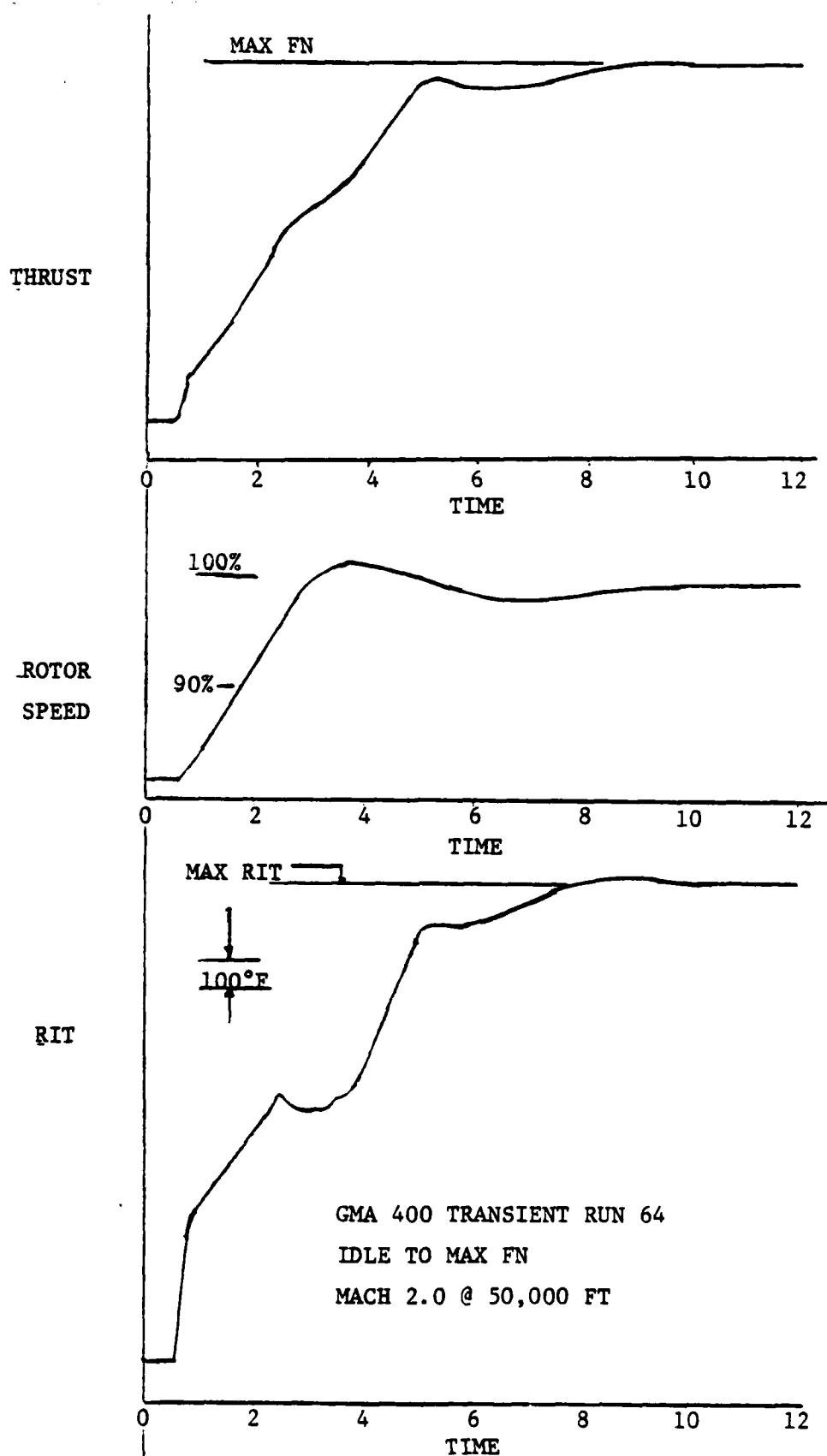


Figure 24. 0.8  $M_N$ /50000 ft. transient response - idle to maximum.

It should be noted that the definition of intermediate power is somewhat arbitrary since there is no true afterburning. This also leaves "idle" thrust which is specified as a percent of intermediate somewhat arbitrary. In this study, intermediate thrust was defined in terms of a RIT which produced an intermediate thrust that is approximately 75% of maximum thrust. Idle thrust was 10% of intermediate thrust since special "geometry spoiling" logic not in the simulation would be required to achieve lower thrusts without dropping to very low speeds.



## VIII. ANALYTICAL METHODOLOGY

The analytical methodology that was explored here involved a simplified steady-state approach for an initial screening of potential control modes as shown in Figure 25. This step does not require a detailed control design (loop gains and compensation) and is somewhat independent of the control implementation (classical or state-variable matrix control). The second step involves transient evaluation of the control modes with the engine and control dynamic simulation. At this point, a more detailed design is required. Then, the effect of dynamics--both pilot inputs and control dynamics--were investigated with respect to mission performance and engine life.

### Steady State Evaluation

The steady state evaluation begins with the development of optimized control schedules which yield "optimal" performance at a few flight conditions as shown in Figure 26. The optimization over the total thrust range is usually limited to a few carefully selected flight conditions because of the high computational cost of optimization.

The "optimized" schedules are then extended to the full flight envelope by normalizing the schedules with respect to inlet conditions. During this step, curve fits are made that compromise the optimal curves which yields "psuedo-optimal" schedules. The control schedules are incorporated into a steady-state engine simulation with a special multiple constraint system to yield steady-state engine match points for the control schedules. The control schedules may represent scheduled geometry control or closed loop geometry control on engine parameters. In the latter case, control schedules are in terms of engine parameters and geometry positions are unknown. The output of this step is a full set of engine performance data at over 300 flight and power conditions which is used for the mission performance evaluation.

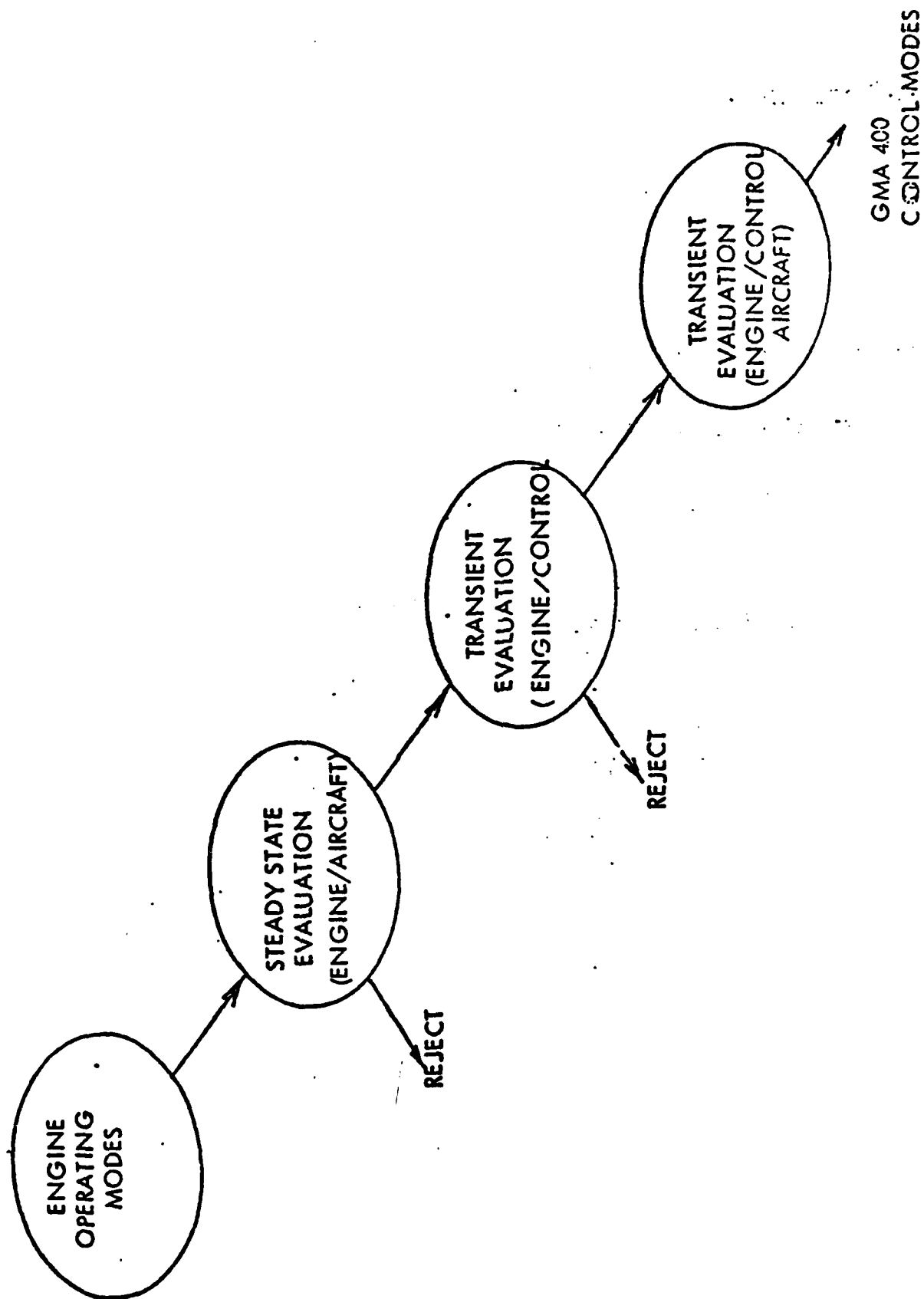


Figure 25. Basic technical approach.

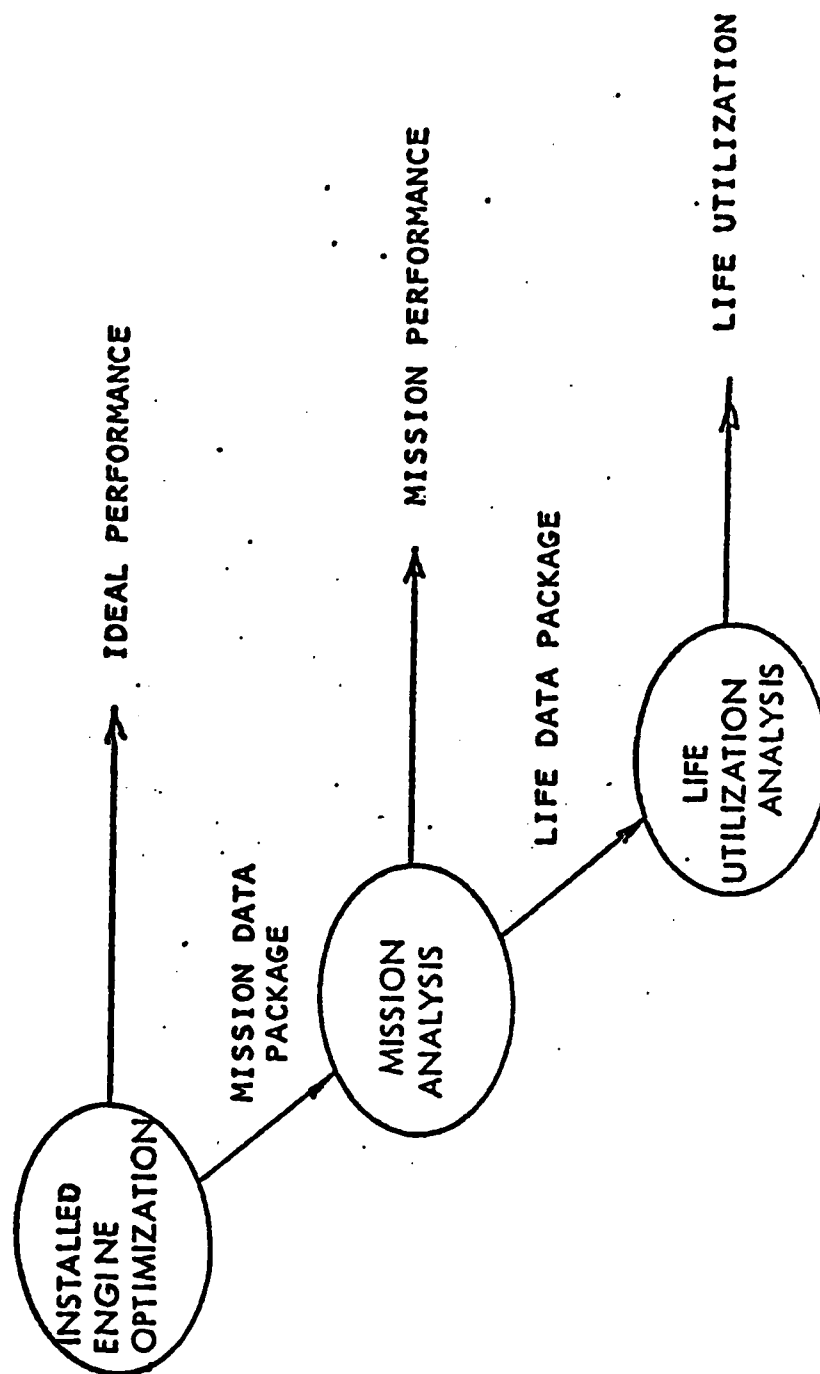


Figure 26. Steady state evaluation (engine).

The mission analysis portion of the control mode evaluations utilized the three missions described in Section III of the Task I report. During this phase of the analysis, the stick-missions with a simulated combat phase (no throttle-jockeying) as shown in Figures 27 through 29 are utilized. The analysis provides mission performance data such as

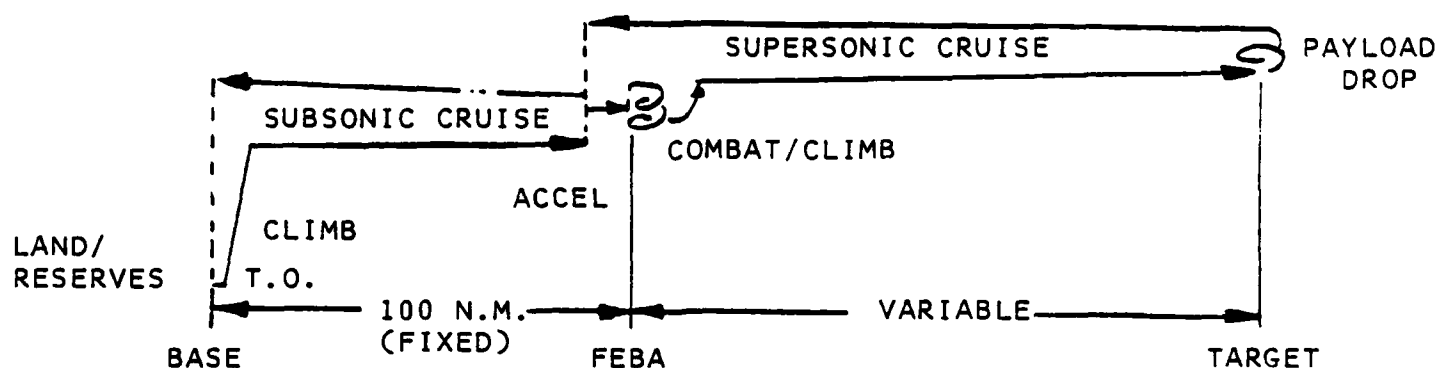
- o maximum range
- o maximum number of combat turns
- o maximum turning rate
- o maximum climb rate
- o maximum accel rate

as well as a time history of critical engine parameters for the life utilization portion of the control mode evaluation.

The life utilization analysis computes the percent life consumed for the turbine blades and vanes due to stress rupture and low cycle fatigue as well as mechanical cycles for the turbine wheel as shown in Figure 30. The computation methodology was developed outside this program and has been validated with TF41 test data. From a control analysis view point, it is important that the control designer understand the assumptions and workings of the program in order to draw correct conclusions. For instance, the DDA life evaluation program has the cooling air schedules built into the thermal analysis which limits control mode studies in this area. The details of the different analysis programs are covered in Section I.

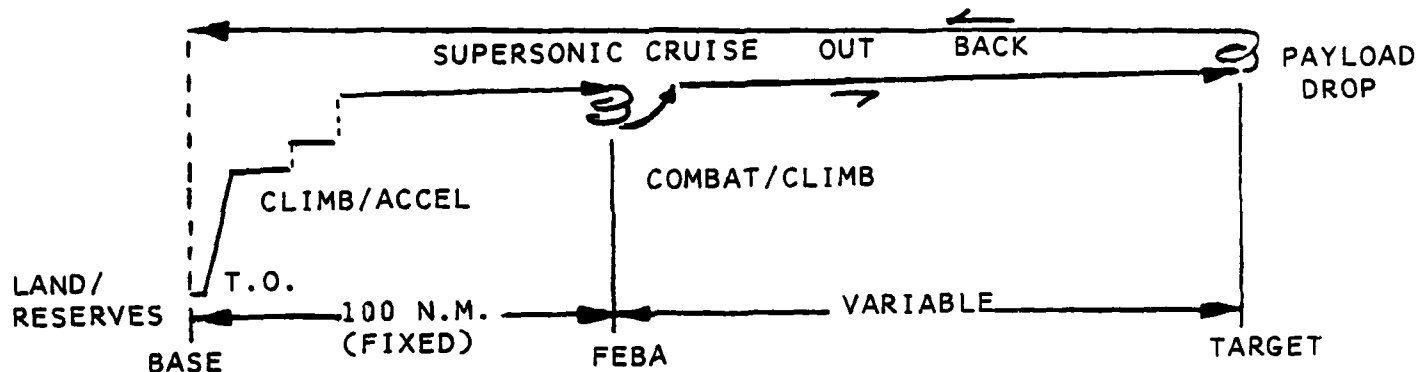
### Dynamic Analysis

The final step is the evaluation of the effect of dynamics on the performance, stability and life utilization evaluation of the control modes. The first step is the effect of control dynamics on the engine response with different control modes. Since this is a step common to all control design and analysis procedures, this portion of the methodology will not be discussed in great detail. It's major effects are in the areas of stability (surge margin during accels) and the life consumption of overshoots.



- MISSION FEATURES:
- O START WITH FULL INTERNAL FUEL
  - O 15 MINUTE TAXI/WARMUP
  - O CRUISE AT CONSTANT MACH NUMBER AT BEST ALTITUDE FOR MAX RANGE
  - O 5000 LB. PAYLOAD
  - O 20 MINUTE LOITER BEFORE LANDING
  - O 5% MISSION FUEL RESERVE

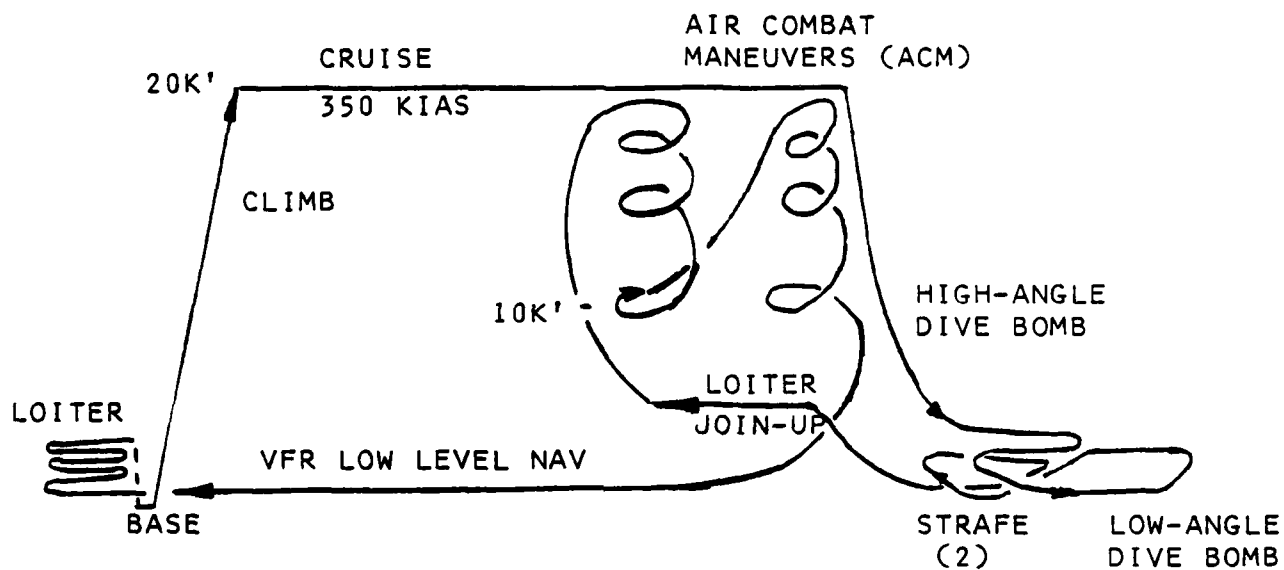
Figure 27. Deep strike mission.



MISSION FEATURES:

- O START WITH FULL INTERNAL FUEL
- O 15 MINUTE TAXI-WARMUP
- O CRUISE AT CONSTANT SUPERSONIC MACH NUMBER AT BEST ALTITUDE FOR MAX RANGE
- O 5000 LB. PAYLOAD
- O 20 MINUTE LOITER BEFORE L. NDING
- O 5% MISSION FUEL RESERVE

Figure 28. Supercruiser mission.



- MISSION FEATURES:
- O FUEL LOAD = TOTAL MISSION FUEL + 5%
  - O 15 MINUTE TAXI/WARMUP
  - O MANUAL CRUISES, CONSTANT KIAS, ALTITUDE
  - O DISTANCE TO WEAPONS RANGE 100 N.M.
  - O 2000 LB. PAYLOAD (2 - 1000 LB. DROPS)
  - O 10-15 MINUTES OVER WEAPONS RANGE
  - O 10 MINUTE LOITER BEFORE LANDING

Figure 29. Training mission.

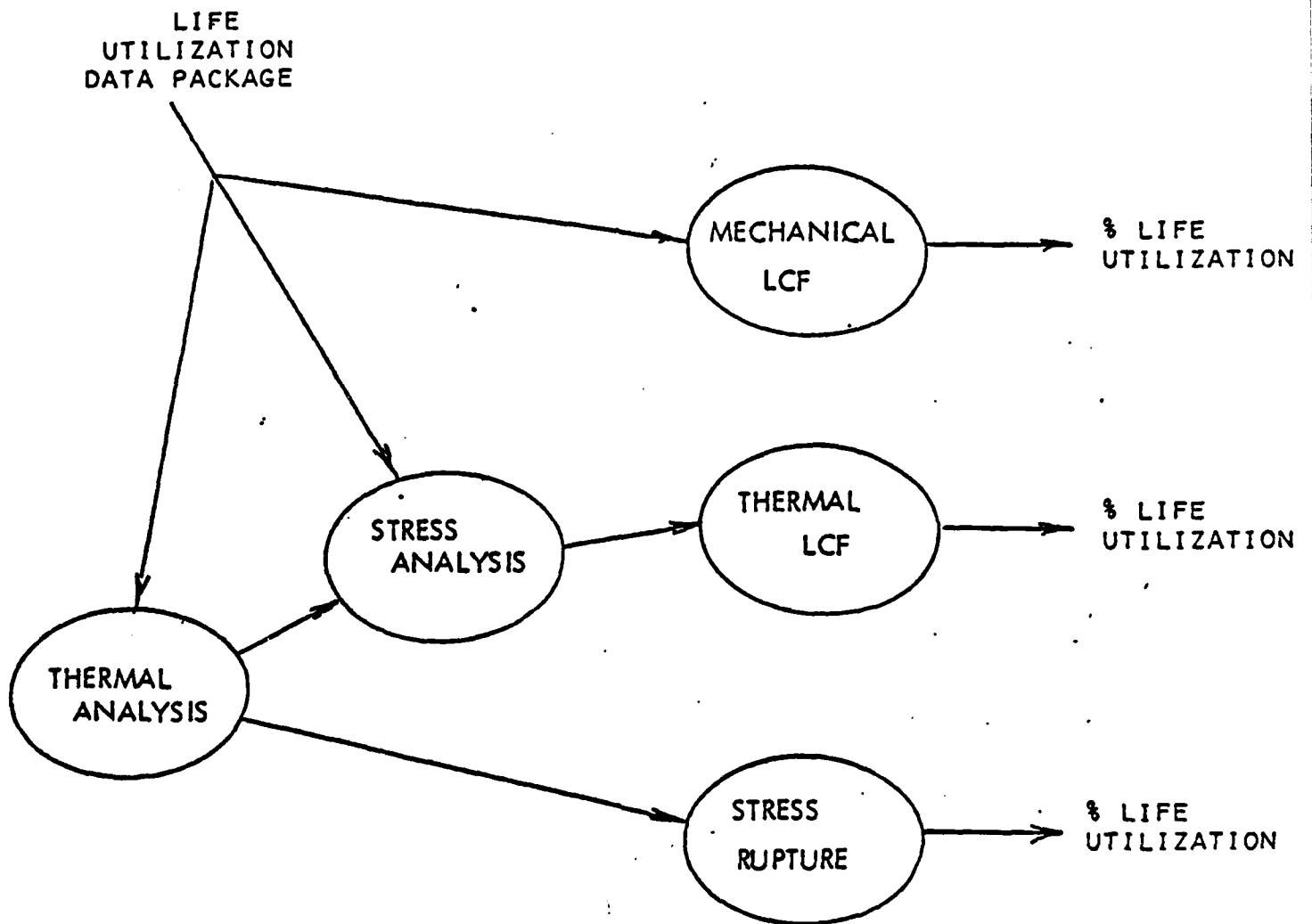


Figure 30. Life Utilization Analysis.



The other area of concern is the evaluation of pilot "throttle-jockeying" on mission performance and life consumption. Here, the steady-state engine data package generated earlier is utilized with missions which include pilot dynamics as described in the Section III report to determine the effect of these dynamics. The mission analysis and life utilization analysis proceeds the same as outlined above for the steady-state analysis with this new dynamic mission definition. The life utilization effects of control dynamic transients are also evaluated and blended into the overall analysis as shown in Figure 31.

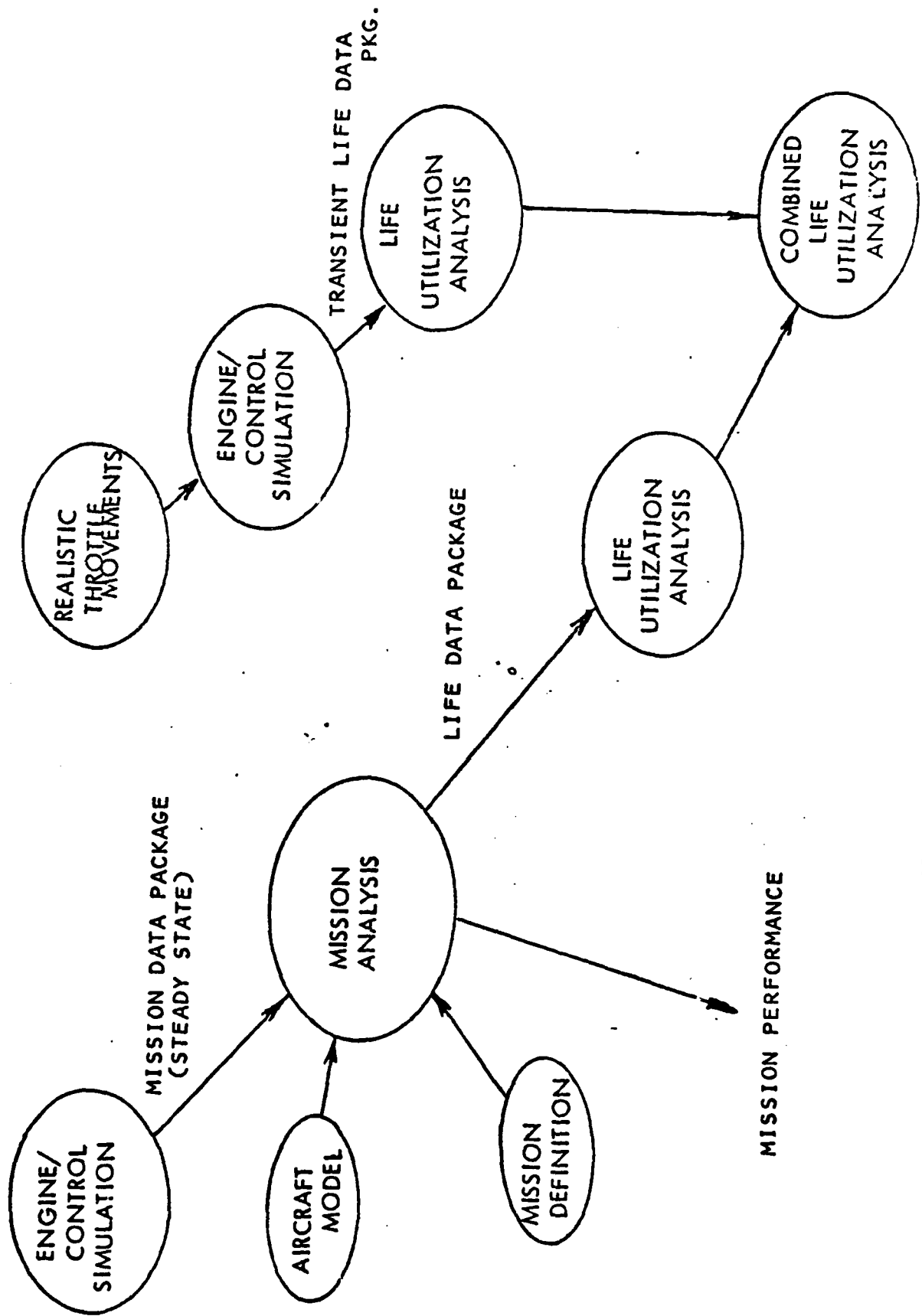


Figure 31. Dynamic Analysis.

AD-A127 503

PERFORMANCE LIFE AND OPERABILITY TRADE-OFFS IN VCE  
(VARIABLE CYCLE ENGINE. (U) GENERAL MOTORS CORP  
INDIANAPOLIS IN DETROIT DIESEL ALLISON DI.

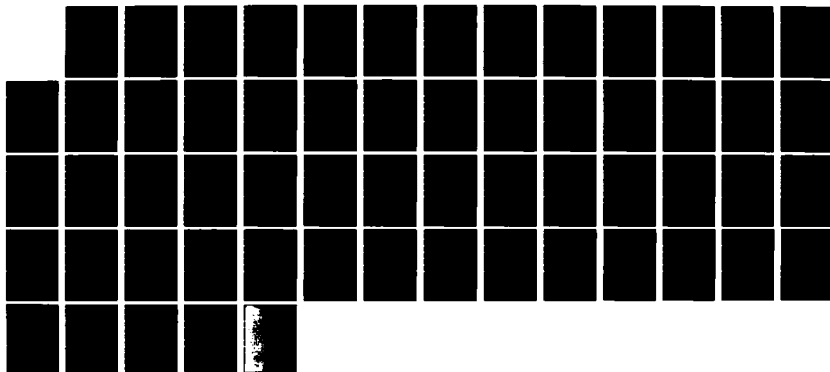
2/2

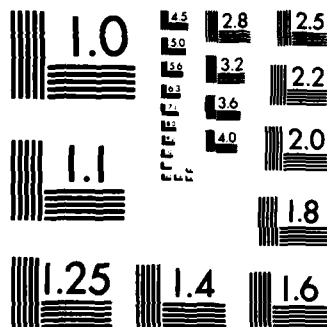
UNCLASSIFIED

DDA-EDR-10456 AFMAL-TR-81-2060

JUL 81  
F/G 21/5

NL





MICROCOPY RESOLUTION TEST CHART  
NATIONAL BUREAU OF STANDARDS-1963-A

## IX. ANALYSIS TOOLS

### Introduction

A major goal of this program was the expansion of the analysis tools available to the control engineer for evaluation of different control modes. The thrust of the work here was the modification of analytical tools developed and used outside the controls area and application of these tools to control mode evaluation rather than the development of totally new programs. The programs utilized here fall into three categories:

1. Steady-state engine performance
2. Mission analysis
3. Life utilization

The steady-state engine performance digital program was developed by the performance analysis group principally for engine sizing, design point calculations, and performance data calculations including off-design point optimization. This digital computer program was modified here to allow full flight envelope steady-state evaluation of control modes in an economical manner.

The mission analysis programs were developed by the preliminary design area to "design" variable engines and aircraft for fixed missions. The programs were modified to "design" variable missions for a fixed engine (control mode) and aircraft.

The life utilization programs were developed for the evaluation of different engine designs against life design goals. These programs were generally used without modification except to overcome computational difficulties generated by a particular control mode.

## Steady-State Performance Deck

DDA computerized steady-state performance programs are designed on the building block concept and consist of a controlling logic routine which links a system of generalized component subroutines into any desired type of engine configuration defined by inputs (see Figure 9). Additional specialized calculations can be easily and efficiently incorporated with only minor modification which allows maximum flexibility in studying a variety of cycle arrangements. The system also features rapid cycle matching procedures and direct transfer from design point to off-design calculation modes.

Transient analysis of a system is rapidly accomplished by interfacing additional dynamic routines with the steady-state simulation. These additional routines perform the control of time functions, rotor dynamics, and heat storage effects to produce engine response time history characteristics. Thus, the dynamic simulation is achieved with little change to the steady-state model and makes maximum use of component characteristics prepared for the steady-state analysis.

The engine definition as contained in CYCLE and its associated subroutines remains unchanged for the various modifications required for control analysis. This structure is especially beneficial during the early engine design phase since engine definition changes are automatically picked up by the control designer. However, the control designer must be constantly aware of engine changes to properly evaluate control mode changes. Detailed description of the engine simulation is found in Section V.

### Basic Cycle Match

The cycle match within the ENGINE subroutine essentially does an iteration on a set of variables to satisfy a set of error equations and constraint equations. For a steady-state "match point", the error equations consist of the continuity equations and the horsepower balance equation. For transient

conditions, the horsepower equations and speed variables are dropped and rotor dynamics are used to provide the horsepower balance. The multiple constraint system is employed to provide greater flexibility in the steady-state mode. In general, the required selection of cycle match variables and equations, as well as the constraints, is made by program inputs without reprogramming. The ENGINE subroutine calls the CYCLE routine for its description of the engine. This subroutine structure allows easy changes to the engine definition by the performance analysis section during the preliminary design.

### Expanded Capability

The cycle match was expanded to include many extra features like engine parameter optimization, control geometry optimization, and steady-state performance evaluation for control geometry position schedules and control engine parameter schedules. Although the same CYCLE routine is preserved, the above ENGINE subroutine disappears because it is necessary to integrate the cycle-match, multiple constraint system, and optimization program for efficient computation. Also, design point computations require a different variable set-up for the cycle-match.

The normal steady-state option can be utilized to determine engine match points with control schedules when the control schedules specify geometry positions. However, the constraint system is utilized when the control schedules are in terms of engine parameters (i.e., speed governor for fuel flow). For a VCE, multiple constraint systems are required so that a particular constraint (engine parameter) can be associated with a particular geometry variable. This approach will yield the same answer as a full engine/control system dynamic simulation running transiently until steady-state is reached if the control loops have integrators to achieve zero steady-state control errors. This is true even if engine limiters are reached since the constraint system holds the engine limit while the geometry moves to a physical limit in an attempt to satisfy the control schedule.

This procedure begins with the steady-state engine model and affects only the size and definition of the Newton-Raphson matrix, independent variables, and constraints. The number of cycle independent variables, (rotor speed, compressor operating line, etc) is increased to include all of the control variables utilizing the indirect method of control. Control variables expressed explicitly in the control schedules can be included in the cycle equations and need not be added to the iteration variables.

The steady-state portion of a control system is incorporated into the engine model. A schedule for each dependent variable (engine pressure ratio, compressor pressure ratio, etc) is maintained in the model by each independent control variable. Constraints for engine limits (turbine temperature, compressor discharge pressure, etc.) and geometry maximum and minimum settings override these schedules when limits are exceeded. Thus, a steady-state match point is defined as not only having flows and shaft horsepower balanced, but also satisfying either the control steady-state schedules or the engine and geometry limits.

The only deficiency in this approach is the inherent assumption that all the control loops are perfect with zero steady-state errors which implies integrator or high dc gain control loops. This limitation is more than offset by the simulation cost savings of this approach--360 data points throughout the flight envelope cost less than 20 steady-state points obtained with the full engine/control dynamic simulation. While these assumptions are acceptable during the preliminary design phase, severe system difficulties can arise when these effects are neglected in the final selection of the schedules and control mode.

### Mission Evaluation

Once the engine and control system performance is known throughout the flight envelope, the performance evaluation phase is limited only by the tools available from the initial engine sizing and cycle definition efforts. These fall into two general categories:



- (1) Engine sizing condition
  - a) acceleration times
  - b) climb rate
  - c) turning rates
- (2) Mission performance
  - a) mission range
  - b) combat turns
  - c) combat engagements
  - d) excess power available

The existing DDA program was developed to size an aircraft-engine combination to meet fixed mission requirements as depicted in Figure 32. The problem to be solved here was the inverse--design a variable mission for a fixed aircraft-engine combination. This was accomplished by modifying the program as shown in Figure 33 which essentially eliminated one iteration loop of the original program and changed the iteration variables for the second loop. Some of the initial sizing computations were also retained which gave additional performance data in terms of aircraft climb and accel times.

#### Life Utilization

The level of stress in a given compressor component is proportional to the square of the rotor speed. These mechanically induced stresses (cycling rotor speed) may cause low cycle fatigue in the compressor section. Although other failure mechanisms may cause minor damage, the critical consumption of life is the result of this low cycle fatigue. Therefore, the rate of compressor life utilization can be obtained from a time history of the compressor speed and a damage map for the given compressor (see Figure 34). The nature of the aircraft and mission, along with the associated performance and control aspects, provides a time history of rotor speed for each control to be studied. The rotor speed history is then input to a damage map generated for a given component at a given temperature to determine how much life of the component has been consumed by the mission. Each mission stress cycle must be assessed

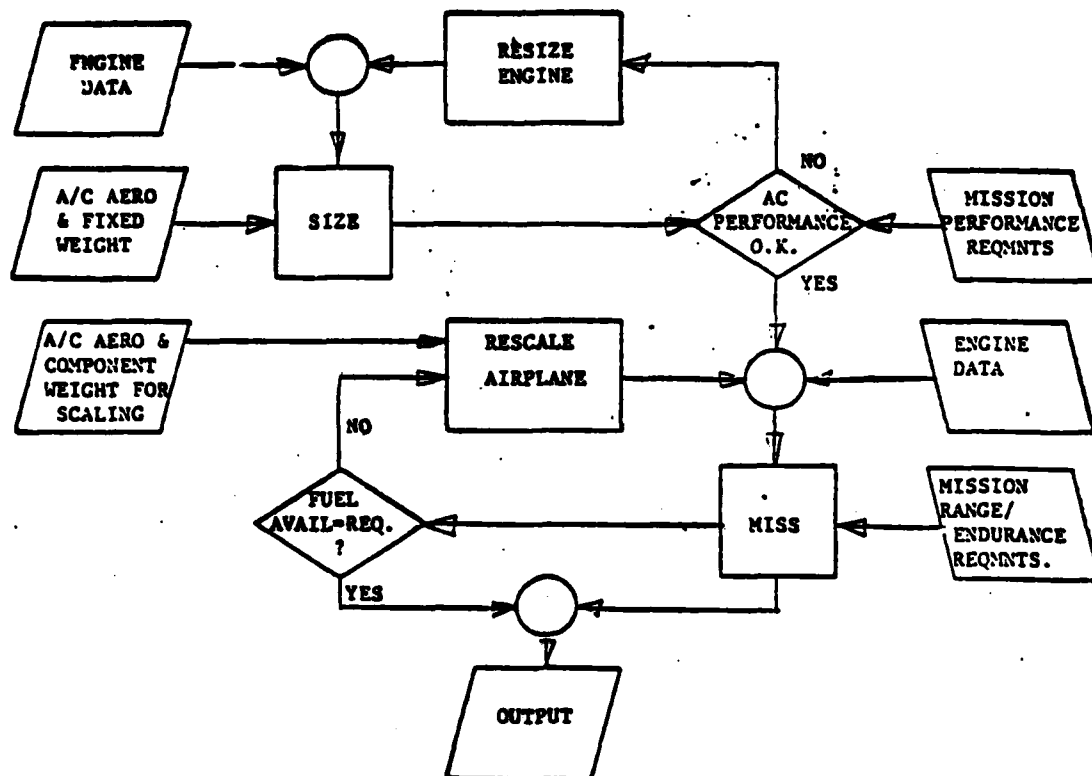


Figure 32. Variable engine mission analysis program.

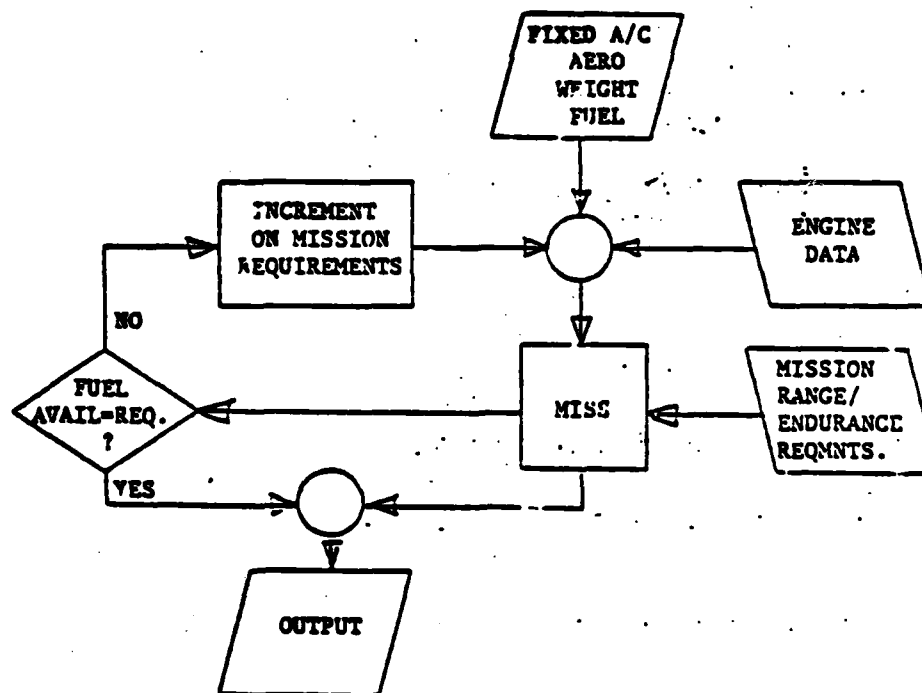


Figure 33. Fixed engine mission analysis program.

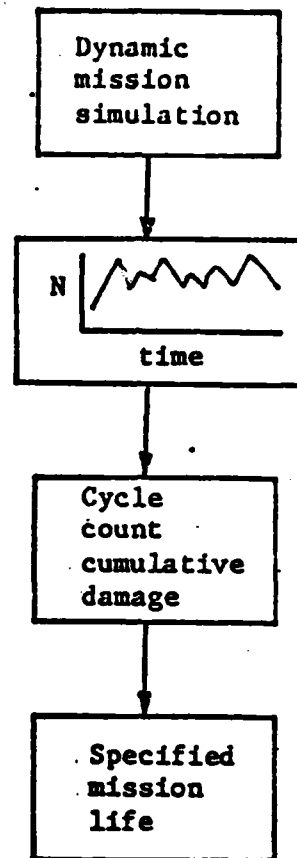


Figure 34. Mechanical LCF.

individually for damage and then converted to the equivalent number of zero-to-max cycles that produce the equivalent damage.

The equivalent zero-to-max damage cycles are additive, so any sequence of stress max and min points may be examined by conversion to damage cycles, via a damage map, and produce thereby a total count of damage-effective equivalent reference cycles corresponding to the original sequence. Because the total life capability expressed in equivalent reference cycles is known for each component, the percent of life consumed and total life of the component in mission hours can be computed.

Figure 35 is a schematic of the logic used to determine the predicted life capability of airfoil components which are subjected to thermally induced low cycle fatigue. Note that the logic is somewhat more complex than that for mechanically induced LCF for two reasons: (1) the stresses which cause damage to the part are now a function of thermal conditions as well as mechanical aspects, which include speed and pressure loads, and (2) the low cycle fatigue properties of a material are temperature dependent. This failure mechanism is most prominent in many areas of the turbine section of the engine because of the large temperature gradients as well as large variations in temperatures and loads that may exist.

The performance analysis of the dynamic mission which produces a time history of rotor speed for the mechanical LCF will also generate time histories of turbine inlet gas temperature (TIT) and pressure (TIP), compressor discharge air temperature (CDT) and pressure (CDP). Local airfoil gas and coolant temperatures are related to TIT and CDT by linear relationships. Steady-state metal temperatures of a film or impingement cooled component are generated from local airfoil gas and coolant temperatures by means of the cooling effectiveness,  $\eta$ , which is a constant. The temperature scaling process for transpiration cooled (Lamilloy)\* components is somewhat more complex depending on

---

\*Lamilloy is a registered GM trademark

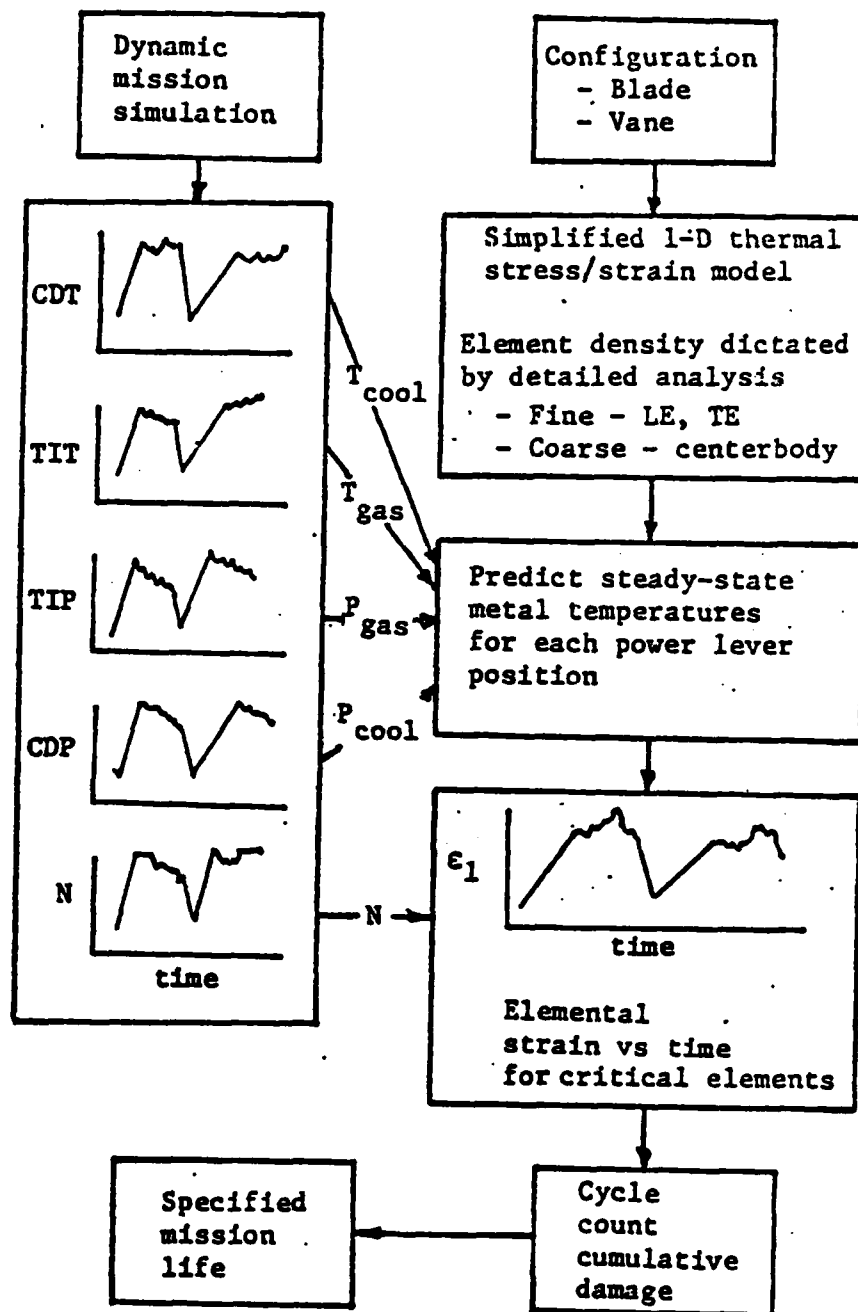


Figure 35. Thermal LCF.

time histories of coolant and gas pressures as well as temperatures. Ultimately, a cooling effectiveness,  $\epsilon$ , is computed from which local element metal temperatures are computed.

The stress/strain state of the component is determined by a simplified model employing one-dimensional thermal stress/strain theory. The model is selected to be simple and inexpensive to run on the computer because the stress/strain state must be evaluated at each moment in time that represents a significant change in either mechanical or thermal conditions. The entire mission is scanned, and stresses/strains are determined for each of these key conditions. From these analyses, the time history of strain for each element location of the component can be determined and evaluated by a cycle counting procedure and a cumulative damage model. The result is the specified-mission life of components which are subjected to thermally induced low cycle fatigue.

The third failure mechanism that is of concern is stress rupture. The logic used to determine the specified-mission life of components which are subjected to stress rupture is similar to the logic used for thermally induced low cycle fatigue. The damage incurred by a component for this mechanism, however, is the result of a continuous high stress at temperature rather than a cycling of stress. Time histories for turbine inlet gas temperature, compressor discharge air temperature, rotor speed, and metal temperature are determined as before.

Because the stress rupture life of an airfoil is assumed to be based on the average section stress (as well as the average section temperature), the stress level is related to rotor speed only. (Average section thermal stresses and gas bending stresses are always zero). This allows a time history of stress to be generated from the history of rotor speed as for the mechanically induced LCF logic. A time history of metal temperatures can be generated from the information of  $T_{\text{gas}}$ ,  $P_{\text{gas}}$ ,  $T_{\text{cool}}$ , and  $P_{\text{cool}}$  in conjunction with the cooling effectiveness,  $\epsilon$ . With the stress and metal temperature as a function of time and with standard Larson-Miller curves relating metal temperature and stress to life, the resultant stress rupture life of the component for the specified mission is determined.

## X. STEADY STATE RESULTS

Experience with the GMA200 ATEGG and GMA200 JTDE control systems has shown that the maximum benefit is obtained from the VCE variable geometry when it is used for closed loop control of engine parameters rather than scheduled (AFAPL-TR-76-49). Therefore, the first step in the design of a control mode is the selection of the engine parameters to be controlled. The next step is the assignment of engine parameters to variable geometry loops and the computation of control loop compensation parameters based upon linear analysis. Finally, control performance is verified and control parameters adjusted on a full range nonlinear engine/control simulation. Generally control mode evaluation is based upon engine and control performance. Here, the performance will be expanded to include mission performance and engine life as well as engine performance and stability.

### Control Mode Development

#### Selection of Control Parameters

Several candidate baseline control systems were investigated. Direct scheduled geometry control had an acceptable loss of performance (when compared to the optimal) over most of the operating range. However, considerable difficulty was encountered at the upper thrust region with "non-optimal" geometry settings that are incompatible with the engine limits. These findings are in line with the APSI study that proved that VCE control on engine parameters was superior to scheduled geometry. Therefore, a scheduled geometry control mode should only be considered as a back-up mode for failed sensors.

Several sensitivity programs were written to evaluate candidate engine parameters for control suitability. The dynamic sensitivity of engine parameters to control inputs was determined to assess control loop and cross coupling dynamics. This sensitivity was also used in developing linear models for the control design. Steady-state sensitivity data was generated for error evaluation. The thrust error generated by a  $10^{\circ}\text{F}$  error in turbine outlet temperature (TOT) measurement (and/or scheduling) is given by:

$$\partial F_N = \left[ \frac{\partial F_N}{\partial HPT} / \frac{\partial TOT}{\partial HPT} \right] * 10.0$$

if the HPT position is controlled by TOT.

where

$\frac{\partial F_N}{\partial HPT}$  is the thrust sensitivity to HPT errors

and

$\frac{\partial TOT}{\partial HPT}$  is the TOT sensitivity to HPT errors

Similar errors can be computed for other critical parameters such as surge margin. These errors were computed for nine candidate engine parameters.

NH	-	spool speed
T(2)	-	compressor discharge temperature
T(4)	-	turbine discharge temperature
T(11)	-	nozzle inlet temperature
WC(1)	-	compressor inlet corrected flow
WC(2)	-	compressor exit corrected flow
WC(11)	-	nozzle inlet corrected flow
P(2)	-	compressor discharge pressure
P(11)	-	nozzle inlet pressure

and the 3 control variables

$W_F$	-	fuel flow
HPT	-	turbine effective area
A8	-	nozzle geometric area

(It should be noted that the compressor geometry is scheduled on corrected speed per the JTDE studies).



The following general conclusions have been arrived at when considering thrust and surge margin error.

- (1) Speed and pressures are the best control parameters for fuel flow.
- (2) Compressor parameters are the best control parameters for the turbine.
- (3) There are many acceptable control parameters for the nozzle.

#### Baseline Control Mode

The following two candidate baseline modes were selected for further study.

##### Mode A

$W_f$  controls  $NH_c = f(PLA, T_1)$

HPT controls  $R_c = f(PLA, T_1)$  or

A8 controls  $EPR = f(PLA, T_1)$

##### Mode B

$W_f$  controls  $EPR = f(PLA, T_1)$

HPT controls  $R_c = f(PLA, T_1)$

A8 controls  $NH_c = f(PLA, T_1)$

where

$NH_c$  = corrected speed

$R_c$  = compressor pressure ratio

$EPR$  = engine pressure ratio

$PLA$  = power lever angle

$T_1$  = compressor inlet temperature

The error analysis work was expanded in two directions. First, engine life critical parameters like speed and temperatures were included. Secondly, predicted control schedule errors were added to the sensor errors. It should be noted that actuator errors do not contribute to the system errors in closed loop control because actuator position is never specified. The analysis shows Mode A better at low power, both equal at mid power, and Mode B better at high power. It is also noted that error trends noted for thrust and surge margin also hold for the engine life critical parameters.

Although the above might suggest a dual control mode, additional work in the areas of transient capability and control loop stability over the entire flight envelope led to the selection of Mode A. Thus the baseline Control Mode includes:

- |                       |           |  |
|-----------------------|-----------|--|
| a) Fuel Flow          | controls  | corrected speed as a function of PLA and $T_1$                             |
| b) HPT                | controls  | compressor pressure ratio as a function of PLA, corrected speed, and $T_1$ |
| c) Nozzle Area        | controls  | engine pressure ratio as a function of PLA and $T_1$                       |
| d) HPC Vane position  | scheduled | as a function of corrected speed   |
| e) Cooling Modulation | scheduled | as a function cooling air and local temperatures and pressures             |

#### Non-Trim Mode

An important function of a control system is maintaining the desired input/output relationship throughout variations in the plant being controlled. These variations may be through manufacturing tolerances between engines or very slow changes with respect to time due to aging. When the control cannot maintain the proper input/output relationship due to engine variations, the control is usually trimmed (adjusted) to achieve the proper input/output correlations. For today's turbine engines, the trim process is an expensive process that is usually repeated to some degree anytime a control component is replaced within the control system. The trim process is expensive in terms of maintenance time and in some cases consumes a high percentage of the engine life (an estimated 20 to 30% for the F100 engine). A majority of the trim procedure is aimed at achieving the desired or rated steady state thrust of the engine while a lesser amount of the trim is aimed at dynamic performance like accel time and transient surge margin.

Therefore, an auxiliary mode, separate from the baseline mode, which absolutely eliminates the requirements for steady-state thrust trimming was investigated. This non-trim mode will maintain the proper rated thrust in the face of expected engine variations due to manufacturing tolerances and aging. The design of this mode can be described by the following three steps.

- a) Determine the expected plant (engine) variations.
- b) Determine candidate control parameters based upon the desire to control thrust.
- c) Evaluate the candidate modes with the engine variations.

There is limited data that gives a history of engine parameter variations due to manufacturing tolerances. The following parameter variations for more than 300 production TF41 engines are plotted in TDR AF.0021-122 by K. Keefer dated 4/12/77.

<u>Parameter</u>	<u>Variations</u>
HPC efficiency	<u>+1.8%</u>
Compressor pressure ratio	+1%, -2%
HP speed	+1%, -.4%
RIT	+1.5%, -1.0%
EPR	<u>+1.0%</u>

It is more difficult to assess the effect of aging on engine component performance. There is no TF41 data for a depreciated engine that yields performance data before and after a repair or overhaul -- only after the overhaul. However, a NASA project with P&W involving the JT9D engine does give limited insight into this area. This work involved engine testing and simulation (modeling) efforts. Some of the conclusions of this program are

- (1) "Very little loss is noted in the high pressure compressor module."

- (2) "The high pressure turbine module exhibits rapid losses in efficiency in the short term, followed by more gradual long-term losses. A greater variation exists between engines in terms of efficiency loss for this module than any other."
- (3) "Post-repair analysis generally show improvements in the HPT with lesser improvements in the cold sections, although generalization is difficult because of the uniqueness of individual engine repairs."

Additional discussions were held with the compressor, burner, and turbine designers which lead to the following conclusions.

- (1) Compressor efficiency build variations generally occur equally distributed between gains and losses while aging will generally decrease efficiency.
- (2) Compressor flow and pressure ratio variations generally occur much more towards the negative side.
- (3) Turbine efficiency changes are similar to those of the compressor with aging effects being more severe.
- (4) Turbine flow variations tend toward the plus side.
- (5) Burner pressure drop variations are small.

Therefore, the following component performance variations were assumed to study the effect of "plant changes" on engine performance with different control logic.

<u>Parameter</u>	<u>Variations</u>
Compressor efficiency	+2%, -2%
Compressor flow	+1%, -3%
Compressor pressure ratio	+4%, -4%
Turbine efficiency	+2%, -2%
Turbine flow	+2%, -1%
Burner pressure drop	+1%, -1%

The non-trim mode must control parameters more closely identified with the desired end product -- net thrust. Although net thrust depends on several non-engine parameters such as inlet and aircraft drag, gross thrust can be linked more directly to engine parameters. The major contributors to the gross thrust calculation are nozzle airflow and expansion ratio. The baseline control comes close to this since compressor corrected speed and pressure ratio determine a nominal airflow at the compressor inlet and engine pressure ratio approximates the nozzle expansion ratio except for inlet and nozzle properties. If a stronger interface is taken between the inlet and engine control, it may be possible to obtain a better approximation to the nozzle pressure ratio than engine pressure ratio. However, this error is non-existent at the normal trim condition - static sea level. Thus, EPR was retained in the non-trim mode.

The errors introduced by assuming a nominal flow characteristic for the compressor can be reduced if the nozzle flow can be controlled directly by the geometry. Application of the error analysis techniques discussed with the baseline mode and consideration of control loop stability problems yielded the following non-trim mode.

- |              |          |  |
|--------------|----------|--|
| a) Fuel Flow | controls | corrected speed as a function of PLA and $T_1$       |
| b) HPT       | controls | engine pressure ratio as a function of PLA and $T_1$ |

c) Nozzle Area	controls	nozzle flow as a function of PLA and $T_1$
d) HPC Vane position	scheduled	as a function of corrected speed
e) Cooling Modulation	scheduled	as a function cooling air and local temperatures and pressures

For the scheduled geometry control mode, the thrust deviations exceeded 5% and the TIT reached its maximum trim tolerance in 4 cases as seen in Table VI. The effect on surge margin was minimal. It must be remembered that these errors are due to engine variations only and do not include control errors in measurement, schedules, etc. Therefore, a scheduled geometry would require trimming for combined engine and control variations and can generate engine and control stability problems noted earlier.

Subjecting the baseline control mode to the same engine variations (Table VII) reduced the thrust deviations to less than 3.5% while generally preserving surge margin (the mode attempts to hold a point on the compressor map). In this mode, trim due to engine and control variations may be required.

In Table VIII, the non-trim mode was subjected to the above engine variations with less than a 1% deviation in thrust. However, there was a significant loss in surge margin in some cases and the TIT ( $T_4$ ) reached or exceeded its maximum trim value (the simulation failed when the TIT limit was enforced on  $T_4$  for the -3% compressor flow variation). In general, this mode handles engine variations very well. However, the errors due to control errors are more than double those cited for the baseline system above, mainly because of the inaccuracy in the flow measurement. Also, the loss in surge margin due to control errors becomes significant. The error sources and surge margin problem must be reduced before the non-trim mode becomes a viable control mode.

Table VI. Scheduled Geometry Control Mode Errors Due to Engine Variations.

	Thrust Pct Dev	WF	ARED	Area(13)	SM	NH	ΔT4	T3	P3	P9
Nominal Engine	0.0	26468.	124.0	223.9	21.5	100.0	0	1215.	214.	85.5
Comp Eff +2 Pct	1.33	25514.	122.8	220.9	21.5	100.0	- 89	1202.	214.	85.5
Comp Eff -2 Pct	-1.37	27482.	125.2	227.1	21.5	100.0	97	1229.	214.	85.5
Comp Flow +1 Pct	-1.13	26826.	125.4	226.5	22.7	100.0	8	1215.	214.	85.5
Comp Flow -3 Pct	3.40	25383.	119.8	216.3	17.8	100.0	- 25	1215.	214.	85.5
Comp Pr +4 Pct	- 0.26	26670.	124.2	224.6	21.5	100.0	19	1218.	214.	85.5
Comp Pr -4 Pct	0.15	26383.	123.9	223.7	21.5	100.0	- 7	1214.	214.	85.5
Turb Eff +2 Pct	1.43	25448.	122.9	220.7	21.5	100.0	16	1215.	214.	85.5
Turb Eff -2 Pct	1.09	26577.	122.1	221.6	18.5	99.0	49	1211.	214.	85.5
Turb Flow +2 Pct	- 0.07	26419.	121.7	223.8	21.5	100.0	- 4	1215.	214.	85.5
Turb Flow -1 Pct	- 0.02	26487.	125.2	224.0	21.5	100.0	1	1215.	214.	85.5
Burner DP +1 Pct	- 0.63	26927.	125.5	225.4	21.5	100.0	37	1215.	214.	85.5
Burner DP -1 Pct	0.75	25930.	122.3	222.2	21.5	100.0	- 45	1215.	214.	85.5
Cust Bld Double	- 0.27	26692.	122.9	224.6	21.5	100.0	49	1215.	214.	85.5
Cust Bld Zero	0.27	26248.	125.1	223.3	21.5	100.0	- 47	1215.	214.	85.5
All Positive	0.26	24964.	123.0	223.3	25.1	100.0	-221	1205.	214.	85.5
All Negative**	59.51	11956.	81.8	-144.9	-27.4	85.0	49	1178.	145.	59.0

\*\* Simulation Failed

Table VII. Baseline Control Mode Errors Due to Engine Variations

	Thrust Pct Dev	WF	ARED	Area(13)	SM	NH	ΔT4	T3	P3	P9
Nominal Engine	0.0	26466.	124.0	223.9	21.5	100.0	0	1215.	214.	85.5
Comp Eff +2 Pct	2.37	25085.	124.0	223.9	23.1	100.0	-126	1198.	211.	83.8
Comp Eff -2 Pct	1.32	26517.	124.0	223.9	20.3	99.0	49	1220.	211.	84.6
Comp Flow +1 Pct	-1.82	27074.	124.0	223.9	21.1	100.0	32	1219.	217.	86.5
Comp Flow -3 Pct	5.09	24831.	124.0	223.9	22.5	100.0	-78	1204.	206.	81.9
Comp Pr +4 Pct	-0.49	26750.	124.0	223.9	21.1	100.0	27	1219.	214.	85.9
Comp Pr -4 Pct	0.27	26314.	124.0	223.9	21.6	100.0	-13	1213.	213.	85.3
Turb Eff +2 Pct	2.72	24882.	124.0	223.9	23.2	100.0	-133	1211.	211.	83.6
Turb Eff -2 Pct	1.22	26626.	124.0	223.9	20.3	99.0	49	1206.	211.	84.7
Turb Flow +2 Pct	-0.23	26937.	124.0	223.9	22.8	99.6	49	1207.	210.	85.7
Turb Flow -1 Pct	0.86	25958.	124.0	223.9	20.9	100.0	-40	1216.	215.	84.9
Burner DP +1 Pct	-0.40	26697.	124.0	223.9	20.2	100.0	21	1218.	216.	85.8
Burner DP -1 Pct	0.46	26187.	124.0	223.9	22.9	100.0	-25	1212.	211.	85.2
Cust Bld Double	1.01	26459.	124.0	223.9	22.1	99.3	49	1205.	209.	84.8
Cust Bld Zero	1.60	25505.	124.0	223.9	21.2	100.0	-105	1216.	214.	84.4
All Positive	-0.19	25240.	124.0	223.9	25.8	100.0	-199	1203.	213.	85.6
All Negative	8.61	24852.	124.0	223.9	19.0	97.5	49	1195.	199.	79.5



Table VIII. Non-Trim Control Mode Errors Due to Engine Variations

	Thrust Pct Dev	WF	ARED	Area(13)	SM	NH	ΔT4	T3	P3	WAC9
Nominal Engine	0.0	26467.	124.0	223.9	21.5	100.0	0	1215.	214.	72.5
Comp Eff +2 Pct	0.07	26419.	126.7	223.8	24.3	100.0	- 20	1195.	209.	72.5
Comp Eff -2 Pct	-0.07	26528.	121.1	224.1	18.4	100.0	23	1237.	219.	72.5
Comp Flow +1 Pct	0.22	25862.	121.1	223.4	19.5	100.0	36	1223.	220.	72.5
Comp Flow -3 Pct	-0.67	28450.	132.1	225.6	26.4	100.0	+213	1197.	199.	72.5
Comp Pr +4 Pct	-0.01	26485.	123.5	224.0	20.9	100.0	5	1219.	215.	72.5
Comp Pr -4 Pct	0.00	26476.	124.3	224.0	21.8	100.0	- 1	1213.	213.	72.5
Turb Eff +2 Pct	0.06	26427.	127.2	223.8	24.5	100.0	- 9	1208.	209.	72.5
Turb Eff -2 Pct	-0.13	26887.	122.7	224.3	19.4	99.6	49	1216.	216.	72.5
Turb Flow +2 Pct	0.01	26484.	121.9	223.9	21.6	100.0	- 1	1215.	214.	72.5
Turb Flow -1 Pct	0.02	26457.	125.0	223.9	21.4	100.0	- 1	1215.	214.	72.5
Burner DP +1 Pct	0.01	26467.	123.5	223.9	20.0	100.0	3	1219.	216.	72.5
Burner DP -1 Pct	0.04	26448.	124.6	223.9	23.2	100.0	- 5	1211.	211.	72.5
Cust Bld Double	-0.03	26643.	122.8	224.1	21.3	99.9	49	1214.	213.	72.5
Cust Bld Zero	0.02	26433.	125.9	223.9	22.1	100.0	- 33	1214.	213.	72.5
All Positive	0.73	24651.	121.6	222.3	24.0	100.0	-245	1207.	216.	72.5
All Negative **	-26.91	21308.	140.9	224.1	27.5	88.0	47	1399.	146.	73.4

\*\* Simulation Failed

## Performance Optimization

A second and somewhat independent step in the control development is determining how the engine is to be run. Here, the engine steady-state performance is optimized to some criteria--usually minimum SFC and maximum thrust. It is necessary to impose engine physical constraints (temperatures, pressures, and speed), geometry physical limits, and engine performance constraints such as minimum surge margin during the optimization. Since minimum SFC is a performance related optimization criteria, additional criteria more closely associated with engine life were sought. Ideally, one would use engine life as an optimization criteria. This is impossible since the optimization deals with steady state performance and LCF is a dynamic problem. However, compressor life is generally consumed by mechanical stress directly related to rotor speed and turbine life consumption is determined by a combination of the above mechanical stress and thermal stress produced by turbine temperatures. Thus, minimization of rotor speed and turbine temperatures could potentially increase engine component life. Unfortunately the two criteria are in opposition since minimization of rotor speed greatly increases turbine temperature and minimization of turbine temperature greatly increases rotor speed.

Thus

- o Minimum rotor speed and
- o minimum turbine inlet temperature

which represent the two extremes of "life conserving modes", were chosen for this study along with the minimum SFC criteria. The maximum thrust criteria was retained in all three cases so that maximum power is identical and the optimization affects only part-power points. (The concept of a derated engine will be introduced later which address the problem of manipulating the maximum power point to conserve engine life).

### Minimum SFC Optimization

The engine performance was optimized at six flight conditions for minimum SFC and maximum thrust. The six points were chosen to span the range of inlet pressures and temperatures in different combinations to provide adequate information for eventual normalization of control schedules to inlet conditions--a necessary step for extending this limited information to the entire flight envelope.

The min. SFC/max.  $F_N$  optimization for the installed engine was run with the following constraints:

- a) geometry physical limits and only engine speed constrained
- b) geometry and engine limited parameters constrained
- c) surge margin greater than 20% in addition to (b) above
- d) hold a single compressor operating line with 20% min. surge margin in addition to (b) above

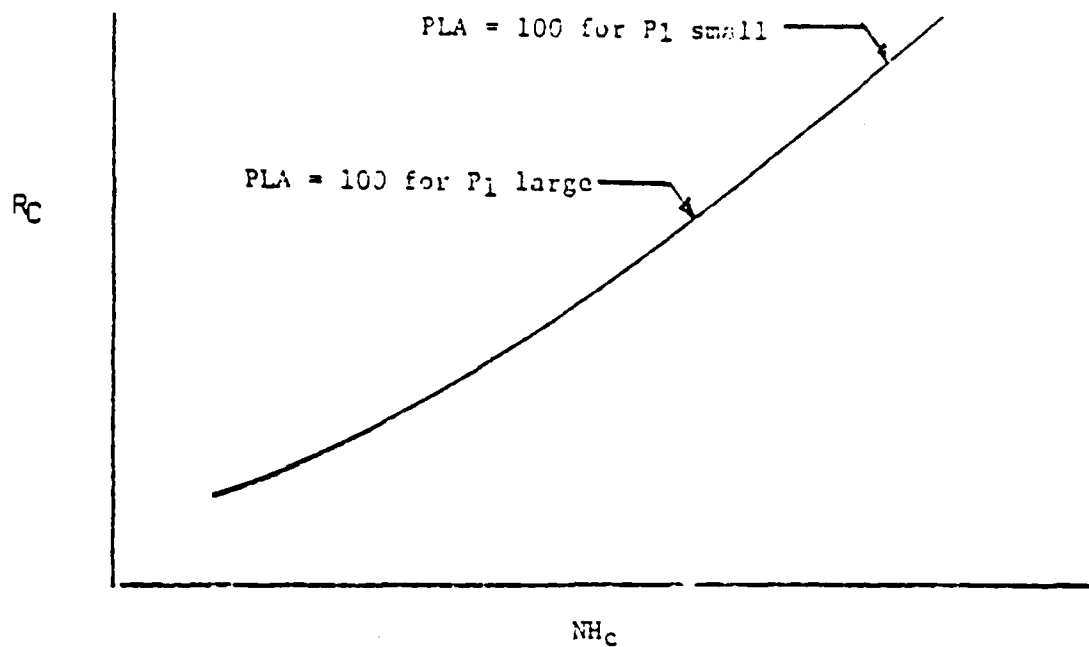
The first two cases were run to get a feel of how engine parameter limits affect the optimization. It was initially felt that ignoring the engine limits would help extend the limited optimized data over the flight envelope. That is, data run at sea level Mach 1.2 ( $T_1 = 667^{\circ}\text{R}$ ) which is restricted by compressor discharge pressure might be extended to other flight conditions with  $T_1 = 667^{\circ}\text{R}$  with a substantially lower inlet pressure, which in turn could run to a higher compressor pressure ratio. However, this was generally unsuccessful because the simulation usually operated some component in an area in which the simulation was ill defined.

While the above problem is solved by imposing the engine limited parameter constraints during the optimization, a second problem occurs. Schedules (engine parameters) described as a function of other engine parameters (namely corrected speed) are generally well behaved. However, when expressed as a function of PLA, most engine parameter schedules require some additional

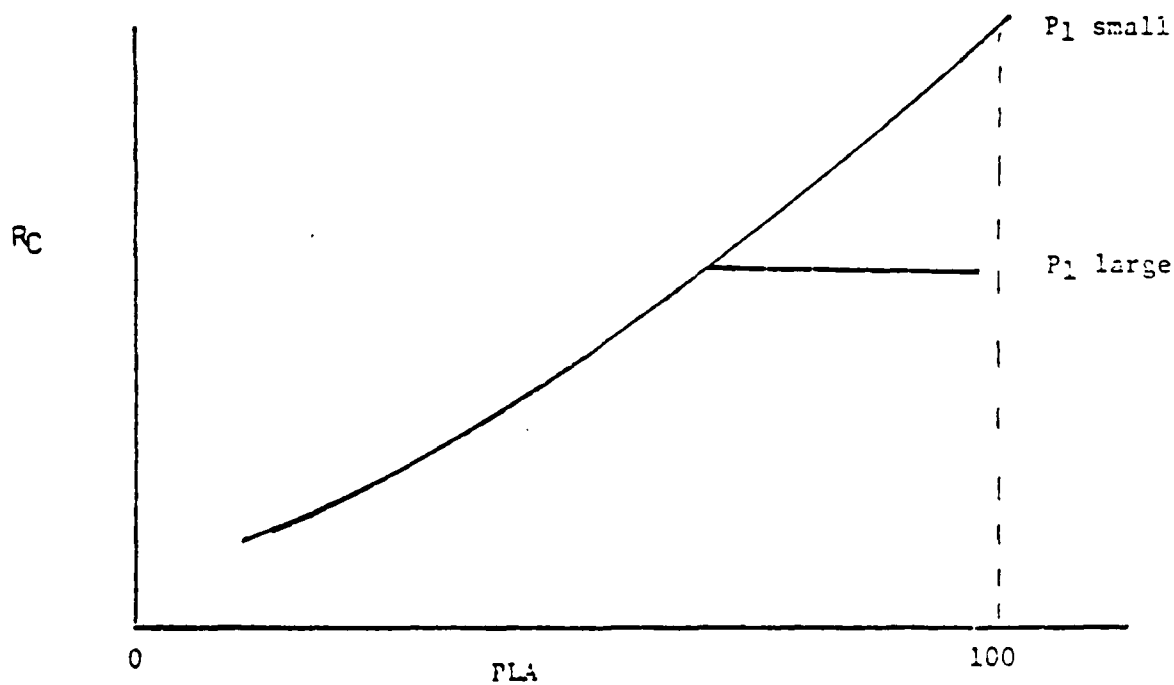
analysis as described in Figure 36. Compressor pressure ratio ( $R_C$ ) described as a function of corrected speed ( $NH_C$ ) is the compressor operating line and is independent of inlet pressure as shown in Figure 36a. However, the functional relationship between  $R_C$  and power lever angle is not unique as seen in Figure 36b. A single schedule for  $R_C$  vs. PLA can be used if an additional limiting test on compressor discharge pressure ( $P_3 = P_1 * R_C$ ) is imposed before determining the required  $R_C$ . It should be noted that corrected speed vs. PLA does not display this problem since it is the first limit reached.

Since the control design requirements specifically require a 20% surge margin, it is necessary to pick the control schedules from optimized data sets (c) or (d). The operating line for optimized data set (a) is shown in Figure 40. The single operating line is suggested very strongly except where the mechanical or corrected speed limit is reached. At this point, the variable geometry generally leaves a minimum or maximum value to hold the speed limit with increased fuel flow (thrust) and the operating point leaves the operating line. Careful study of the optimized data in this area has shown that the optimizer finds a better SFC by trading poorer compressor efficiency for higher efficiencies elsewhere, generally in the turbine. The effects of variable cooling also affects deviation from a single operating line.

However, if the operating point goes above the operating line, surge margin is often less than 20% while surge margin increases if the operating point drops below the operating line. Therefore,  $R_C$  from the optimized data set (c) is similar to Figure 37 except only the excursions below the operating line remain. Examination of this data did not uncover a simple way to describe the excursions below the operating line, so the optimized data set (d) was run as a "practical" optimized data set with the single operating line concept.



a)  $R_C$  as a function of an Engine Parameter.



b)  $R_C$  as a function of  $PLA$ .

Figure 36. Effects of engine limits.

NUMERICAL VALUES CLASSIFIED

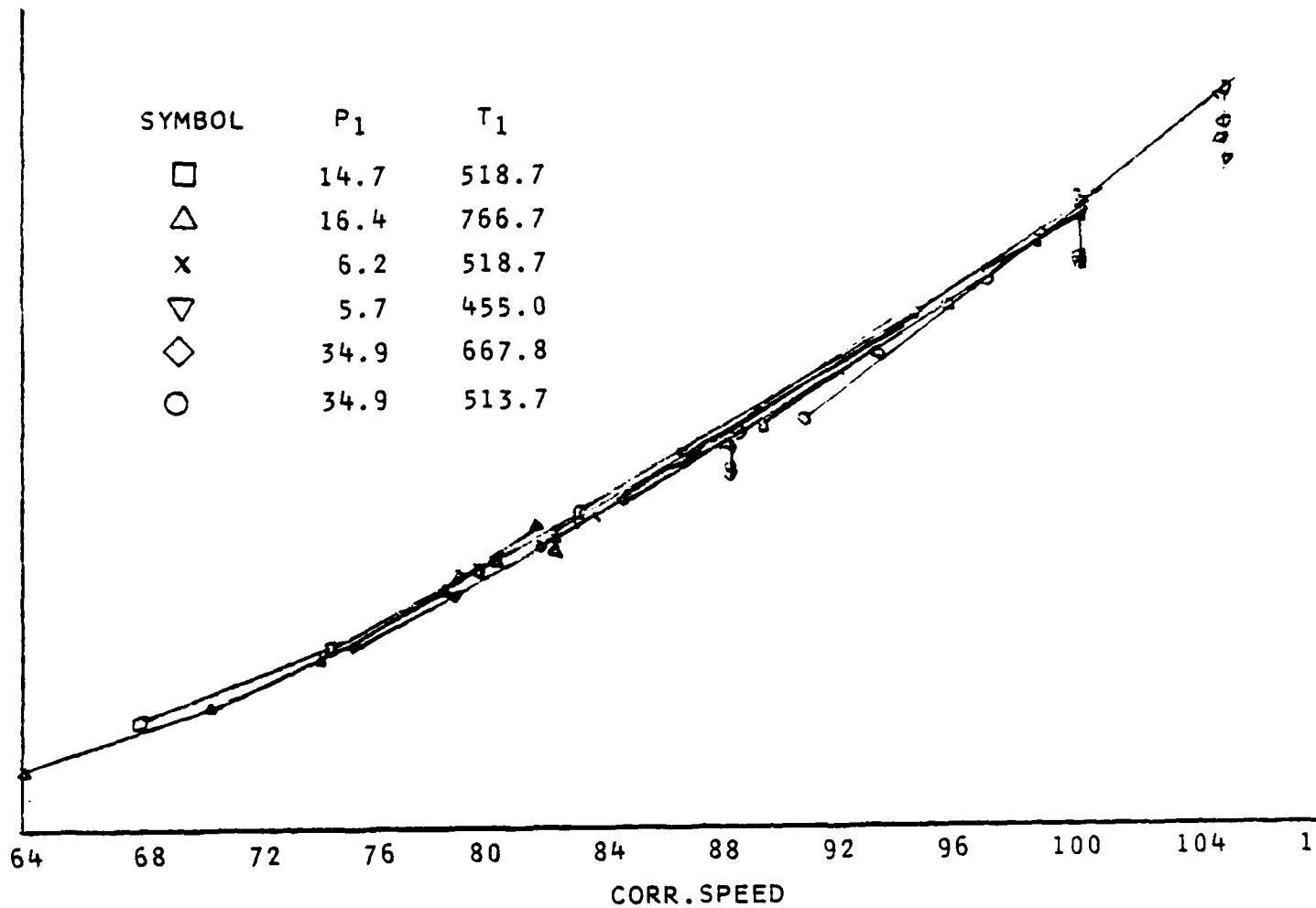


Figure 37. Installed operating line.

## Minimum Speed and Minimum Turbine Inlet Temperature

A very interesting phenomena occurred when the other two optimizations were performed--the "optimal" compressor operating line was preserved from the minimum SFC optimization. However, the actual operating point on the operating line for a given part-power condition (i.e., 90% thrust at S.S.L.) changes for each of the criteria. The minimum SFC and minimum Turbine Inlet Temperature optimization results were almost identical since they are both heavily biased towards minimum fuel flow and maximum airflow.

### Control Schedules

#### Baseline Control Schedules

The baseline control system requires the following schedules:

$NH_c$  vs. PLA for the fuel flow  
 $R_c$  vs.  $NH_c$  for the HPT  
EPR vs. PLA for the primary nozzle

Ideal performance (schedules built into the engine simulation) is assumed for the HPC, turbine blade cooling, aft cooling, and divergent nozzle area.

Since the operating line deviations generated in (c) cannot be easily described, the compressor and engine pressure ratio schedules were chosen from optimized data set (d). However, the corrected speed vs. PLA did not fit a neat family of lines vs. inlet temperature at the low power settings. There was an indication that the optimal corrected speed lines for inlet temperature between 50°F and 200°F cross each other as shown in Figure 38. However, since only the static sea level case showed a strong crossing, a second schedule shown in Figure 39 was also run to determine the performance differences between the two approximations. The optimal  $R_c$  and EPR curves shown in Figures 40 and 41 were used with the speed schedule of Figure 38 to form

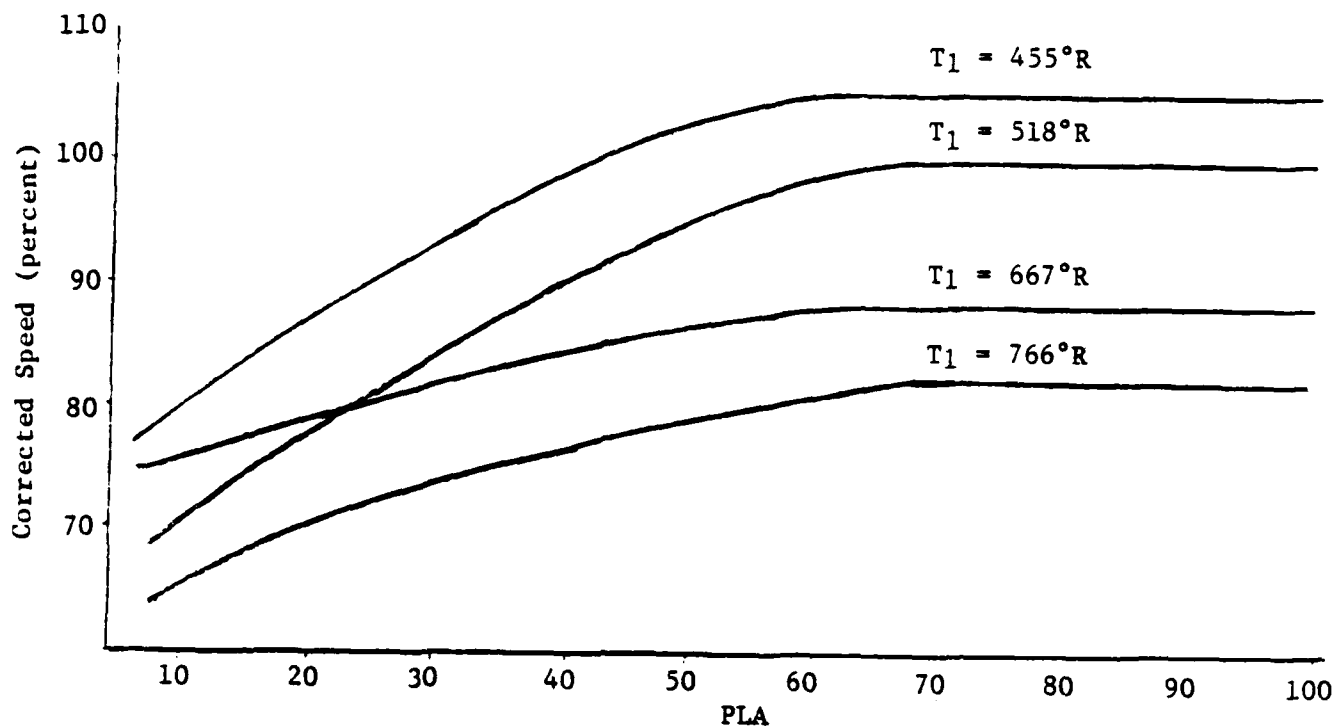


Figure 38. Speed schedule #1.

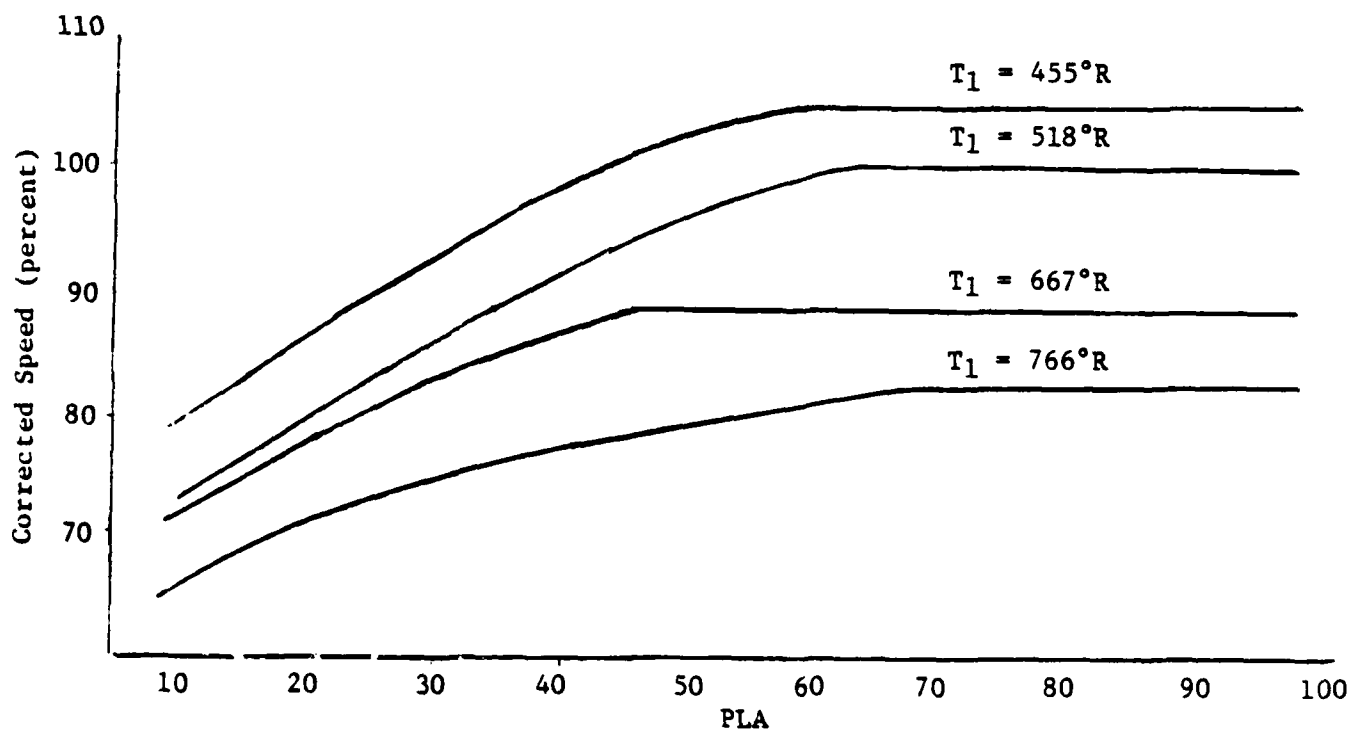


Figure 39. Speed schedule #2.



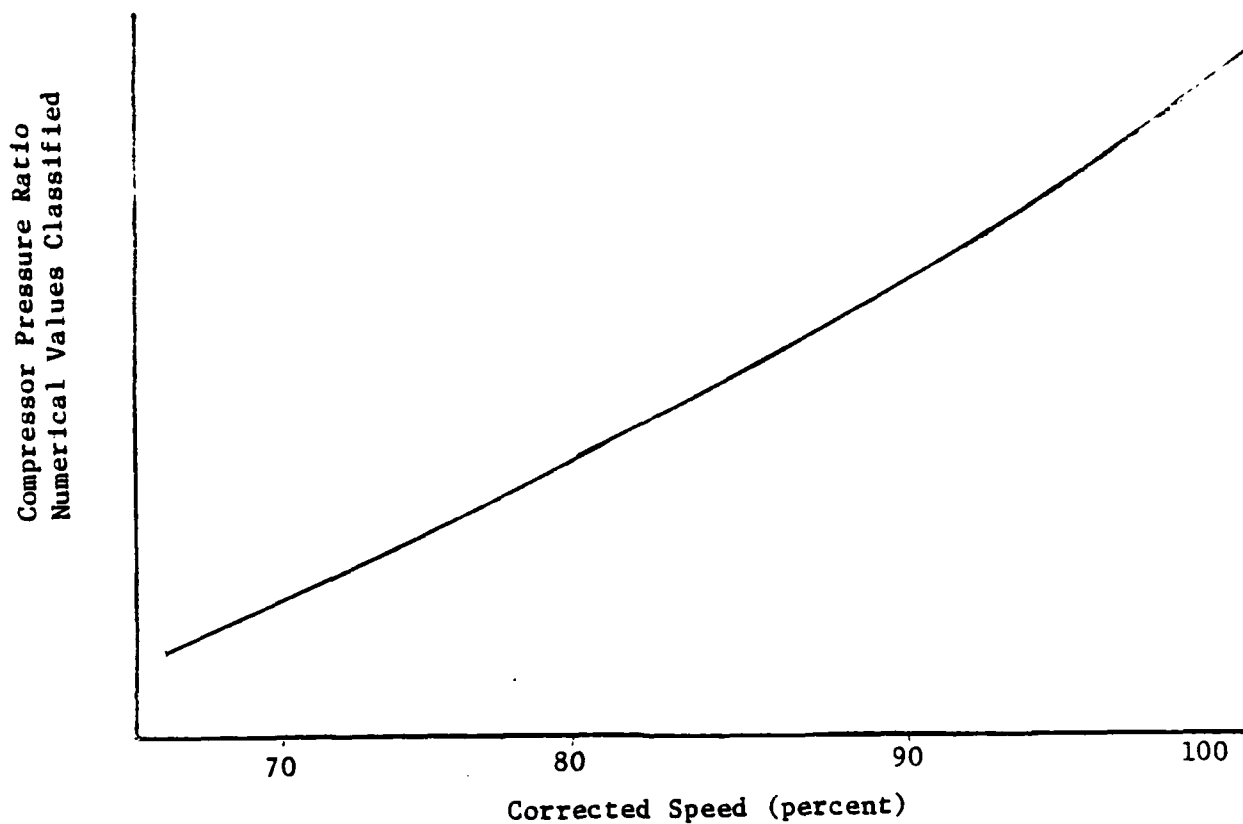


Figure 40. Operating line.

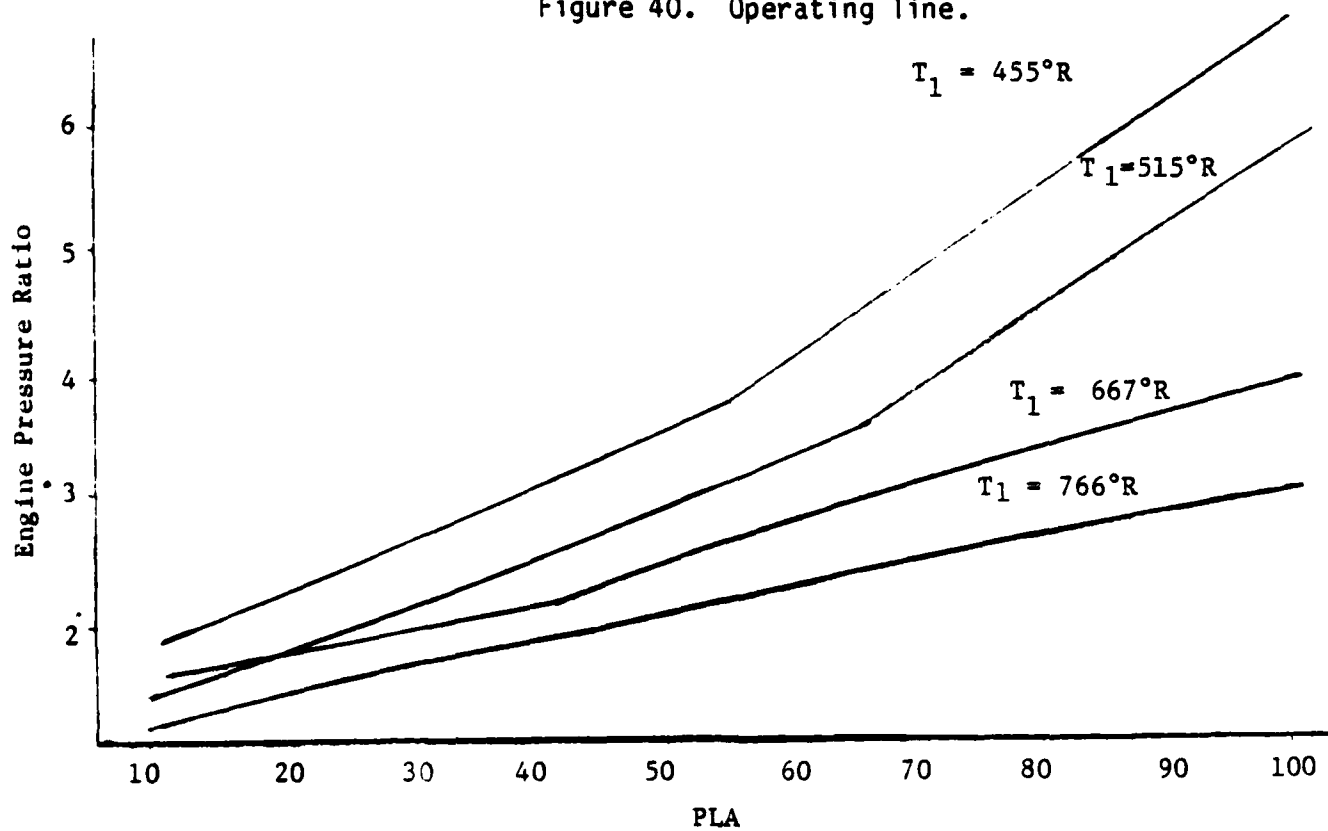


Figure 41. EPR schedule.

one baseline mode and the  $R_C$  and EPR schedules of Figures 40 and 42 were used with the speed schedule of Figure 39 to form a second baseline mode for further evaluation in the mission analysis phase. The steady state performance (thrust, surge margin, SFC, etc.) for the control schedules was also compared to the optimized to verify that general performance had not been severely compromised (especially surge margin).

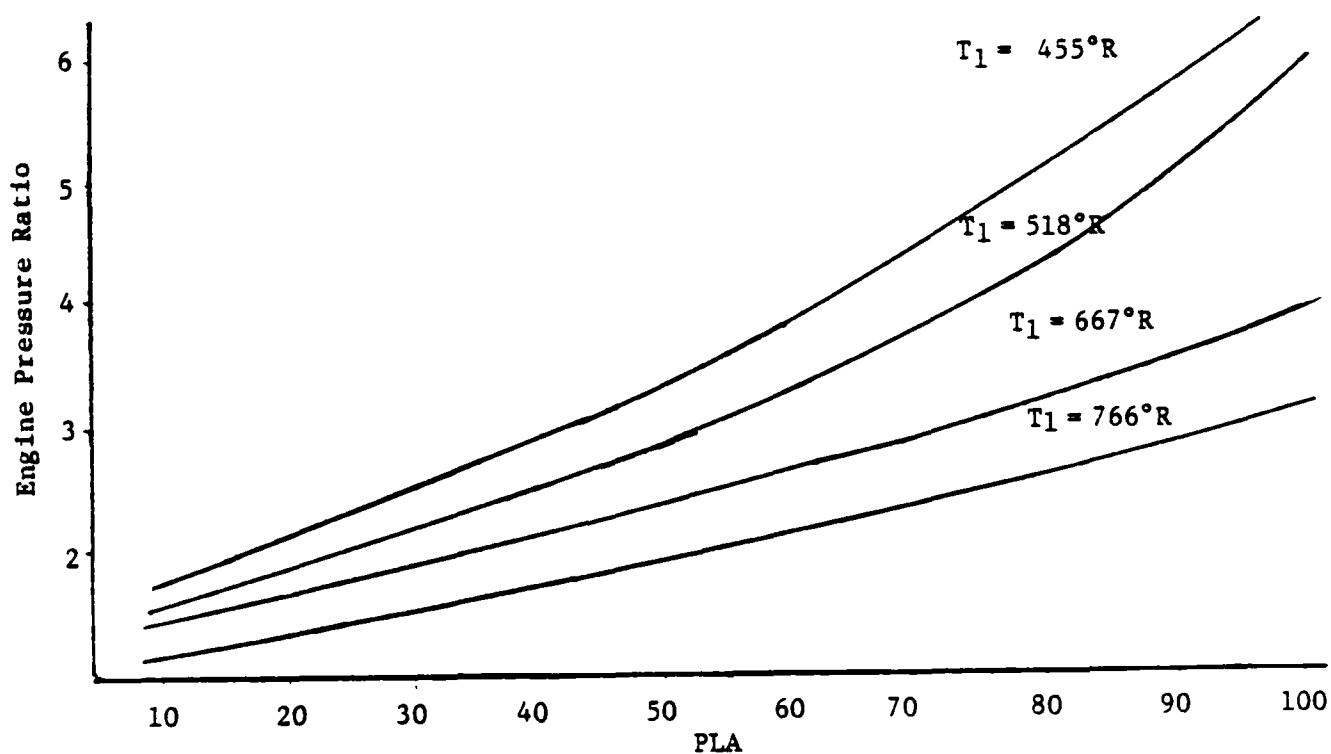


Figure 42. EPR schedule #2

### Non-Trim Mode

The control schedules required for the non-trim mode are

$NH_c$  vs. PLA for the fuel flow

EPR vs. PLA for the HPT

$WC_5$  vs. PLA for the nozzle

where the nozzle corrected flow ( $WC_5$ ) is computed from schedules of compressor corrected flow ( $WC_1$ ) vs.  $NH_c$ ,  $T_5/T_1$  vs. PLA, and EPR vs. PLA ( $WC_1$  vs.  $NH_c$  is transformed to  $WC_1$  vs. PLA to be consistent with the  $\theta_5$  and  $\delta_5$  schedules through the speed schedule).

The speed curves used for the non-trim mode were the same as those used for the baseline mode and a set of EPR,  $WC_1$ , and  $T_5/T_1$  schedules was constructed from the optimized data (d). The same mission and steady-state performance evaluation were made on the schedules shown in Figures 43 and 44. (EPR curves are the same as the baseline mode).

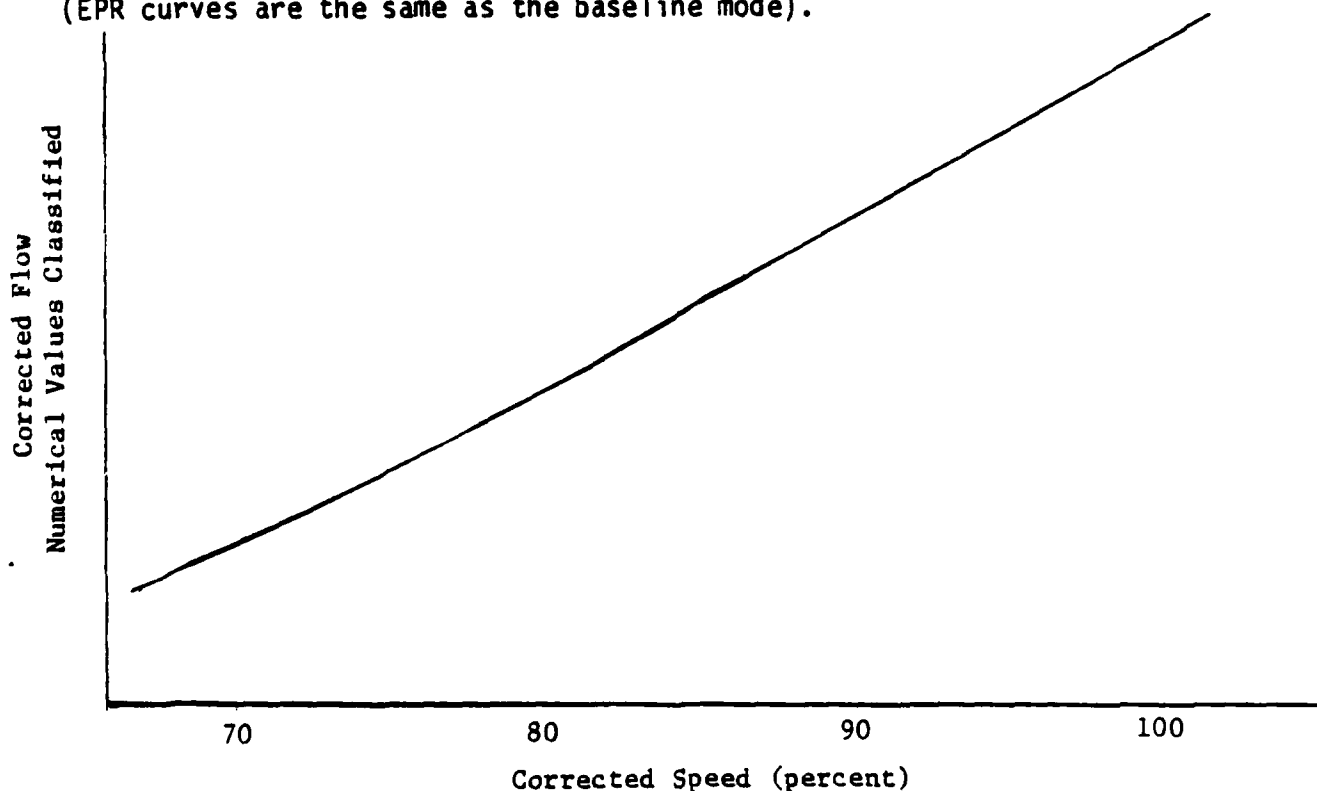


Figure 43. Corrected flow schedule.

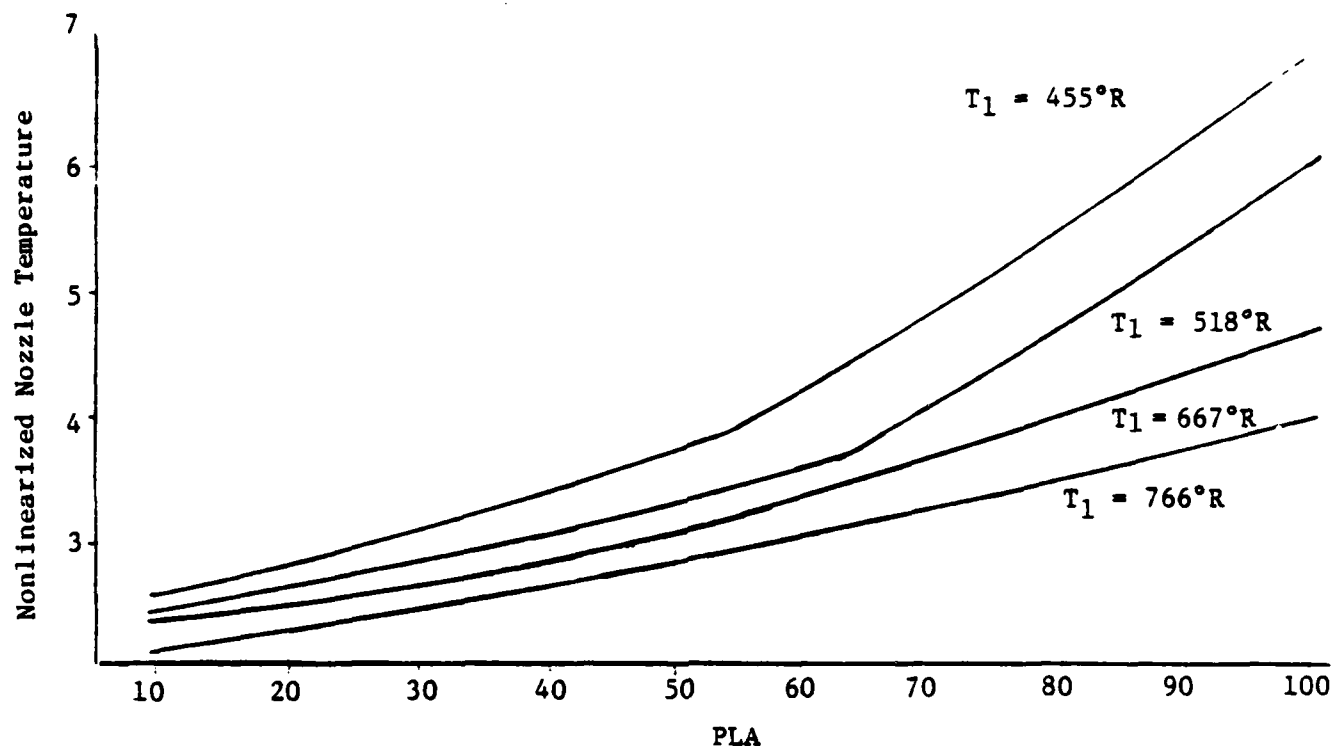


Figure 44. Nozzle temperature schedule

#### Steady State Evaluation

The results are divided into three areas -- (1) performance, (2) life utilization, and (3) stability. The first seven performance parameters are determined from the mission analysis. The final performance factor compares the maximum thrust achieved to the optimal (theoretical) maximum thrust for 30 flight conditions within the flight envelope. This is determined from the flight envelope data used as input to the mission analysis program.

The life utilization analysis includes mechanical LCF for the turbine wheel and thermal stress rupture and thermal LCF for the turbine blades and vanes. This data is normalized to the baseline control mode, minimum SFC results for the supercruiser mission.

The stability comparisons were drawn from over 300 operating conditions within the flight envelope from the same mission input data packages. This procedure gives a fast look at how the control will be operated steady state over the entire flight envelope.

The seven control modes evaluated with the screening process were

Baseline Mechanization (controls  $N_H$ ,  $R_C$ , and EPR)

- (1) Min. SFC #1
- (2) Min. SFC #2 (crossing speed lines)
- (3) Min. SFC #3 (increased EPR schedule)
- (4) Min. RIT
- (5) Min.  $N_H$
- (6) Min. SFC #3 with 200°F derated RIT

Non-Trim Mechanization (controls,  $N_H$ , flow, and EPR)

- (1) Min. SFC #3

The first evaluation was between the three Min. SFC modes under the baseline mechanization. The first two modes are different full flight envelope approximations (curve fits) to minimum steady-state SFC optimized schedules derived at 6 flight conditions representing combinations of four inlet temperatures and four inlet pressures.

A closer look at the flight envelope data showed that the TIT for the maximum power cases for minimum SFC #1 was less than the limiting temperature in more instances than minimum SFC #2. In the case of minimum SFC #2 data, geometry limits or corrected speed limits kept the turbine inlet temperature below its maximum in most of the cited instances. However, for minimum SFC #1, many

additional cases were noted where the maximum RIT was not reached even though the schedule was met.

Remember that the schedules were derived from optimized data for 6 flight conditions representing only 4 temperatures and 4 pressures, and then extrapolated throughout the flight envelope. Therefore, maximum thrust optimization was performed throughout the flight envelope to provide insight into the problems. Comparison of the extrapolated schedule values and optimal engine parameters showed that the flow values were close, but the scheduled EPR values were not consistent with optimal. Figure 45 shows a plot of the EPR values for maximum thrust for 30 points throughout the flight envelope.

It can be noted that EPR for maximum thrust is not just a function of inlet temperature ( $T_1$ ) as assumed in the original schedules and a schedule drawn through the original flight conditions will produce a lower EPR than the optimal in many cases.

Only the maximum power EPR settings were increased on minimum SFC #1 to form minimum SFC #3 and a new mission data set was generated. In this data set, only 2 of the 30 maximum power points did not achieve 98% of the optimal -- a 1/3 increase in the number of points that achieved 98% of the optimal. (It should be noted that here we used the optimal as a measure of goodness rather than an absolute to be achieved.)

The results for these three modes are shown in Table IX. The life utilization results have been normalized to the supercruiser minimum SFC #3 control mode results. A value greater than 1.0 signifies that the mode consumes more engine life than the Min SFC #3 baseline mode. This mode was chosen as the baseline mode for the remainder of the study because it exhibited better performance and less life utilization at the expense of engine stability (steady-state surge margin).

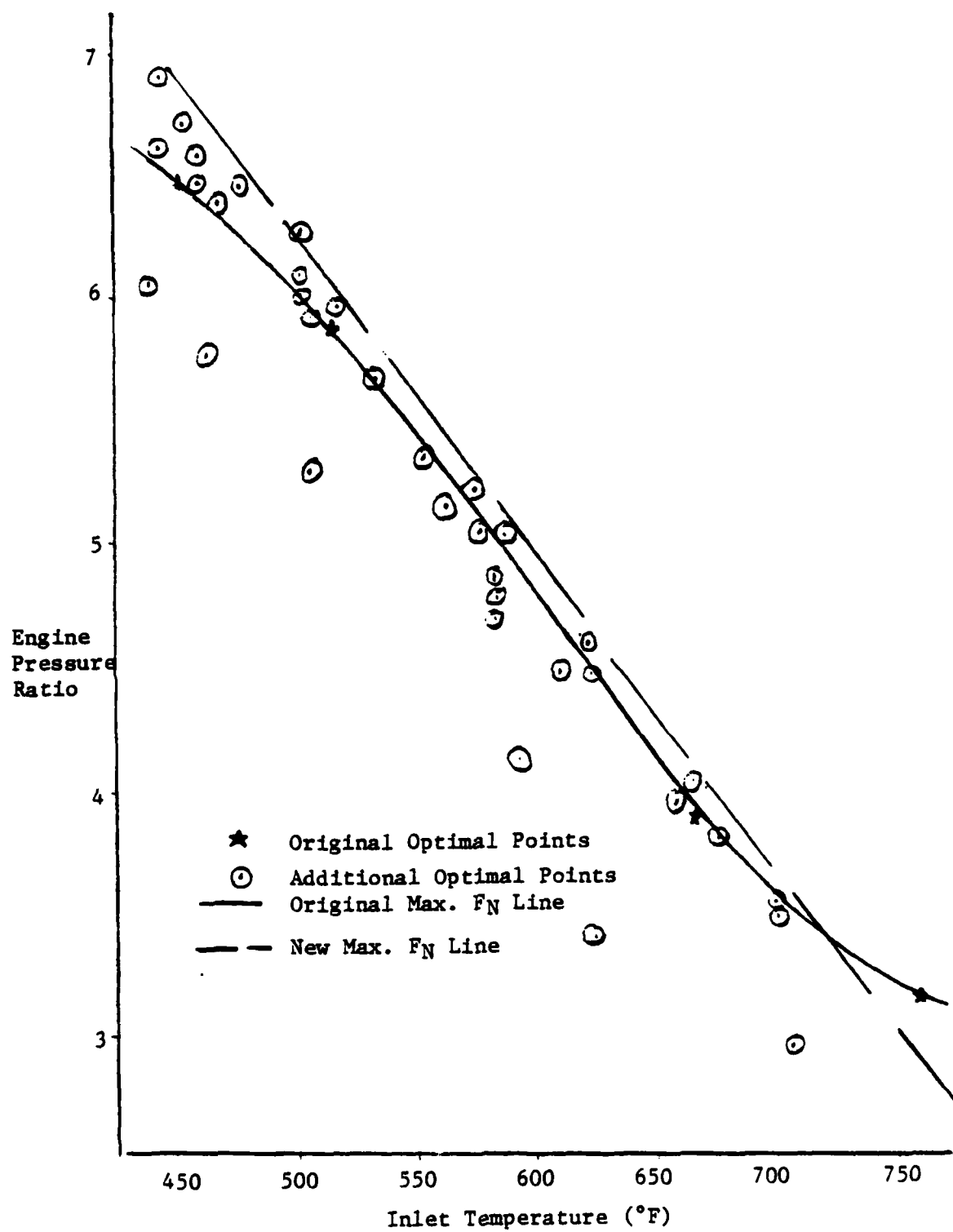


Figure 45. EPR at max thrust.

Table IX. Minimum SFC evaluation

CRITERIA		MIN SFC #1	MIN SFC #2	MIN SFC #3
P E R F O R M A N C E	DEEP STRIKE (D.S.) RANGE	131.3	128.9	131.2
	SUPERCRAISER (S.C.) RANGE	116.8	114.5	117.4
	TRAINING (TR) MISSION TURNS	4.1	4.0	4.1
	MAXIMUM TURNING RATE (DEG/SEC)			
	AT 3,000FT (TR. MISSION)	12.63	12.63	12.69
	AT 20,000FT (TR. MISSION)	10.15	10.18	10.15
	AT 40,000FT (D.S. MISSION)	2.91	2.91	2.89
	AT 50,000FT (D.S. MISSION)	1.55	1.50	1.56
	EXCESS POWER @ 36,30K FT, .9 MN	-.3 FT/SEC	14.0 FT/SEC	13.4 FT/SEC
	MAX FN WITHIN 98% OF OPTIMAL	21 OF 31	25 OF 31	28 OF 31
	ACCEL TIME .85 TO 1.6MN @ 30K FT	69.72	68.61	68.52
L I F E  C O N S U M P T I O N	VANE STRESS RUPTURE			
	DEEP STRIKE MISSION	.96979	1.0947	.71746
	SUPERCRAISER MISSION	1.3469	1.5766	1.0000
	TRAINING MISSION	1.5477E-05	1.6734E-05	1.8349E-05
	VANE LCF			
	DEEP STRIKE MISSION	.97306	.98175	.89194
	SUPERCRAISER MISSION	1.1325	1.1335	1.0000
	TRAINING MISSION	6.0076E-02	6.3615E-02	7.2799E-02
	BLADE STRESS RUPTURE			
	DEEP STRIKE MISSION	.80945	.89338	.81089
	SUPERCRAISER MISSION	1.0360	1.1187	1.0000
	TRAINING MISSION	1.2735E-04	1.4109E-04	1.6849E-04
	BLADE LCF			
	DEEP STRIKE MISSION	1.0482	1.0152	1.0252
	SUPERCRAISER MISSION	1.0271	.99726	1.0000
	TRAINING MISSION	1.0894	1.0899	1.0319
	WHEEL MECHANICAL CYCLES			
	DEEP STRIKE MISSION	.920	.921	.920
	SUPERCRAISER MISSION	1.0	1.003	1.0
	TRAINING MISSION	.938	.944	.936
S A F E T Y	POINTS LESS THAN 20% S.M.	.74	111	103
	POINTS LESS THAN 17% S.M.	7	16	43
	POINTS LESS THAN 15% S.M.	2	9	17
	MINIMUM SURGE MARGIN	14.8%	12.3%	10.9%



The surge margin degraded significantly to the point where approximately 10% of the flight and power conditions had less than 17% surge margin. In the final control design, it would be desirable to adjust the schedules to increase the surge margin, but the schedules are acceptable at this point in the design (only a paper engine exists).

In the remaining discussion, this mode will be referred to as the BASELINE MODE.

The BASELINE MODE is compared to the minimum RIT mode in Table X. Minimum SFC and minimum RIT are generally synonymous in a fixed geometry configuration. However, with a variable turbine, RIT is influenced by turbine position as well as fuel flow. As expected, the performance of the two modes was about equal with the BASELINE MODE superior in the SFC related items (i.e., range). However, the min. RIT mode consumed less turbine life in both the blades and vanes, with the largest improvement in the blades as a result of more direct control of the blade temperature (the cooling scheme was not altered). The wheel mechanical cycles were not affected as expected. There also was little change in engine stability. In summary, the min RIT mode offers a 10% increase in turbine blade life in trade for a 3% decrease in mission range with little effect on engine stability.

Since rotor speed is a factor in engine component life as well as metal temperature, a minimum  $N_H$  mode is compared to the BASELINE MODE in Table XI. In both modes, maximum power generally denotes maximum speed and temperature. As power decreases, speed remains at 100% and turbine temperature decreases in the minimum SFC mode until turbine loading requires a decrease in speed. Generally, the rotor remains at maximum speed for the upper 1/3 of the power range for the min SFC mode. However, speed immediately drops as power is reduced from the maximum power for the minimum  $N_H$  mode while turbine temperature remains at the maximum for up to a 10% power decrease. Thus, this mode trades a lower speed for a higher temperature (generally 200°F to 400°F higher than the minimum SFC mode). Therefore, this comparison provides the maximum differential between the two prime life utilization factors.

Table X. Minimum RIT evaluation

CRITERIA		BASELINE MIN SFC	BASELINE MIN RIT
P E R F O R M A N C E	DEEP STRIKE (D.S.) RANGE	131.8	128.0
	SUPERCRAISER (S.C.) RANGE	117.4	113.3
	TRAINING (TR) MISSION TURNS	4.1	4.0
	MAXIMUM TURNING RATE (DEG/SEC)		
	AT 3,000FT (TR. MISSION)	12.69	12.71
	AT 20,000FT (TR. MISSION)	10.18	10.20
	AT 40,000FT (D.S. MISSION)	2.89	2.87
	AT 50,000FT (D.S. MISSION)	1.56	1.48
L I F E  C O N S U M P T I O N	EXCESS POWER @ 3G, 30K FT, .9 MN	13.4 FT/SEC	13.4 FT/SEC
	MAX FN WITHIN 98% OF OPTIMAL	28 OF 31	27 OF 31
	ACCEL TIME .85 TO 1.6MN @ 30K FT	68.52 SEC	68.62
	VAHE STRESS RUPTURE		
	DEEP STRIKE MISSION	.71746	.56583
	SUPERCRAISER MISSION	1.0000	.79092
	TRAINING MISSION	1.8349E-05	1.8165E-05
	VAHE LCF		
	DEEP STRIKE MISSION	.89194	.84118
	SUPERCRAISER MISSION	1.0000	.95808
	TRAINING MISSION	7.2799E-02	7.3010E-02
	BLADE STRESS RUPTURE		
	DEEP STRIKE MISSION	.81089	.54290
	SUPERCRAISER MISSION	1.0000	.78657
	TRAINING MISSION	1.6849E-04	1.6829E-04
	BLADE LCF		
	DEEP STRIKE MISSION	1.0252	.89615
	SUPERCRAISER MISSION	1.0000	.96645
	TRAINING MISSION	1.0319	1.0353
	WHEEL MECHANICAL CYCLES		
	DEEP STRIKE MISSION	.920	.918
	SUPERCRAISER MISSION	1.0	1.0
	TRAINING MISSION	.936	.945
S A B I L I T Y	POINTS LESS THAN 20% S.M.	103	93
	POINTS LESS THAN 17% S.M.	43	47
	POINTS LESS THAN 15% S.M.	17	17
	MINIMUM SURGE MARGIN	10.9%	10.2%

Table XI. Minimum  $N_H$  Evaluation

CRITERIA		BASELINE MIN SFC	BASELINE MIN $N_H$
P E R F O R M A N C E	DEEP STRIKE (D.S.) RANGE	131.8	75.0
	SUPERCRAISER (S.C.) RANGE	117.4	64.3
	TRAINING (TR) MISSION TURNS	4.1	2.1
	MAXIMUM TURNING RATE (DEG/SEC)		
	AT 3,000FT (TR. MISSION)	12.69	12.94
	AT 20,000FT (TR. MISSION)	10.18	10.21
	AT 40,000FT (D.S. MISSION)	2.89	2.91
	AT 50,000FT (D.S. MISSION)	1.56	1.83
	EXCESS POWER @ 3G, 30K FT, .9 MN	13.4 FT/SEC	13.1 FT/SEC
	MAX FN WITHIN 98% OF OPTIMAL	28 OF 31	27 OF 31
	ACCEL TIME .85 TO 1.6MN @ 30K FT	68.52 SEC	68.55
L I F E  C O N S U M P T I O N	VAINE STRESS RUPTURE		
	DEEP STRIKE MISSION	.71746	4.3149
	SUPERCRAISER MISSION	1.0000	10.980
	TRAINING MISSION	1.8349E-05	1.3961E-05
	VAINE LCF		
	DEEP STRIKE MISSION	.89194	.99089
	SUPERCRAISER MISSION	1.0000	1.1808
	TRAINING MISSION	7.2799E-02	5.3947E-02
	BLADE STRESS RUPTURE		
	DEEP STRIKE MISSION	.81089	.44705
	SUPERCRAISER MISSION	1.0000	.87559
	TRAINING MISSION	1.6849E-04	2.4364E-03
	BLADE LCF		
	DEEP STRIKE MISSION	1.0252	.74372
	SUPERCRAISER MISSION	1.0000	.75760
	TRAINING MISSION	1.0319	1.0332
	WHEEL MECHANICAL CYCLES		
	DEEP STRIKE MISSION	.920	1.107
	SUPERCRAISER MISSION	1.0	1.177
	TRAINING MISSION	.936	1.674
S A B I L I T Y	POINTS LESS THAN 20% S.M.	103	102
	POINTS LESS THAN 17% S.M.	43	52
	POINTS LESS THAN 15% S.M.	17	23
	MINIMUM SURGE MARGIN	10.9%	9.8%

The higher temperature in the min  $N_H$  mode drops the SFC significantly and this is reflected in a 40% decrease in the three SFC related mission performance factors. However, since the maximum thrust is not affected, the other performance factors are unaffected.

The life utilization data also yields some interesting contrasts. The following factors should be considered in the evaluation of the vane life utilization.

- 1) The speed differences affect the airflow since both modes still use essentially the same compressor operating line.
- 2) With fixed percentage vane cooling air, the lower speed mode will provide less cooling air.
- 3) The vane does not see the mechanical cycles.

The higher gas temperature and lower cooling air significantly increases the vane stress rupture life utilization. However, in absolute values, this life consumption mechanism is several orders of magnitude less than the other mechanisms shown in the table. The LCF differences between the two modes for the vanes are not as significant because the higher temperatures are partially offset by the lower level of the mechanical cycles (reduced aerodynamic loading). When considering the turbine blade, one must remember that the modulated cooling will partially compensate for the higher gas temperatures.

However, in this case the modulated cooling completely distorted the results because of a phenomena that was not discovered until missions with dynamics were studied later in the program. An analysis of the detailed calculations for each time segment revealed that the major differences occurred in one

area, the two combat turns. This maneuver, which is broken into six similar sections by "throttle chops", was analyzed in more detail. Metal temperature and gas stream temperature are plotted for the deep strike mission for the two modes for three of the six similar sections in Figure 46. The modulated cooling air is scheduled to protect the metal temperature as opposed to closed loop control on metal temperature. Because the schedules must maintain safe metal temperature over the entire flight envelope, there are conditions of over-cooling even with cooling modulation. In the conditions shown in Figure 46, the cooling is optimum when the gas stream is at 94% of maximum, which results in a maximum safe metal temperature. However, as the gas stream temperature increases or decreases about this point, overcooling occurs and the metal temperature drops. In the minimum SFC mode, the stick mission requires a power setting ( 95% thrust) equivalent to approximately 94% TIT which yields the maximum metal temperature for most of the "life critical" combat turns. However, for the minimum  $M_N$  mode, the same power setting results in 100% TIT with the associated overcooling producing a 40°F decrease in metal temperature and life utilization decreases by a factor of 2. Since the stress rupture life utilization is about the same for the remainder of the mission, and the critical section accounts for 90% of the life utilization, the overall effect is a 50% decrease in life consumption for the mission.

There is no appreciable difference in the steady-state surge margin of the two modes because they both hold the same general compressor operating line. This comparison does show that the performance gained with the constant speed operation of the min SFC mode does cost turbine blade life.

Table XII shows a comparison between the BASELINE MODE and the same control derated by 200°F. As expected, the performance factors that reflect maximum thrust capabilities were significantly reduced by the deratings. However, the SFC related factor showed improvement because the fuel consumed at maximum power during the fixed portion of the mission was reduced which provided more fuel for the variable leg. It should be noted that the mission time for the

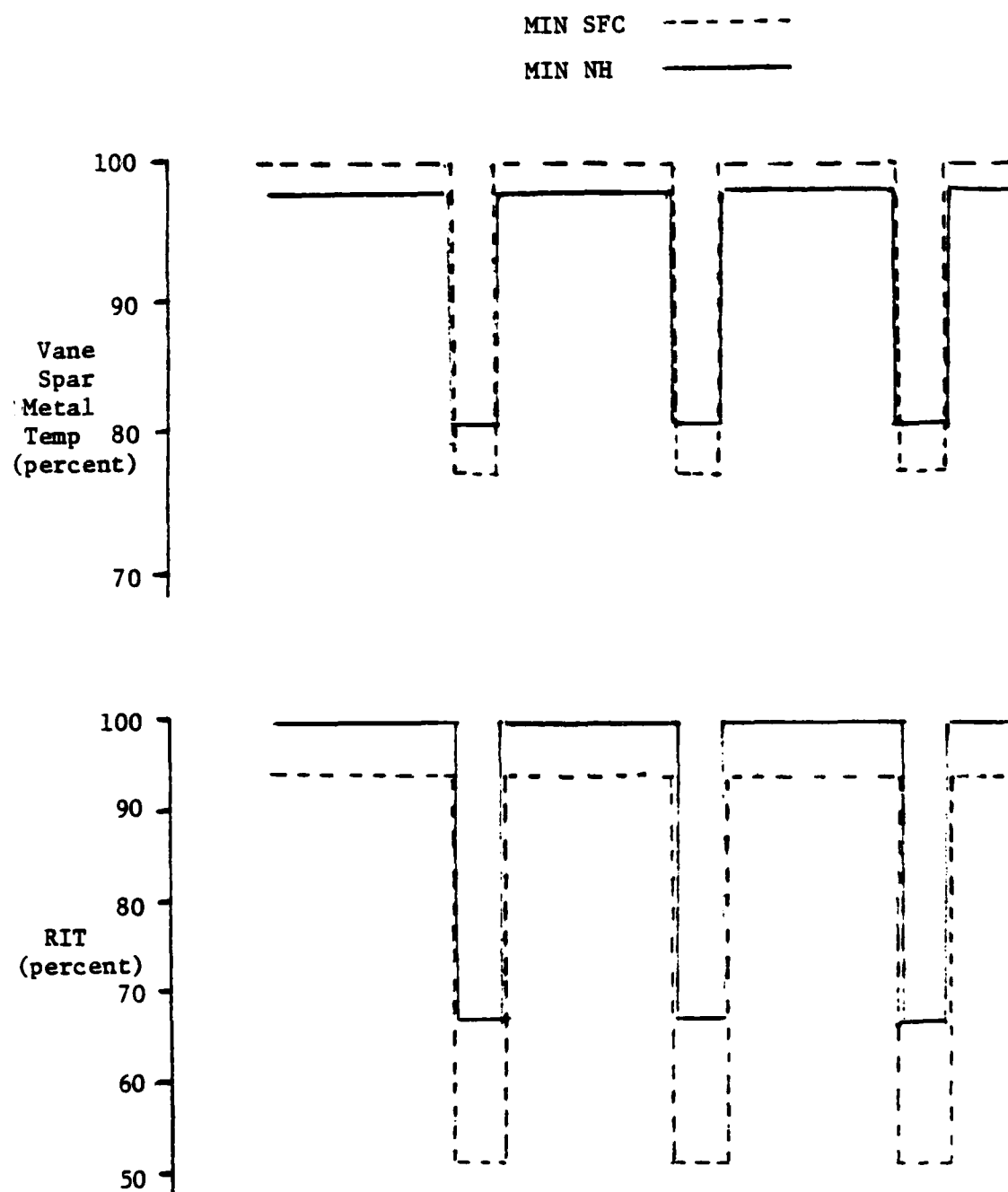


Figure 46. Gas and metal temperatures during critical period

Table XII. Derated control evaluation

CRITERIA		BASELINE MIN SFC	BASELINE DERATED
P E R F O R M A N C E	DEEP STRIKE (D.S.) RANGE	131.8	147.1
	SUPERCRAISER (S.C.) RANGE	117.4	133.2
	TRAINING (TR) MISSION TURNS	4.1	4.6
	MAXIMUM TURNING RATE (DEG/SEC)		
	AT 3,000FT (TR. MISSION)	12.69	12.21
	AT 20,000FT (TR. MISSION)	10.18	9.86
	AT 40,000FT (D.S. MISSION)	2.89	2.72
	AT 50,000FT (D.S. MISSION)	1.56	1.49
	EXCESS POWER @ 3G, 30K FT, .9 MN	13.4 FT/SEC	6.1 FT/SEC
	MAX FN WITHIN 98% OF OPTIMAL	28 OF 31	--
	ACCEL TIME .85 TO 1.6MN @ 30K FT	68.52 SEC	75.1
L I F E  C O N S U M P T I O N	VANE STRESS RUPTURE		
	DEEP STRIKE MISSION	.71746	.87318
	SUPERCRAISER MISSION	1.0000	1.1933
	TRAINING MISSION	1.8349E-05	8.3831E-06
	VANE LCF		
	DEEP STRIKE MISSION	.89194	.47331
	SUPERCRAISER MISSION	1.0000	.54337
	TRAINING MISSION	7.2799E-02	2.3294E-02
	BLADE STRESS RUPTURE		
	DEEP STRIKE MISSION	.81089	.41931
	SUPERCRAISER MISSION	1.0000	.60193
	TRAINING MISSION	1.6849E-04	4.7933E-05
	BLADE LCF		
	DEEP STRIKE MISSION	1.0252	.87352
	SUPERCRAISER MISSION	1.0000	.88537
	TRAINING MISSION	1.0319	.87643
	WHEEL MECHANICAL CYCLES		
	DEEP STRIKE MISSION	.920	.899
	SUPERCRAISER MISSION	1.0	.973
	TRAINING MISSION	.936	.958
S T A B I L I T Y	POINTS LESS THAN 20% S.M.	103	68
	POINTS LESS THAN 17% S.M.	43	8
	POINTS LESS THAN 15% S.M.	17	1
	MINIMUM SURGE MARGIN	10.9%	11.4%

derated modes was over 1 minute longer. As expected, the derating decreased turbine blade and vane life consumption. The increased stability reflects the fact that most of the low surge margin points in the BASELINE MODE occur in the area of maximum power.

The final comparison involves two different mechanizations of the Min SFC optimization. The non-trim mode was developed to provide automatic adjustment of the operating line to assure the design thrust within the engine constraints even with engine depreciation and engine build variations. Theoretically (neglecting the mechanization errors), the BASELINE MODE will hold thrust within 5% for expected engine variations while the NON-TRIM MODE will limit thrust deviations to less than 1%.

Direct application of the BASELINE MODE NHC and EPR schedules to the NON-TRIM MODE resulted in unacceptable steady-state surge margin. Over 1/2 of the 300 points in the flight envelope had less than 20% surge margin. This was expected to some extent since the control sensitivity analysis performed in the stability audit showed that additional surge margin was required for the NON-TRIM MODE. The stability loss was shown to be caused by a lower than nominal turbine setting. The EPR schedule was decreased to increase the surge margin (open the turbine). This adjustment also decreased the turbine temperature and thrust.

Only a small degradation was noted in SFC related performance parameters with the NON-TRIM MODE and the decreased EPR schedule as seen in Table XIII. However, the lowered EPR schedule significantly reduced the ability to achieve the desired maximum thrust throughout the flight envelope. The performance of this mode was closer to that of the derated engine since that was the effect of the lower EPR schedule. The slight improvements in life consumption in the NON-TRIM MODE can be attributed to this effect. However, the main life conserving feature of the NON-TRIM MODE is the elimination of field trimming the engine which can consume as much as 20% of the engine life.



Table XIII. Trim mode evaluation

CRITERIA		BASELINE MODE	TRIM MODE
P E R F O R M A N C E	DEEP STRIKE (D.S.) RANGE	131.8	128.2
	SUPERCRAISER (S.C.) RANGE	117.4	113.1
	TRAINING (TR) MISSION TURNS	4.1	4.4
	MAXIMUM TURNING RATE (DEG/SEC)		
	AT 3,000FT (TR. MISSION)	12.69	12.54
	AT 20,000FT (TR. MISSION)	10.18	9.13
	AT 40,000FT (D.S. MISSION)	2.89	2.54
	AT 50,000FT (D.S. MISSION)	1.56	1.58
	EXCESS POWER @ 3G, 30K FT, .9 MN	13.4 FT/SEC	-7.5 FT/SEC
	MAX FN WITHIN 98% OF OPTIMAL	28 OF 31	10 OF 31
	ACCEL TIME .85 TO 1.6MN @ 30K FT	68.52 SEC	75.99
L I F E  C O N S U M P T I O N	VANE STRESS RUPTURE		
	DEEP STRIKE MISSION	.71746	.71090
	SUPERCRAISER MISSION	1.0000	.98759
	TRAINING MISSION	1.8349E-05	1.8686E-05
	VANE LCF		
	DEEP STRIKE MISSION	.89194	.75714
	SUPERCRAISER MISSION	1.0000	.88167
	TRAINING MISSION	7.2799E-02	5.4759E-02
	BLADE STRESS RUPTURE		
	DEEP STRIKE MISSION	.81089	.67510
	SUPERCRAISER MISSION	1.0000	.97370
	TRAINING MISSION	1.6849E-04	1.4697E-04
	BLADE LCF		
	DEEP STRIKE MISSION	1.0252	.89358
	SUPERCRAISER MISSION	1.0000	.95124
	TRAINING MISSION	1.0319	.87889
	WHEEL MECHANICAL CYCLES		
	DEEP STRIKE MISSION	.920	.924
	SUPERCRAISER MISSION	1.0	1.001
	TRAINING MISSION	.936	.932
S T A B I L I T Y	POINTS LESS THAN 20% S.M.	103	94
	POINTS LESS THAN 17% S.M.	43	9
	POINTS LESS THAN 15% S.M.	17	43
	MINIMUM SURGE MARGIN	10.9%	4.7%

The screening evaluation has yielded several different contrasting modes to select from for evaluation with dynamics. The min RIT offers very small differences which could be accentuated or reduced by the dynamics. The minimum  $N_H$  mode offers the greatest differences for comparison while a NON-TRIM MODE represents a completely different mode. Investigation of the NON-TRIM MODE with dynamics was not considered for the dynamics analysis because it requires reprogramming the control logic in the engine/control simulation. The other modes only revise schedules (input data) in the simulation. In light of the above considerations, the minimum  $N_H$  mode was evaluated with dynamics in addition to the BASELINE MODE.

## XI. DYNAMIC ANALYSIS

The main purpose of this phase is to quantify the effects of neglecting the dynamic aspects of the mission and control during the steady-state analysis. The two particular points in question are

- 1) Does neglecting the dynamics give the wrong relative answers when comparing control modes?
- 2) What percentage additional life utilization does dynamics create?

The addition of dynamics greatly increases the cost of running the mission analysis and life utilization programs. Therefore, only two of the candidate modes--baseline system with minimum SFC and baseline system with minimum NH schedules--were evaluated with dynamics. There was no change in the performance and stability parameters. However, the life consumption generally increased with the addition of dynamics.

### Evaluation of Mission Life Consumption with Dynamics

The addition of dynamics to the stick missions used in the screening process made a significant change in the life consumption rate for the two modes evaluated. Unfortunately, the initial results with dynamics when compared to the stick missions were not consistent with the general trends exhibited with TF41 data during the life utilization validation. During the TF41 evaluations, the addition of dynamics to the stick mission increased the life consumption by about 10%. As seen in Table XIV, the addition of dynamics with the baseline mode increased life consumption up to several orders of magnitude and decrease life consumption in a couple of cases. The values circled in Table XIV are considered suspect and required further investigation.

The results for the minimum NH mode given in Table XV are much more reasonable. The vane stress rupture life consumption is several orders of magnitude less than the vane thermal LCF which makes the minor inconsistency in this area

Table XIV. Baseline Min SFC Comparison

<u>Life Criteria</u>	<u>Baseline Minimum SFC</u>		
	<u>No Dynamics</u>	<u>Dynamics</u>	<u>Increase</u>
VANE STRESS RUPTURE*			
Deep Strike Mission	.717	.987	+38%
Supercruiser Mission	1.000	1.34	+34%
Training Mission	$1.835 \times 10^{-5}$	$2.16 \times 10^{-5}$	+18%
VANE LCF			
Deep Strike Mission	.892	1.868	+110%
Supercruiser Mission	1.000	2.146	+114%
Training Mission	0.0728	0.0841	+16%
BLADE STRESS RUPTURE			
Deep Strike Mission	.811	.384	-53%
Supercruiser Mission	1.000	.427	-57%
Training Mission	.000168	.0787	+31267%
BLADE LCF			
Deep Strike Mission	1.0252	1.140	+11%
Supercruiser Mission	1.000	1.076	+ 8%
Training Mission	1.0319	1.471	+42%
WHEEL MECHANICAL CYCLES			
Deep Strike Mission	.920	1.032	+12%
Supercruiser Mission	1.0	1.004	+ 1%
Training Mission	.936	1.076	+15%

\*Vane Stress Rupture is negligible in absolute terms

Table XV. Baseline Min NH Comparison

<u>Life Criteria</u>	<u>Baseline Minimum NH</u>		
	<u>No Dynamics</u>	<u>Dynamics</u>	<u>Increase</u>
VANE STRESS RUPTURE*			
Deep Strike Mission	4.3149	3.894	-10%
Supercruiser Mission	10.980	10.883	- 1%
Training Mission	$1.396 \times 10^{-5}$	$1.63 \times 10^{-5}$	+17%
VANE LCF			
Deep Strike Mission	.991	1.165	+18%
Supercruiser Mission	1.181	1.3587	+15%
Training Mission	0.0539	0.0569	+ 6%
BLADE STRESS RUPTURE			
Deep Strike Mission	.447	.501	+12%
Supercruiser Mission	.876	.917	+ 5%
Training Mission	.00243	.00279	+15%
BLADE LCF			
Deep Strike Mission	.744	.908	+17%
Supercruiser Mission	.757	.830	+10%
Training Mission	1.033	1.185	+15%
WHEEL MECHANICAL CYCLES			
Deep Strike Mission	1.107	1.409	+27%
Supercruiser Mission	1.177	1.345	+14%
Training Mission	1.674	1.838	+10%

\*Vane Stress Rupture is negligible in absolute terms

negligible at this time. Therefore, dynamics introduced an increased life consumption consistent with TF41 experience with this mode.

#### Unusual Effects Created by Adding Dynamics

The five discrepancies noted in the minimum SFC mode with dynamics will be discussed next. All three missions with dynamics yielded unusual blade stress rupture results. The life utilization in the training mission increased by 32 fold with dynamics while the stress rupture life consumption decreased in the other two missions when dynamics were added.

Investigation of the discrepancies between the baseline minimum SFC mode with and without throttle dynamics revealed a potential problem in the construction of the mission approximations at maximum power conditions. It was assumed that the throttle dynamics would occur about a mean power less than maximum power since the engine control has tight bounds at maximum power. Therefore maximum power with dynamics were generated by superimposing the throttle dynamics on a mean power level of 95% thrust. The engine protection logic of the control was simulated by limiting the resulting power to 100% thrust by "clipping" any excessive spikes created by the dynamics. From TF41 data, this is the best representation of "throttle jockeying" at maximum power.

However, this left a dilemma for the stick-mission. One would expect a stick-mission at maximum power to be more severe than the dynamic mission with no excursions above maximum power. Thus, for the evaluation, maximum power for the stick-mission was reduced to the mean thrust (95% thrust) used in the corresponding dynamic segments.

The reduced power without dynamics and an unusual affect from the turbine blade modulated cooling combined to produce about a 50% decrease in stress rupture when dynamics was added to the deep strike and supercruiser missions. An analysis of the detailed calculations for each time segment revealed that the major difference in stress rupture with and without dynamics occurred in

one area of the mission combat turns. This maneuver, which is broken into six similar sections by "throttle chops", was analyzed in more detail. Metal temperature and gas stream temperature are plotted for the supercruiser mission with and without dynamics for two of the six similar sections in Figure 47. In the baseline system, the modulated cooling air is scheduled to protect the metal temperature as opposed to closed loop control on metal temperature. Because the schedules must maintain safe metal temperature over the entire flight envelope, there are conditions of over-cooling even with cooling modulation. In the conditions shown in Figure 47, the cooling is optimum when the gas stream temperature is at 94% of maximum, which results in a maximum safe metal temperature. However, as the gas stream temperature increases or decreases about this point, overcooling occurs and the metal temperature drops. In these two missions, the stick mission requires a power setting equivalent to the maximum metal temperature for most of the "life critical" combat turns. However, when "throttle jockeying" is added to the mission, overcooling occurs for both increasing and decreasing PLA and life utilization decreases by a factor of 2. Since the stress rupture life utilization is about the same for the remainder of the mission, and the combat turns account for 90% of the life utilization, the overall effect is a 50% decrease in life consumption for the mission.

It should be noted that this phenomena did not show up with the minimum  $N_H$  mode because throttle movements in this mode result in a constant turbine gas temperature (maximum value) for power changes between 90% and 100% thrust. Thus, there would be no metal temperature differences with and without dynamics at the critical conditions of maximum power in the combat turns.

However, in the case of the turbine vane LCF which has fixed cooling air, the reduced maximum thrust had the opposite effect. In the case without dynamics, approximately 1/2 of the LCF life consumption occurs during one major cycle which goes from mission start to maximum stress in the combat turn to mission end. Most of the remaining LCF damage is induced by the 6 throttle chops

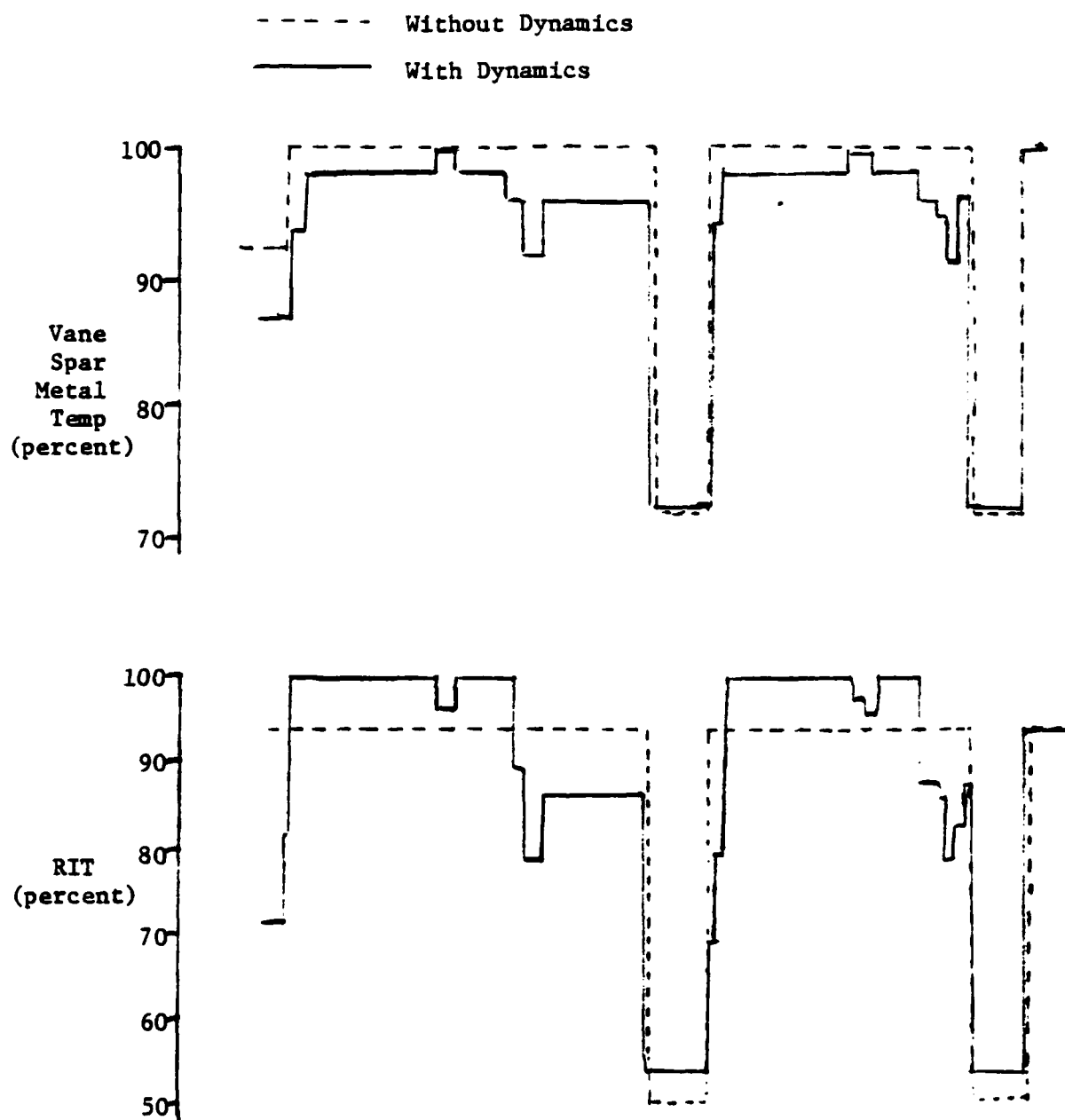


Figure 47. Gas stream and metal temperature during combat turns.



introduced in the combat turns. Similarly, 1/3 of the LCF life consumption when dynamics are added, occurs in a similar major cycle. Again, most (80%) of the additional damage was due to the throttle chops during the combat turns. Thus, the 110% increase in damage which occurs when dynamics are added is not directly due to additional cycles introduced by the throttle jockeying.

In each case--both major cycles and throttle chops--the LCF cycles in the stick mission are only half as damaging as the mission with dynamics. Detailed examination of the LCF computations revealed that the maximum metal temperature in the stick mission was approximately 40°F less than the dynamic enhanced mission for all the critical cycles. This occurred because all the critical cycles occur during the mission section where the thrust level was reduced to 95% in the stick mission and with fixed cooling, lower thrust means lower metal temperature. However, the thrust reach 100% during the dynamic mission due to the throttle jockeying which produced the maximum metal temperature. Therefore, the 110% increase in LCF life consumption was due to the reduced thrust level assumption in the stick mission. The LCF's would have been comparable if the stick-mission had allowed 100% thrust during the combat turns.

In the case of the training mission, the stress rupture life utilization is 4 orders of magnitude less than the other two missions. Further investigation showed that there were four small time segments which accounted for most of the additional damage. Because of the very low level of initial damage, a 200°F increase in metal temperature generated an order of magnitude increase in stress rupture and a 300°F increase caused a two orders of magnitude increase in the stress rupture life utilization. Although these four time segments accounted for less than a minute of the overall mission, the 200°F metal temperature increase in these four time segments amount to the 32 fold increase in life utilization because of the initial low life consumption.

## EVALUATION OF LIFE CONSUMPTION WITH CONTROL SYSTEM DYNAMICS

A verification study was run between a typical control transient output segment and the comparable mission dynamic output segment. The specific purpose was to determine the applicability of the mission dynamic program in predicting control performance parameter time histories. The time histories form the raw data from which life prediction is made. The mission analysis program requires parameter time histories as input. The original mission parameter time histories were generated by superimposing dynamics on steady state stick missions. The dynamic thrust profile of this mission can be correlated to a suitable control input, PLA, to generate comparable control/engine simulation time histories. By inputting each time history separately and comparing results, the original mission analysis procedure can be verified for the control study application. The primary concern is that the original mission time history dynamics are indicative of control/engine dynamics such that the mission analysis results produce consistent qualitative life usage indicators that can be used in control mode studies.

A typical dynamic time history segment was chosen from the original supercruiser mission. The chosen segment exhibited significant dynamics in a short time frame and was flown at a single Mach Number/altitude condition, thereby meeting previously determined selection criteria. The thrust response of the chosen supercruiser mission segment was transformed into a corresponding PLA time history for input to the control/engine simulation.

The PLA time history was input to the GMA400 engine/control digital transient computer simulation. The purpose was to generate an actual control time history for comparison. The resulting time histories were saved on tape. The format was rearranged to suit the mission analysis program input requirements. The data was then input to the mission life usage program. Table XVI shows a comparison between the vane and blade stress rupture and low cycle fatigue for the original supercruiser mission segment and the comparable control transient. The control transient used more life, as was expected. The percent increase in life used is also shown in Table XVI. The average increase for both failure modes is 9.8%.

Table XVI.  
Normalized Life Consumption Comparison

<u>Component/Failure Mechanism</u>	<u>Mission Baseline*</u>	<u>Control Transient</u>
Vane Stress Rupture	1.0	1.071
Vane Low Cycle Fatigue	1.0	1.031
Blade Stress Rupture	1.0	1.067
Blade Low Cycle Fatigue	1.0	1.222

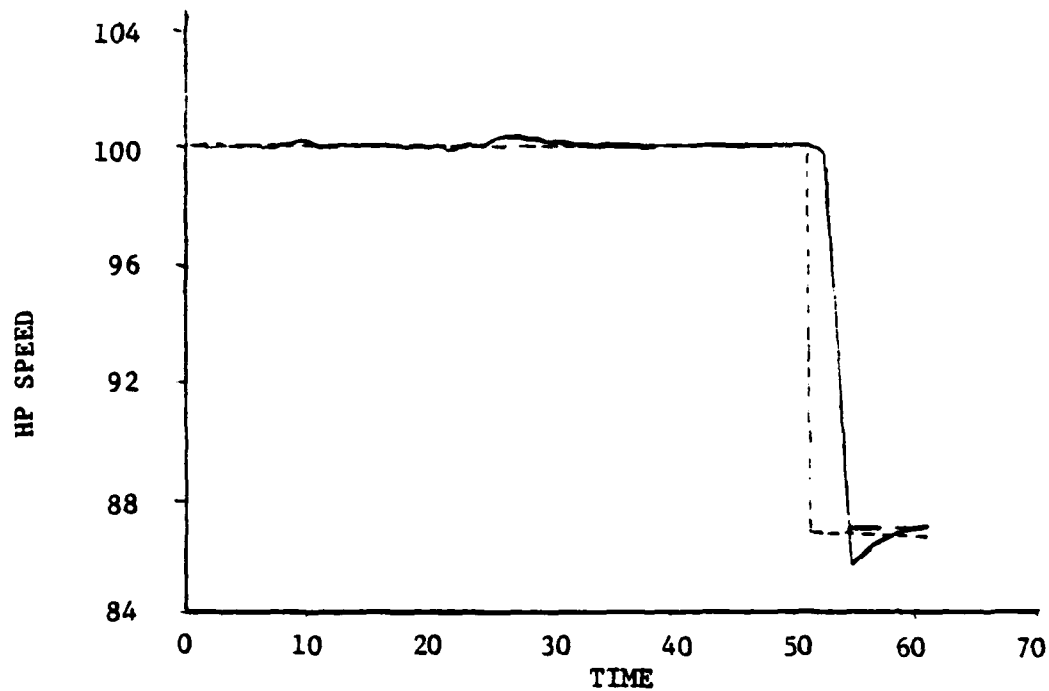
\*Normalized

The increase in life consumption noted for the control transient data is the result of several factors. Most obvious among these are the overshoots and undershoots. Figure 48 depicts time plots of both turbine inlet temperature,  $T_4$ , and rotor speed,  $N_H$ , for the mission baseline and for the control transient. The curve shapes are very similar with discrepancies mainly attributable to the control action about the point. There is a level shift noticeable at the non-max power points due to a flight difference in schedules. This schedule difference along with the overshoots/undershoots and the program sensitivities caused the life consumption differences.

The program calculations are sensitive to shifts in cooling flows or cooling temperature and in particular, to new parameter combinations resulting from slight skewing of time histories in relationship to each other (such as occurs with control/engine lags). Calculations at high temperatures can vary significantly in such a situation and indeed contributed to the noted differences. The difference of 9.8% overall is considered acceptable and explainable and shows a good degree of correlation between the mission life program dynamic parameter generation and the equivalent control transient.\* In conclusion, the mission analysis program is a useful tool in the control mode selection process.

\*It should be noted that the error would be present in the same direction and approximate magnitude in all mission time histories, such that qualitative analysis between missions is unaffected.

MISSION LIFE CONTROL TRANSIENTS  
TIME VS SPEED



MISSION LIFE CONTROL TRANSIENTS  
TIME VS T4

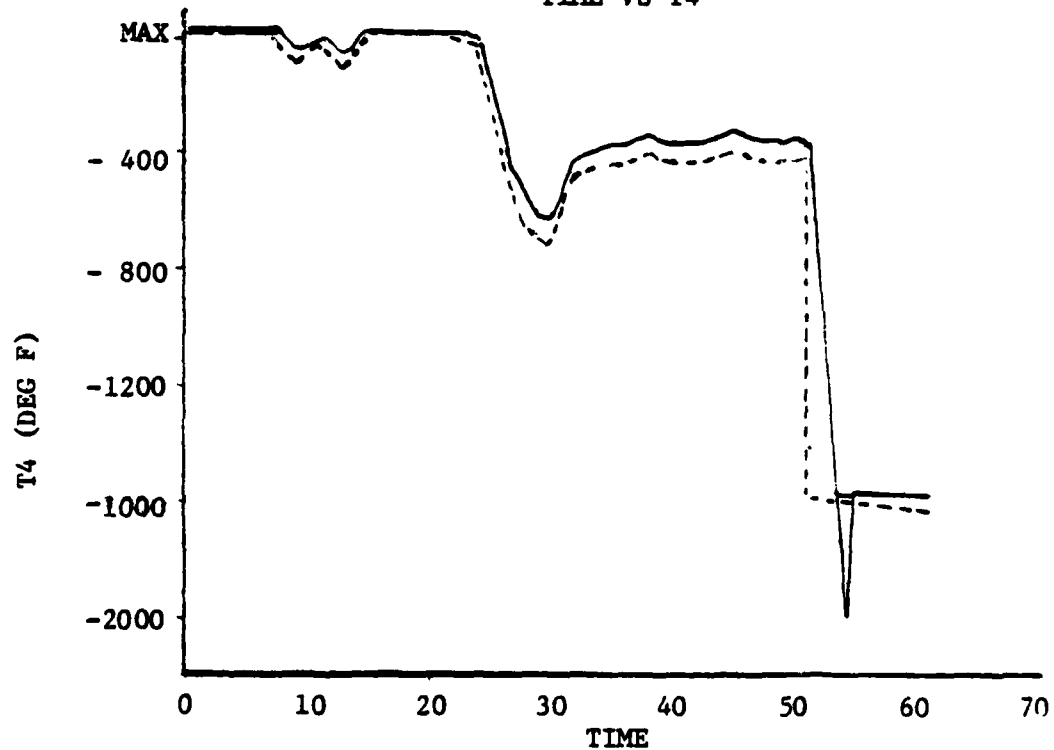


Figure 48. Mission life control transients.

## XII. CONCLUSIONS

The design and analysis methodology presented in this study has added a new dimension to control design procedures and clearly demonstrates that the control design can influence the life of engine components. This influence is distributed throughout the many choices made in the control design procedure.

Some of these choices, when made on classical values, also lead to greater engine life. Control parameters and loop gains are typically chosen for closed loop accuracy and system stability. When the control parameters are related to engine life, and established procedures for assuring system accuracy and stability are applied, the final result will generally provide a life-conserving control mode. However, when the parameters are performance oriented and life related parameters like speed or temperature are "uncontrolled", engine life is generally traded away for performance (i.e., the minimum trim mode in this study).

However, the other major variable in the control design, the control schedule, is generally a trade-off between performance and engine life. Typically, the schedules are derived by optimizing a steady-state criterion such as minimizing SFC or maximizing thrust. Direct optimization of control schedules to minimize engine life consumption is impractical because of the mathematical complexity of engine life computation models. However, engine life limiting parameters such as speeds and temperature can be minimized to provide a pseudo life optimization. The analysis procedure presented in this study provides quantified results that allow the control designer to make the proper trades depending upon the application and life goals of the engine. It must be noted that the results are generally influenced by the missions (applications) selected for the study.

A word of caution is also necessary. In this study, the control designer used several design tools from disciplines outside his area of expertise -- namely in the areas of performance analysis, mission analysis, and life consumption

analysis. It is important that the control designer become familiar with the computations utilized in these design tools, especially any assumptions required in their useage, in order to avoid erroneous answers. This was illustrated in the dynamics study which produced inconsistent results because of peculiarities in the cooling calculation.

#### RECOMMENDATIONS

The design and analysis procedures presented in this study should be applied to advanced variable geometry engines. The full flight envelope data evaluation and mission performance analysis can be applied early in the design to evaluate different control schedules. The control parameters should be chosen on the basis of engine life criticality as well as performance. However, detailed life consumption computation should be delayed until the mission is well defined and the life models are verified because of the great expense in this analysis.

More specifically, for the high temperature engines with variable cooling, the above analysis should be used to determine the type of variability and degree of modulation required to provide adequate performance and the desired life for hot section components.

**END**

**FILMED**

**5-83**

**DTIC**